

Final Project Report: Marine Species Density Data Gap Assessments and Update for the AFTT Study Area, 2016-2017 (Opt. Year 1)

Cooperative Agreement Number N62470-15-2-8003

Jason J. Roberts, Laura Mannocci, and Patrick N. Halpin

Marine Geospatial Ecology Lab (MGEL), Duke University

Document Version 1.4 – 2017-10-06

This document should be cited:

Roberts JJ, Mannocci L, Halpin PN (2017) Final Project Report: Marine Species Density Data Gap Assessments and Update for the AFTT Study Area, 2016-2017 (Opt. Year 1). Document version 1.4. Report prepared for Naval Facilities Engineering Command, Atlantic by the Duke University Marine Geospatial Ecology Lab, Durham, NC.

1. Introduction

In the United States, national laws protect cetaceans. The Marine Mammal Protection Act (MMPA) prohibits intentional or incidental killing, injuring, or harassment of marine mammals and specifies the circumstances and rules under which permits may be issued for such activities. The Endangered Species Act (ESA) prohibits harm to species threatened with extinction and requires conservation of their habitat. The National Environmental Policy Act (NEPA) specifies a process by which U.S. federal government agencies must evaluate the potential environmental effects of their actions, consider alternatives, and conduct public reviews. For certain actions this may culminate in the development of an Environmental Impact Statement (EIS). Agency actions that involve decisions to issue permits under the MMPA or ESA are often subject to this process.

The US Navy is responsible for compliance with a suite of federal environmental and natural resources laws and regulations that apply to the marine environment, including MMPA, ESA, the Magnuson-Stevens Fishery Conservation and Management Act, the Marine Protection, Research and Sanctuaries Act (MPRSA), Clean Water Act (CWA), Executive Order 13089 on Coral Reef Protection, and NEPA/Executive Order 12114 (EO 12114). Additionally, Federal Activities that have the potential to affect the state coastal zone are required to be consistent with respective state coastal zone management plans mandated by the Coastal Zone Management Act (CZMA).

To evaluate the potential effects of proposed activities on marine mammal populations, the Navy requires a detailed understanding of the spatiotemporal distributions of these populations. To facilitate development of the Atlantic Fleet Training and Testing (AFTT) Phase III EIS, the Navy funded us (the Duke Marine Geospatial Ecology Lab, or MGEL) to develop density surface models (Hedley & Buckland 2004; Miller et al. 2013) for all cetacean species sighted in the AFTT Study Area (Fig. 1) during scientific surveys conducted with protocols compatible with density surface modeling methodology. This culminated in the development and publication of regional models for the U.S. Atlantic coast and northern Gulf of Mexico (Roberts et al. 2016a) and the wider AFTT Study Area (Mannocci et al. 2017). From these results, we prepared a new version of the Navy Marine Species Density Database (NMSDD), the authoritative source of marine species density data maintained by the Navy, for the AFTT Phase III EIS (Roberts 2015; Roberts et al. 2015).

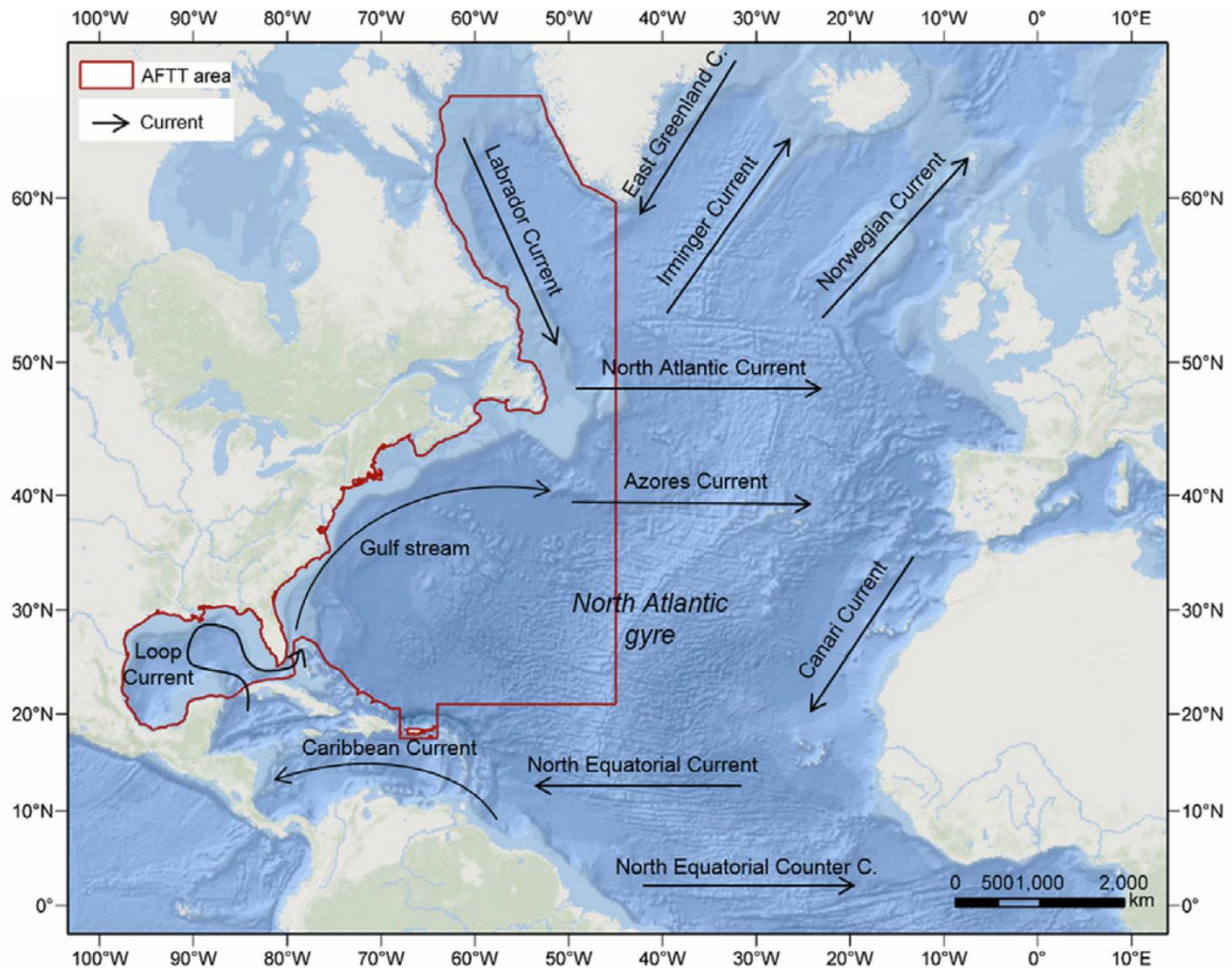


Figure 1. U.S. Navy AFTT Study Area with major current systems. Reproduced from Mannocci et al. (2017).

In 2015, the Navy initiated the project “Marine Mammal Density Gap Assessments and Update for the AFTT Study Area”, a Cooperative Agreement (#N62470-15-2-8003) with us to prepare revised models using newly available data and methodology; these “second generation” models would replace those in Phase III. In the Base Year (2015-2016) of the project, we acquired and integrated a large quantity of additional survey data in preparation for developing revised models (Roberts et al. 2016b). We prioritized acquisition of data in the U.S. Atlantic EEZ, which the Navy indicated was the highest priority for model refinement. Of particular interest were the first phase of the Atlantic Marine Assessment Program for Protected Species (AMAPPS) surveys¹, which provided aerial coverage of the U.S. Atlantic continental shelf in all four seasons and shipboard coverage of the offshore portion of the U.S. Atlantic EEZ in summer for multiple years. Also of high interest were the Southeast U.S. North Atlantic Right Whale (SEUS NARW) aerial surveys that covered right whale calving habitat in December-March since the 1990s². These surveys, together with others that were also integrated, more than doubled the data available for density analysis.

¹ The first phase of AMAPPS surveys (“AMAPPS I”) were conducted in 2010-2014 but were not released to us by NMFS until 2015 and 2016, which was too late to be incorporated into the original AFTT Phase III analysis. The second phase of surveys (“AMAPPS II”) started in 2015 and were a secondary priority for us. As of this writing, none of the AMAPPS II surveys have been released yet by NMFS.

² The SEUS NARW surveys comprised a very large amount of data and required special treatment to be used for density surface modeling. There was insufficient time to incorporate these into the original AFTT Phase III analysis. In the Base Year and Option Year 1 of the new analysis, we incorporated the SEUS NARW surveys from the 2003/04 season forward. This was the first season the SEUS NARW teams sufficiently standardized their protocols to allow the data to be used in our analysis (please see Roberts et al. (2016b) for more information).

Here we document work performed in Option Year 1 (2016-2017) of the Cooperative Agreement. During this period, we:

- Completed the integration of additional surveys into our analysis framework
- Validated the published density models (Roberts et al. 2016a) using newly-available acoustic monitoring data and geographical cross-validation, to inform development of updated models
- Updated density surface models for 11 cetacean taxa for the East Coast (EC) study area using the expanded collection of surveys and improved statistical methods
- Prepared an NMSDD update for the AFTT area and associated web services for the 11 updated taxa
- Coauthored two scientific publications relating to the density models

The following sections describe each task in detail.

2. Integration of Additional Surveys

We integrated most of the new surveys into our analysis framework during the Base Year of the Cooperative Agreement; Roberts et al. (2016b) describe these in detail. Here we describe additional surveys we incorporated after the Base Year, how we redefined the spatial extent of the east coast (EC) regional model study area, and re-summarize the total collection of surveys.

2.1. *Additional surveys integrated during Option Year 1*

During Option Year 1, we received and integrated additional data from three collaborators:

- From the North Atlantic Right Whale Sighting Survey (NARWSS) program, conducted at the NOAA Northeast Fisheries Science Center (NEFSC), we received 16,500 linear km of aerial surveys conducted between January and June 2016. This complemented the 70,600 km from November 2013 – December 2015 we integrated during the Base Year.
- From the SEUS NARW programs, we received 62,000 linear km of aerial surveys conducted between December 2015 and March 2016. These new data were conducted by the Florida Wildlife Research Institute (FWRI) and Sea to Shore Alliance (SSA), and complemented the 1,275,000 km of SEUS NARW surveys from December 2013 – March 2015 that we integrated during the Base Year.
- From the University of North Carolina, Wilmington (UNCW) we received 17,400 linear km conducted during all months of 2016 in the UNCW Jacksonville, Cape Hatteras, and Norfolk Canyon study areas. This complemented the 32,300 km from all months of 2014 and 2015 that we integrated during the Base Year.

These new data were collected in similar locations and seasons to the data already integrated, thus while they are not geographically or seasonally unique, they represent important geographic and seasonal replicates. (Please see Roberts et al. (2016b) for maps showing these areas.)

2.1.1. *Reprocessing of all NARWSS surveys to utilize multiple species per sighting*

In addition to integrating the new data described above, we reprocessed all NARWSS surveys (1999-2016, totaling 528,000 km) to allow our workflow to utilize multiple cetacean species when more than one were reported during a sighting and suitable records are logged, as follows.

The primary goal of NARWSS is to find, count, and photograph right whales, thus NARWSS conducts surveys in *closing mode* rather than *passing mode*. In closing mode, when a sighting is made the aircraft departs the trackline and circles the sighted group to confirm group size and species identification, and, if appropriate, collect photographs for identification of individuals. In passing mode, the aircraft remains on the trackline and does not collect additional information.

The use of closing mode presents a problem in the NARWSS study area, within which multiple species occasionally co-occur, e.g. right whales and sei whales at zooplankton prey patches. Under the NARWSS data recording protocol, only one species and group size is logged when the break is made from the trackline. When multiple species are present, these are logged as additional off-effort sightings while the aircraft is circling. NARWSS observers are required to log both sightings that are part of the original group and those that are “off in the distance”, but these additional sightings are not flagged as being one or the other. Because of this, in the original Phase III analysis (and related publications) we only counted the species logged when the break was initiated. We did not count sightings of additional species because we could not determine whether they were plausibly part of the original group (which would allow us to consider them on-effort and correct their detection probability by perpendicular distance from the trackline).

For the reprocessing, we adjusted our workflow to count species sighted during circling when the records were flagged as “actual positions”, meaning that the aircraft overflew the animals and collected a GPS coordinate, allowing us to establish that they were part of the originally-sighted group (Fig. 2), rather than other animals off in the distance that were coincidentally sighted during circling. This resulted in the recovery of approximately 300 additional sightings (mostly baleen whales) relative to the prior workflow, across the NARWSS surveys spanning 1999-2016.

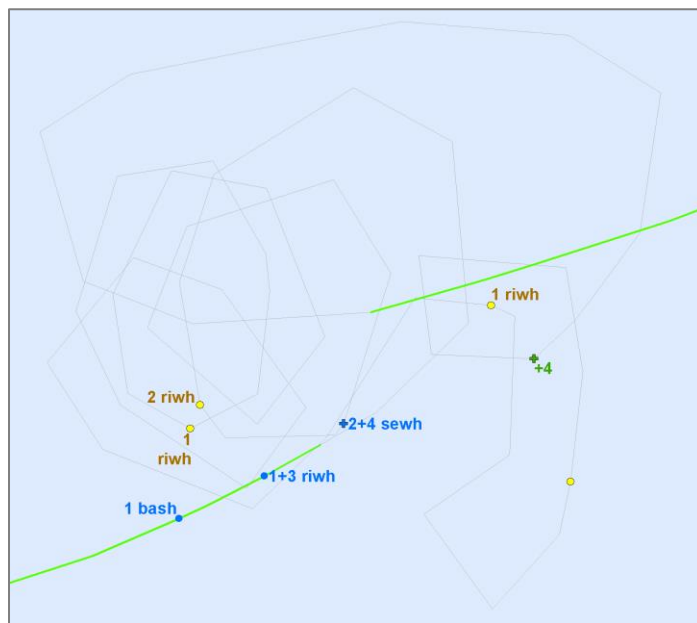


Figure 2. Example of new treatment of NARWSS multi-species sightings that allows both species to be utilized for modeling. Here, the aircraft entered from the lower right. Observers first logged a basking shark (bash) but did not break from the trackline. Then they logged a right whale (blue point labelled 1+3 riwh) and broke from the trackline to circle. During circling they located a total of four right whales and logged their actual positions (yellow points). The initial group size was corrected to four (i.e., 1+3). They also sighted six associated sei whales and logged their actual positions (blue point labelled 2+4 sewh and green point labelled +4). In this sighting, both the 4 right whales and the 6 sei whales were used in their respective density models. For the purposes of correcting for detectability, the same perpendicular distance was used in both models, obtained by the observer by measuring the declination angle to the first sighted group of 1 right whale.

2.2. New East Coast (EC) model study area

The expansion of survey coverage to new areas allowed us to expand the geographic extent of the EC model study area slightly (Fig. 3). AMAPPS surveys added coverage to Long Island Sound (A) and several offshore areas (B) slightly beyond the U.S. EEZ. NARWSS surveys of parts of the Gulf of St. Lawrence (C) will facilitate experimental models of right whales in this area. These will be performed at some future time in collaboration with NARWSS colleagues. Although the Gulf of St. Lawrence is outside of the AFTT study area, the Navy has indicated interest in models of this area because they may help explain shifts in right whale distributions in recent years.

The updated EC regional models presented in this report all terminate at the south edge of the Laurentian Channel (orange line D). The original Phase III EC models' predictions extended northeast to the opposite side of the Laurentian Channel but we decided to discontinue predicting this area from the EC regional models until additional survey data can be acquired for it. Until that time, we will predict the Laurentian Channel from the AFTT-wide models instead.

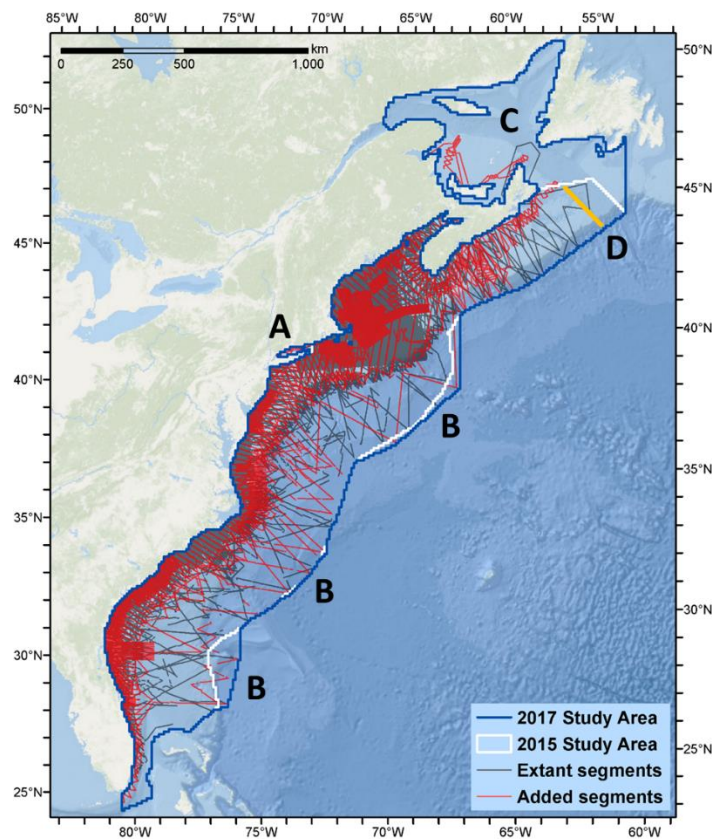


Figure 3. New East Coast (EC) model study area (blue line). New surveys allowed us to expand the study area at several locations from what was used in the original Phase III models (white line).

2.3. Summary of surveys available for analysis

The SEUS NARW surveys only systematically logged sightings of large whales and were not usable for other species. The remaining added surveys boosted the aerial and shipboard survey effort available for species other than large whales by 31% and 47%, respectively, relative to the data available for the original Phase III analysis (Table 1). For large whales, the SEUS NARW surveys boosted aerial effort by a further 158% (Table 2), but this was concentrated in the months of December-March within 50 miles of the coastlines of Florida, Georgia, and South Carolina (see Fig. 6 of Roberts et al. (2016b)).

Table 1. Survey effort usable for species other than large whales. “Extant” effort was used in the original Phase III models (Roberts et al. 2016a; Mannocci et al. 2017). “Added” effort was acquired and integrated into our modeling workflow in 2015-2017.

Platform	Provider	Program	Survey Effort (1000 km)			
			Extant	Added	Total	% Increase
Aerial	NEFSC	Marine mammal abundance surveys	70	41	112	59
		NARWSS harbor porpoise survey	6		6	
		NARWSS right whale surveys	432	87	520	20
	NJDEP	New Jersey Ecological Baseline Study	11		11	
	SEFSC	Marine mammal abundance surveys	43	66	108	154
	UNCW	Cape Hatteras Navy Surveys	19	16	35	86
		Jacksonville Navy Surveys	65	22	87	34
		Marine mammal surveys, 2002	18		18	
		Norfolk Canyon Navy Surveys		12	12	
		Onslow Bay Navy Surveys	49		49	
		Right whale surveys, 2005-2008	114		114	
	VAMSC	MD Wind Energy Area surveys		16	16	
		VA Wind Energy Area surveys	17	5	21	28
	All			844	264	1108
Shipboard	NEFSC	Marine mammal abundance surveys	16	12	28	76
	NJDEP	New Jersey Ecological Baseline Study	14		14	
	SEFSC	Marine mammal abundance surveys	28	15	43	52
	All			58	27	85

Table 2. Survey effort usable for large whale species. “Extant” effort was used in the original Phase III models (Roberts et al. 2016a; Mannocci et al. 2017). “Added” effort was acquired and integrated into our modeling workflow in 2015-2017.

Platform	Provider	Program	Survey Effort (1000 km)				
			Extant	Added	Total	% Increase	
Aerial	NEFSC	Marine mammal abundance surveys	70	41	112	59	
		NARWSS harbor porpoise survey	6		6		
		NARWSS right whale surveys	432	87	520	20	
	NJDEP	New Jersey Ecological Baseline Study	11		11		
	SEFSC	Marine mammal abundance surveys	43	66	108	154	
	SEUS NARW	FWRI surveys		521	521		
		NEAq surveys		237	237		
		SSA surveys (Skymaster)		279	279		
		SSA surveys (Twin Otter)		291	291		
		UNCW	Cape Hatteras Navy Surveys	19	16	35	86
		Jacksonville Navy Surveys	65	22	87	34	
		Marine mammal surveys, 2002	18		18		
		Norfolk Canyon Navy Surveys		12	12		
		Onslow Bay Navy Surveys	49		49		
		Right whale surveys, 2005-2008	114		114		
	VAMSC	MD Wind Energy Area surveys		16	16		
		VA Wind Energy Area surveys	17	5	21	28	
	All			844	1591	2435	189
	Shipboard	NEFSC	Marine mammal abundance surveys	16	12	28	76
NJDEP		New Jersey Ecological Baseline Study	14		14		
SEFSC		Marine mammal abundance surveys	28	15	43	52	
All			58	27	85	47	

The added surveys filled critical seasonal gaps throughout the study area, yielding complete coverage of the continental shelf (0-200m) from southern Florida to the Bay of Fundy, and much of the continental slope (200-2000m) from Cape Hatteras to Georges Bank, in all seasons (Fig. 4). However, nearly all additional distant deep-water effort occurred in summer, and effort remained sparse here in other seasons.

For more information about the added surveys, please see Roberts et al. (2016b).

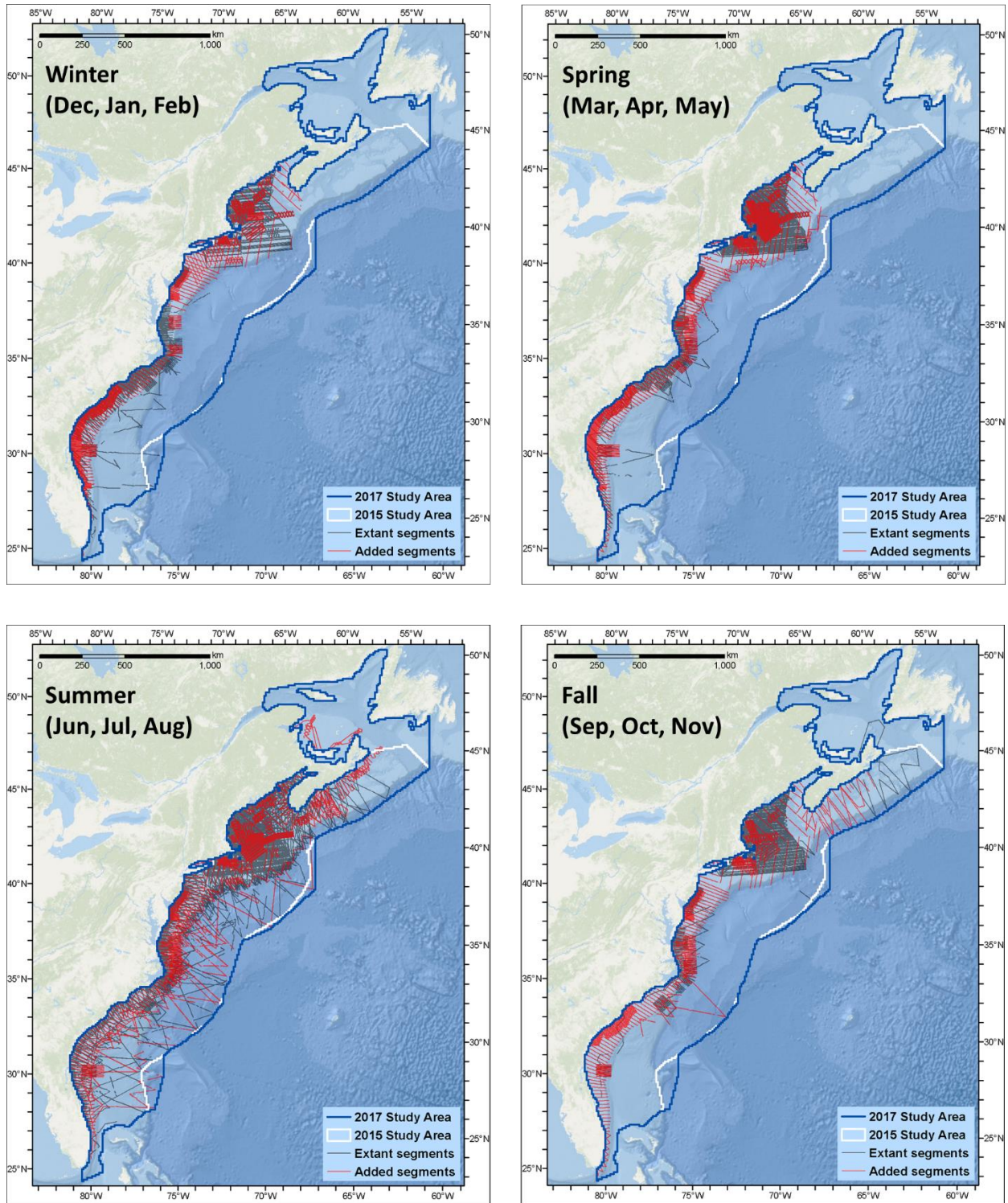


Figure 4. Seasonal distribution of survey effort used in the original Phase III models (“extant” segments) and of survey effort acquired and integrated into our modeling workflow in 2015-2017 (“added” segments).

3. [Omitted]

[This section contains acoustic analyses that we cannot release without obtaining permission from a large number of collaborators. These analyses are ancillary to the documentation of the updated density models, which appears in sections above and below. Obtaining permission from all of the collaborators would take a long time. Thus, to facilitate quick release of the documentation of the density models, we are omitting the acoustic analyses from our except of this report.]

4. Updated Density Surface Models

The central objective of Option Year 1 was to produce updated density models for 6-10 marine mammal species considered to be high priority by the Navy for the AFTT Study Area. In discussions, the Navy identified baleen whales—particularly the North Atlantic right whale—beaked whales, pilot whales, the sperm whale, and the harbor porpoise as the highest priority species, owing to their endangered status or sensitivity to acoustic disturbance. Additionally, the Navy prioritized breaking up the “beaked whales” and “pilot whales” guild models of the original Phase III models into multiple, more taxonomically-precise models, if this was feasible given improvements in species identifications made by NOAA and others in newly-integrated surveys. Finally, the Navy called for investigation of, and if feasible, development of density models for four species of sea turtles.

The Navy indicated that it was a priority to update regional models for the east coast (EC) region (Fig. 3), and that it was not necessary to update the Gulf of Mexico (GOM) regional models or the AFTT-wide models (Mannocci et al. 2017) as part of the Option Year 1 updates, indicating that updates to these models could come in later Option Years, should they become a priority for the Navy. The Navy also identified or suggested various methodological improvements that could be considered during development of updated models, which we investigated, discussed with the Navy, and implemented when feasible.

4.1. *Summary of work performed*

- We produced new and updated EC regional density models for 11 taxa: fin whale, humpback whale, minke whale, North Atlantic right whale, sei whale, Cuvier’s beaked whale, Mesoplodont beaked whales (a guild), unidentified beaked whales (a guild), pilot whales (a guild), sperm whale, and harbor porpoise.
- After reviewing new and revised beaked whale identifications contributed by collaborators and discussing them with colleagues and the Navy, we successfully split the original Phase III “beaked whales” guild into the three models noted above.
- We investigated the possibility of splitting up the “pilot whales” guild, either by classifying the numerous “unidentified pilot whale” sightings into one species or the other with a classification model from definitive sightings (as we did with “fin or sei whale” sightings; see section 4.2.7), or by leveraging an experimental classification model built by L. Garrison and colleagues at the NOAA Southeast Fisheries Science Center from definitive sightings identified with genetics. Both options proved infeasible; there were too few definitive sightings to build our own classification model, and Garrison expressed considerable uncertainty about his model’s performance in non-summer months. Accordingly our updated model for pilot whales remains a guild of the two species.
- We investigated the possibility of developing sea turtle density models but lacked the time to overcome the turtle-specific challenges that impede their development during this Option Year. We summarize these below. Sea turtle models could be attempted in a future Option Year if prioritized by the Navy.

- We investigated various methodological improvements, implemented some of them, and deferred some to the future. One notable improvement we implemented, discussed below, was estimation of coefficients of variation (CV) surfaces for AFTT-wide models. Many deferred improvements, such as a tractable method for propagating uncertainty in multiple detection functions and $g(0)$ estimates into a single spatial density model, require innovations from outside experts in the statistics of density modeling. We hope to leverage the upcoming “DenMod” working group, funded by the Navy’s Living Marine Resources Program, to make progress on these innovations.

4.2. *New and updated East Coast (EC) models*

Here, we briefly discuss each of the 11 new or updated EC density models we are delivering in our NMSDD update. These models are intended to eventually replace the corresponding Phase III models published by Roberts et al. (2016a). We met with and reviewed all of these models with peer modelers and species experts, including colleagues at NOAA NEFSC and SEFSC and other institutions responsible for collecting the data (including D. Palka, L. Garrison, P. Corkeron, W. McLellan, T. Gowan, M. Swingle) as well as those not involved in this work (including E. Becker, A. Read, and D. Nowacek).

Although we believe, at the time of this writing, that these models have reached final publishable formulations, we will continue to informally examine them and discuss them with additional experts, in preparation for submitting a publication. It is possible these examinations and discussions will move us to further adjust some models. If this happens we will make any changes available to the Navy as additional NMSDD updates.

As we prepare the publication, the results that appear here and other diagnostics will be consolidated and placed in species-specific reports designed as supplementary information for the publication. As was done with the original Phase III density models, we will provide these reports to the Navy as they are produced.

4.2.1. *Methods*

This project used the same methodology as the published Phase III models (Roberts et al. 2016a) with several updates and improvements.

4.2.1.1. *Improvements to detection function formulations*

The Roberts et al. (2016a) detection functions only supported continuous covariates. This was sub-optimal for certain situations. Notably, for some species we observed a nonlinear relationship between detectability and sea state (Fig 17). When we inquired with observer teams about this, they found it reasonable. For example, Christin Khan, an observer and data manager with the NOAA NARWSS program, explained “There appears to be a bit of a step function in detectability at higher Beauforts. From Beaufort 1-3 the whales' bodies are a primary cue. At 4-5 it becomes the white water around the whales as the waves break over the whales' back, and I think at the right Beaufort it increases our detection distance. From 5-6, the whitecaps become bigger and we can no longer distinguish between them and the breakers created by the backs of whales.”

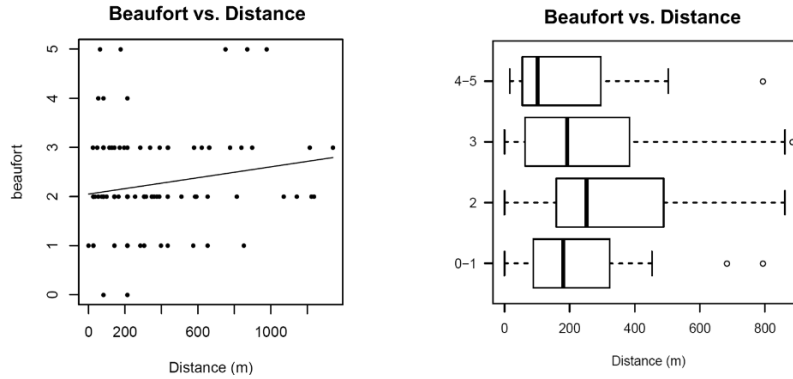


Figure 17. Left: example of treatment of Beaufort sea state as a continuous detection function covariate, as was done in Roberts et al. (2016a). The black line represents a linear trend line; in this plot it suggests that detection distance increases as sea state increases, which seems counter-intuitive. Right: example of treatment of Beaufort sea state as a categorical covariate. Here we see that the relationship between detection distance and sea state is nonlinear, peaking at 2. In the example shown here, the best model is obtained with a categorical covariate.

For the new models, we enabled the ability to utilize categorical covariates. This handled nonlinear relationships between sea state and detectability, and was more appropriate for sea state generally, as the Beaufort scale is a categorical (actually ordinal) scale, not a continuous scale.

A second major improvement was that we reprocessed most surveys used in Roberts et al. (2016a) and replaced the single, synthetic “Quality” detection function covariate that Roberts et al. had computed from various survey-specific covariates with those individual covariates instead. For example, in surveys that had Glare and Visibility covariates, Roberts et al. (2016a) computed Quality by taking the mean of Glare and Visibility, weighted equally, and rescaling the result onto a 0-5 scale similar to Beaufort sea state. This experimental approach attempted to standardize these organization-specific covariates other than Beaufort sea state into a synthetic covariate that was comparable across organizations, to facilitate using it in detection functions that pooled sightings across organizations. We found that this synthetic covariate was, in fact, not very comparable across organizations and could not use it in the way it was originally intended. In the new models, we largely abandoned the synthetic Quality covariate and replaced it with the original covariates (e.g. Glare and Visibility) collected by the surveyor organization. This allowed detection functions to consider such covariates independently or together in a multi-covariate model, rather than as the synthetic covariate that used a predetermined weighting scheme.

Finally, we improved our reporting of diagnostic information by computing the Kolmogorov-Smirnov and Cramer-von Mises goodness-of-fit tests.

4.2.1.2. *New detection hierarchy*

In Roberts et al. (2016a), we organized the detection hierarchy for shipboard surveys under the assumption that the specific ship used made more of a difference in detectability than the organization (NEFSC vs. SEFSC) or survey program (e.g. AMAPPS vs. surveys that came before). With several new shipboard surveys available from AMAPPS and other programs, including an NEFSC survey conducted on one of SEFSC’s primary survey vessels (R/V Gordon Gunter), we were able to test this assumption more carefully. The results suggested that the survey organization and program made more of a difference than the ship used. We lacked sufficient information to determine whether this might be due to organizational or historical differences in the observers used, their training, the survey protocols, regional differences in observation conditions or species behaviors, or other factors. In any case, we reorganized the detection hierarchy to reflect this new view.

4.2.1.3. New detection functions

After integrating the new surveys, reprocessing the old surveys to recover original survey-specific detectability covariates, and reconfiguring the detection hierarchies, we fitted new detection functions from scratch for the 11 taxa for which we created updated density models. For brevity, we omit these results from this report, as they constitute many 10s of pages of plots and statistical output. As with the original Phase III models, these will appear in the species-specific supplementary reports that will accompany the submitted publication.

A notable feature of the new detection functions relative to those from the original Phase III models is that the addition of categorical covariates allowed us to test species identification as a categorical covariate. When sightings were sparse, we were able to pool similar species (e.g. baleen whales) into a single detection function but allow some difference in detectability through the species ID categorical covariate. For example, we used this approach for baleen whales sighted from the 1999 NEFSC Abel-J naked eye shipboard survey (Fig. 18). In this survey, right and humpback whales had higher detection probability, potentially owing to behaviors such as breaching and other surface activity visible from a long distance, followed by fin and sei whales. Minke whales, known for their cryptic behavior and relatively small size, exhibited the lowest detection probability.

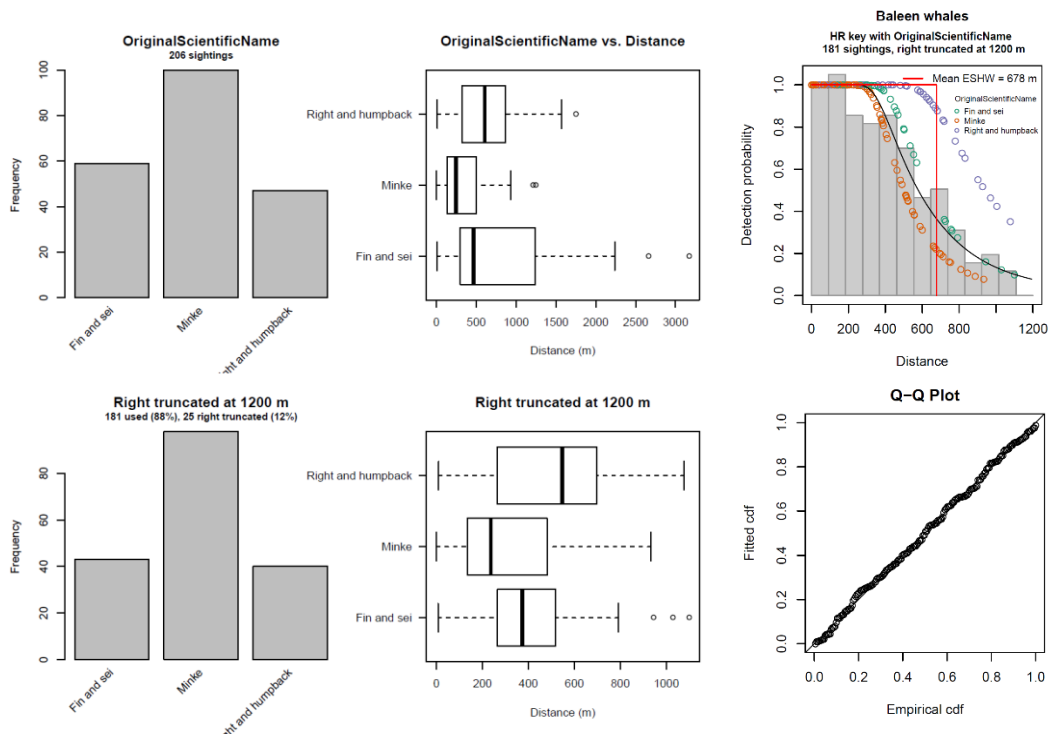


Figure 18. Left and center: histograms and boxplots showing distribution of sightings of baleen whales sighted on the 1999 NEFSC Abel-J naked eye shipboard survey. Right: resulting detection function (top) and diagnostic Q-Q plot (bottom).

4.2.1.4. Technical changes to spatial modeling statistical approach

As before, for the spatial models we fitted generalized additive models (GAMs) with the R mgcv package. For the new models, we made two important technical changes to our statistical approach to fitting them.

First, Roberts et al. (2016a) restricted the maximum degrees of freedom of univariate spline smoothers to 4, in keeping with an approach originally advocated by Forney (2000) that sought to preserve the ecological interpretability of spline fits and mitigate against overfitting by requiring “simple” (i.e. not “too wiggly”) covariate relationships. After discussing this approach extensively since 2015 with K. Forney, E. Becker, D. L. Miller, and

others, and testing various alternatives, we collectively decided to relax this constraint. The new models utilize the default recommended by mgcv, which is 9 degrees of freedom for univariate spline smoothers.

Second, for certain models we utilized bivariate smooths of spatial coordinates (longitude and latitude, projected with GIS to a coordinate system appropriate for density estimation). This practice is advocated by experts at the University of St. Andrews, where the “distance sampling” and “density surface modeling” methods originated (Buckland et al. 2001; Hedley & Buckland 2004). However, to work well it requires sufficient spatial coverage by line transect surveys. Large gaps in spatial coverage are unlikely to be interpolated or extrapolated well. Faced with that problem, we favored models built on univariate smooths of habitat-based covariates (e.g. depth of the seafloor or sea surface temperature) that were more completely sampled by available surveys. For Roberts et al. (2016a), in which there were many seasonal gaps in coverage, we utilized univariate habitat-based covariates exclusively. In the models presented here, we selectively utilized spatial bivariate smooths when we judged that surveys sufficiently covered the subregion and months that were modeled. We used $k=50$ when parameterizing bivariate spatial smooths.

Finally, we updated software packages to the latest versions. Final models were fitted with R 3.3.3, mrds 2.1.18 (for detection functions), mgcv 1.8-17 (for GAMs), and party 1.2-3 (for classification of ambiguous sightings).

4.2.1.5. Updated habitat covariates for spatial modeling

For spatial models, we used the same habitat-based covariates as Roberts et al. (2016a), with a few changes. We updated all covariates to the latest reprocessings performed by their original providers and extended their time durations to the end of 2016 (or the latest date available). We also added or changed a few covariates:

- We added an experimental Finite-Size Lyapunov Exponent (FSLE) covariate published by AVISO (see <https://www.aviso.altimetry.fr/en/data/products/value-added-products/fsle-finite-size-lyapunov-exponents/fsle-description.html>). This covariate identifies front-like structures where particles are likely to be separated, as on the edges of the Gulf Stream or geostrophic eddies. In modeling performed so far, we did not find that this covariate was frequently selected over more traditional hydrodynamic covariates such as eddy kinetic energy. Perhaps this results from using the FSLE covariate as-is, and instead we should formulate a “distance to FLSE front” index. This remains a topic for future research.
- We replaced the NOAA NCDC 1/4° Blended Sea Winds covariates with a newer product, the Cross-Calibrated Multi-Platform (CCMP) Wind Vector Analysis Version 2, produced by Remote Sensing Systems (RSS) (<http://www.remss.com/measurements/ccmp.html>). The CCMP v2 product integrates more data, uses a more recent algorithm, and extends beyond the temporal extent of the NOAA NCDC product used in Roberts et al. (2016a).
- We added another formulation of SST fronts (DistToSSTFront3) intended to capture distance to only the strongest fronts, such as the Gulf Stream wall or shelf break front.
- We discovered a temporal discontinuity in the SEAPODYM epipelagic micronekton biomass and productivity time series that necessitated removing these two covariates from the list of candidate contemporaneous covariates. In short, values in recent years were extremely high relative to historical years; this appeared to correspond to a change in the SEAPODYM algorithm that we were not aware of. In the future, we will consult the SEAPODYM team to see if it is possible to cross-calibrate the two algorithms. Until then, SEAPODYM epipelagic micronekton remains usable only as a climatological covariate. In this formulation, we tested as candidate covariates the climatological means of both algorithms independently, in case one or the other performed better.

4.2.2. Beaked whale models

In the Phase III EC regional models (Roberts et al. 2016a) the majority of beaked whale sightings reported in the EC region were of unidentified beaked whales (Table 3). Collaborators who were experts for these species agreed that these were likely to be either Cuvier’s beaked whale (*Ziphius cavirostris*) or one of the *Mesoplodon* species, but unlikely to be northern bottlenose whale (*Hyperoodon ampullatus*), which was easier to distinguish from the others.

For the AMAPPS surveys, NMFS NEFSC and SEFSC undertook a concerted effort to boost the taxonomic precision of beaked whale sightings relative to prior surveys (D. Palka, pers. comm.). Separately, the University of North Carolina, Wilmington (UNCW) team led by W. McLellan revisited all beaked whale sightings they collected since 2010 to try to fully identify them from photographs taken of each sighted group. These efforts resulted in a large increase in sightings identified to the genus or species level, relative to unidentified sightings, as compared to sightings reported by the surveys available for the original Phase III models (Table 3, Fig. 19).

This raised the possibility of fitting species or genus-specific models, which we investigated. Unfortunately the high overlap in habitats between the *Z. cavirostris* and the *Mesoplodon* species ruled out the nontrivial use of a habitat-based classification model. Another limiting factor was that most of the *Mesoplodon* sightings were not resolved to the species (e.g. “unidentified *Mesoplodon*”), which ruled out species-specific *Mesoplodon* models. Finally, there were still enough completely ambiguous sightings (“unidentified beaked whale”) that we could not simply ignore them without biasing composite density of beaked whales low by an unknown but substantial factor.

We discussed these limitations with collaborators and the Navy and all parties agreed that the best alternative for improving the taxonomic precision of beaked whale density estimates was to split beaked whales into three models: a Cuvier’s beaked whale model built from the fully resolved *Z. cavirostris* sightings, a *Mesoplodonts* guild model built from the *Mesoplodon* sightings (both fully resolved and unidentified *Mesoplodonts*), and an unidentified beaked whales model built from the “unidentified beaked whales” sightings. The Navy agreed that this breakdown would be useful for environmental compliance—specifically that the “unidentified beaked whales” model would not cause onerous compliance problems. We present these models below.

Finally, all parties agreed that it was not necessary to build another northern bottlenose whale model at this time, as no new sightings were reported. In principle, if we were to rebuild the Phase III model, abundance and density would decrease, as the added surveys represent additional effort for which no new northern bottlenose whales were sighted. The bottlenose whale model will likely be updated in a future Option Year, subject to Navy priorities.

Table 3. Summary of beaked whale sightings available for new models. “Extant” sightings were used in the Phase III regional models (Roberts et al. 2016a). “Added” sightings were incorporated during the Base Year and Option Year 1 for the updated models.

Platform	Provider	Program	Mesoplodon			Ziphius			Hyperoodon			Unidentified		
			Extant	Added	Total	Extant	Added	Total	Extant	Added	Total	Extant	Added	Total
Aerial	NEFSC	Marine mammal abundance surveys					1	1	1		1	15	7	22
		NARWSS right whale surveys										7		7
	UNCW	SEFSC Marine mammal abundance surveys				1	2	3						
		Cape Hatteras Navy Surveys	20	11	31	19	31	50						
		Norfolk Canyon Navy Surveys			2		1	1						
		Onslow Bay Navy Surveys	3		3									
	Right whale surveys, 2005-2008										2		2	
All			23	13	36	20	35	55	1	1	24	7	31	
Shipboard	NEFSC	Marine mammal abundance surveys	19	71	90	26	80	106	4		4	83	49	132
	SEFSC	Marine mammal abundance surveys	14	15	29	2	7	9				16	15	31
	All		33	86	119	28	87	115	4	4	99	64	163	

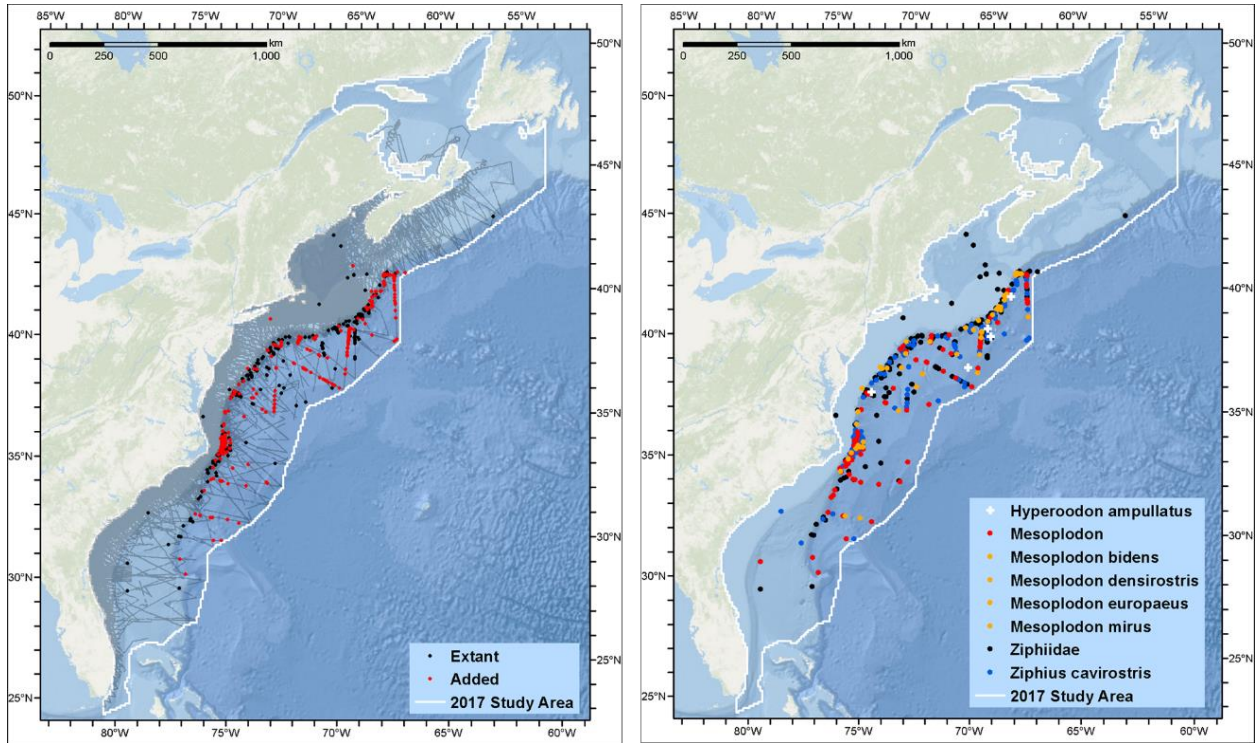


Figure 19. Left: beaked whale sightings used in the original Phase III models (black) and added for the new models (red), with survey tracklines. Right: the same sightings classified by genus, showing high overlap between *Ziphius cavirostris* and the *Mesoplodon* species.

4.2.2.1. $g(0)$ estimates

In the Phase III models, with so many unidentified beaked whales, we based $g(0)$ estimates on *Ziphius cavirostris* estimates from Barlow (1999) as a precautionary measure, with it being lower than the estimate for *Mesoplodon* species. In the updated models, having a relatively large number of sightings identified to the genus, we switched to genus-specific estimates from Barlow (1999) and used the simple mean between the two for unidentified beaked whales (Table 4).

Table 4. Beaked whale $g(0)$ estimates.

Platform	Surveys	Taxa	$g(0)$	Biases Addressed	Notes
Shipboard	AJ 98-01, 98-02	All	0.46	Perception	Survey specific $g(0)$ from Palka (2006)
Shipboard	EN 04-395	All	0.31	Perception	Survey specific $g(0)$ from Palka (2006)
Shipboard	All others	<i>Ziphius cavirostris</i>	0.23	Both	From Barlow (1999) simulations
		<i>Mesoplodon</i> spp.	0.45	Both	From Barlow (1999) simulations
		Unidentified	0.34	Both	Simple mean of two above
Aerial	All	<i>Ziphius cavirostris</i>	0.074	Both	Est. from dive data in Barlow (1999)
		<i>Mesoplodon</i> spp.	0.116	Both	Est. from dive data in Barlow (1999)
		Unidentified	0.095	Both	Simple mean of two above

4.2.2.2. *Cuvier's beaked whale (Ziphius cavirostris) model*

As with the original Phase III beaked whales guild model, we split the study area at the shelf break, represented by the 125m isobath, under the presumption that beaked whales—deep diving squid specialists—over the shelf would exhibit different species-environment relationships than those over the slope and abyss, their primary habitats. We fitted a stratified model to the sightings over the shelf and a habitat-based spatial model to the sightings over the slope and abyss (Figs. 20, 21).

Multiple lines of evidence, including passive acoustic monitoring (Stanistreet et al. 2017) and telemetry (A. Read, unpublished data), suggest that beaked whales do not undertake large seasonal movements like cetaceans such as baleen whales. Additionally, multiple years of surveying at Cape Hatteras reported sightings of Cuvier's beaked whales in all seasons. Finally, the model selection procedure selected dynamic covariates relating to fronts and eddies that remain relatively stable throughout the year. Reflecting this stability, monthly predictions did not exhibit much variation from month to month. Given that, and lacking external evidence for strong seasonality, we elected to provide a year-round mean density surface for Cuvier's beaked whale for use in the NMSDD, as we did with the original Phase III beaked whales guild model (Roberts et al. 2016a), rather than monthly density surfaces. For similar reasons, we also provided year-round density surfaces for *Mesoplodont* beaked whales and unidentified beaked whales, discussed below.

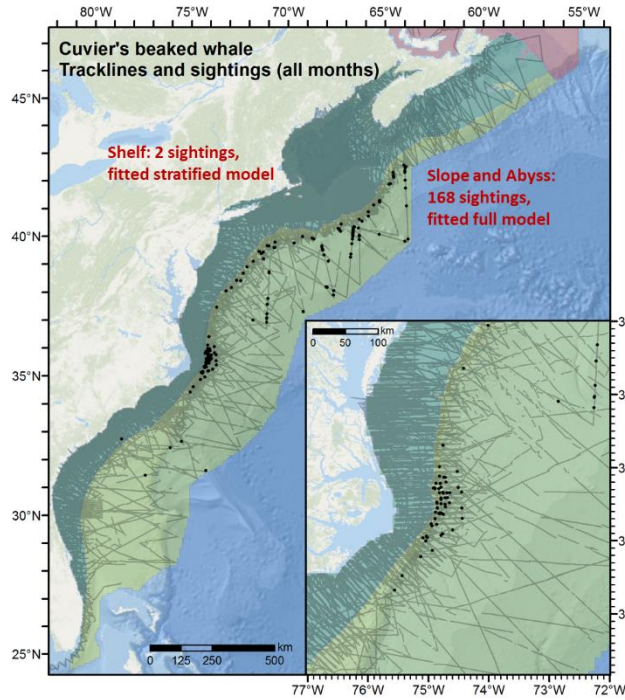
4.2.2.3. *Mesoplodont beaked whales model*

We configured the *Mesoplodont* beaked whales model similar to the Cuvier's beaked whale model and obtained similar results (Figs. 22, 23). The resulting model for the slope and abyss habitat was similar; several static covariates were retained during model selection, as well as total kinetic energy (TKE), a relatively stable covariate probably used by the model to capture high density along the slope just south of Cape Hatteras, where the Gulf Stream departs the continental shelf. Predicted abundance was slightly lower than for Cuvier's beaked whale and the spatial distribution was slightly more southerly.

4.2.2.4. *Unidentified beaked whales model*

We configured the unidentified beaked whales model similar to the Cuvier's and *Mesoplodont* beaked whales models and obtained similar results (Figs. 24, 25). The resulting model for the slope and abyss habitat was similar, as it identified habitats that beaked whales are known to associate with, including the continental slope, submarine canyons, and seamounts. However, the model displayed an interesting negative correlation with TKE (term plot, Fig. 24), which manifested as a band of very low density predicted within the Gulf Stream (Fig. 25), an oceanographic feature exhibiting very high TKE. In contrast, the Cuvier's and *Mesoplodont* models showed a positive correlation with TKE.

Our interpretation is that the unidentified beaked whales model reflects spatial patterns in two processes: the distribution of beaked whales according to their habitat preferences, but also the probability that a beaked whale sighting will be fully identified. Nearly all of the sightings of beaked whales near Cape Hatteras, an area of high TKE, were reported by UNCW, which undertook a focused, multi-year effort specifically designed to document all beaked whale sightings sufficiently to allow full identification. This likely resulted in a dearth of “unidentified beaked whale” sightings near Cape Hatteras, where the Gulf Stream separates from the continental shelf. Farther from the shelf, the Gulf Stream passes through an area where fewer beaked whales were sighted, but NMFS successfully identified them to the genus or species and reported no “unidentified beaked whale” groups. Reflecting these patterns of very few unidentified beaked whales in the Gulf Stream, the model selected a covariate, TKE, associated with this habitat. Thus we suspect the apparent absence of unidentified beaked whales in the Gulf Stream reflects a pattern in beaked whale identification efficiency, rather than an aversion of beaked whales to this habitat.



Slope and Abyss

```

Family: Tweedie(n=1.296)
Link function: log
Formula:
Abundance ~ offset(log(Area)) + s(log10(Depth), bs = "ts") +
s(log10(Slope), bs = "ts") + s((ClimDistToSTFront2*(1/3)),
bs = "ts") + s((ClimDistToAEddy9/1000), bs = "ts") +
s((ClimDistToEddy9/1000), bs = "ts")
Parametric coefficients:
Estimate Std. Error t value Pr(>|t|)
(Intercept) -8.0029 0.5391 -13.58 <2e-16 ***
Approximate significance of smooth terms:
edf Ref.df F p-value
s(log10(Depth)) 3.4576 9 6.218 4.77e-14 ***
s(log10(Slope)) 1.0384 9 3.208 2.73e-08 ***
s((ClimDistToSTFront2*(1/3))) 1.0299 9 2.773 2.50e-07 ***
s((ClimDistToAEddy9/1000)) 4.2161 9 1.954 0.000668 ***
s((ClimDistToEddy9/1000)) 0.9127 9 0.868 0.002599 **
---
Signif. codes: 0 '***' 0.001 '**' 0.01 '*' 0.05 '.' 0.1 ' ' 1
R-sq (adj) = 0.0108 Deviance explained = 39.5%
REML = 1353.3 Scale est. = 79.403 n = 25822

```

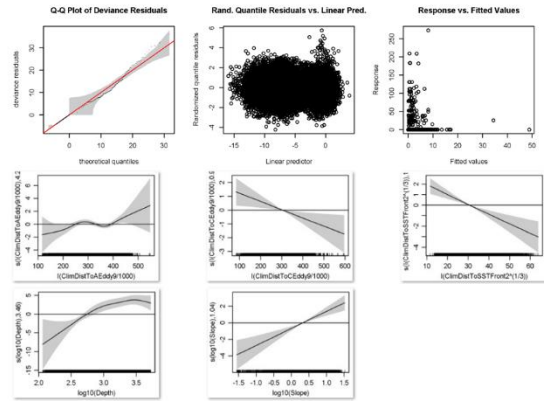


Figure 20. Left: Cuvier's beaked whale model schematic. Right: spatial model selected as best.

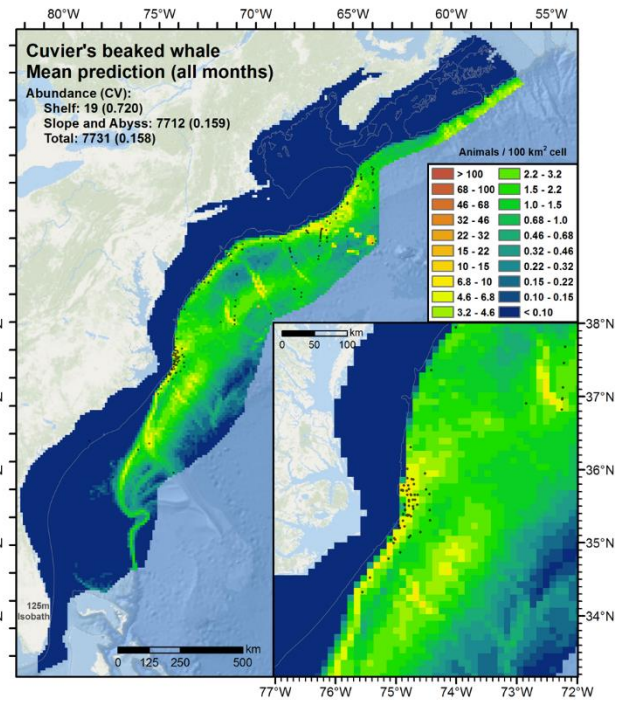
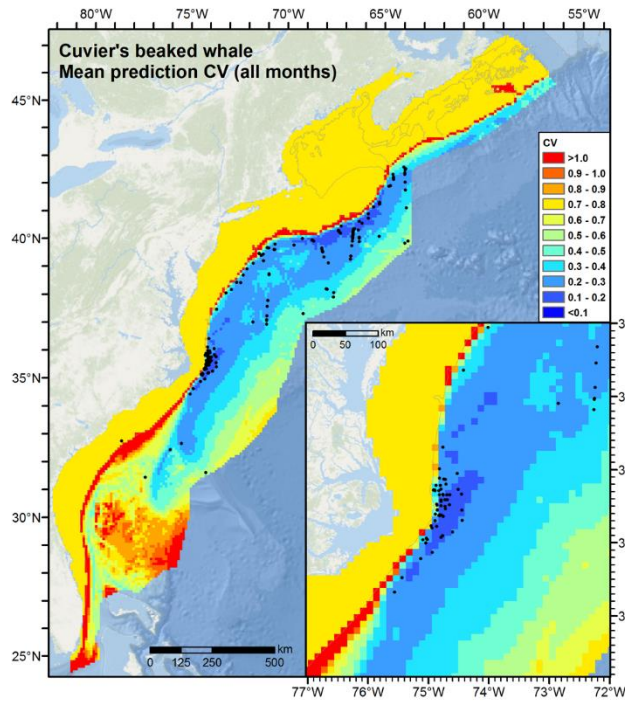
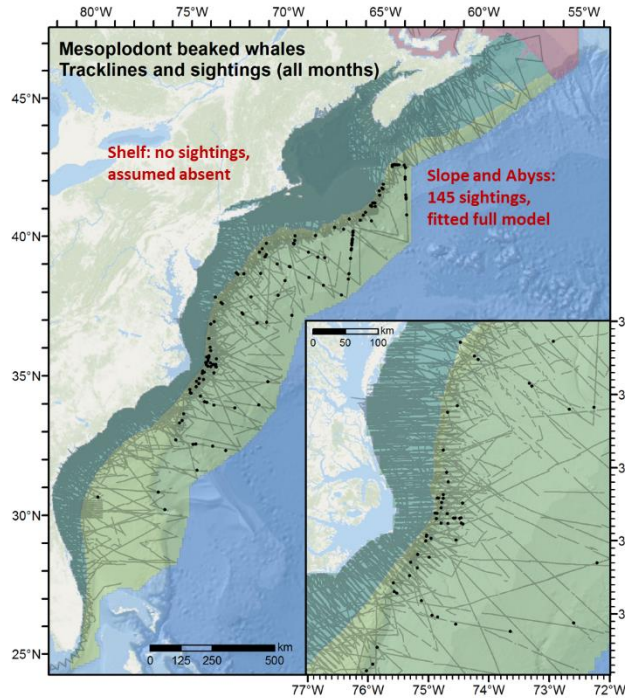


Figure 21. Left: Predicted mean coefficient of variation (CV) for Cuvier's beaked whale, with sightings overlaid. Right: Predicted mean density and total abundance for Cuvier's beaked whale.



Slope and Abyss

```

Family: Tweedie(p=1.43)
Link function: log
Formula:
Abundance ~ offset(log(Area)) + s(log10(Depth), bs = "ts") +
s(log10(Slope), bs = "ts") + s(I(DistTo1500m/1000), bs = "ts") +
s(log10(pmax(ClimTKE, 1e-04)), bs = "ts")
Parametric coefficients:
              Estimate Std. Error t value Pr(>|t|)
(Intercept)  -7.4864    0.3998  -18.73  <2e-16 ***
Approximate significance of smooth terms:
              edf Ref.df  F  p-value
s(log10(Depth))    2.919    9 4.275 6.90e-11 ***
s(log10(Slope))    1.022    9 2.745 1.19e-07 ***
s(I(DistTo1500m/1000)) 2.395    9 1.230 0.00173 **
s(log10(pmax(ClimTKE, 1e-04))) 1.799    9 1.706 9.81e-05 ***
Signif. codes:  0 '***' 0.001 '**' 0.01 '*' 0.05 '.' 0.1 ' ' 1
R-sq.(adj)  = -0.00837  Deviance explained = 35.7%
-REML      = 1303.1    Scale est. = 106.07    n = 25835

```

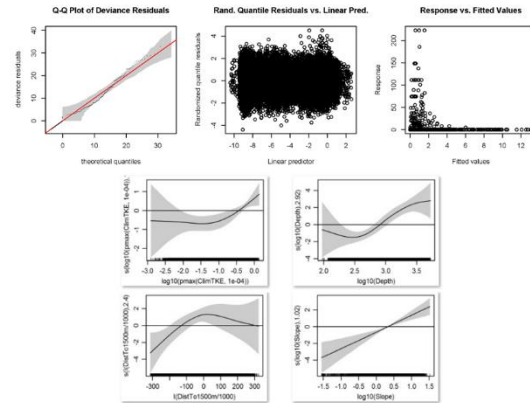


Figure 22. Left: *Mesoplodont* beaked whale model schematic. Right: spatial model selected as best.

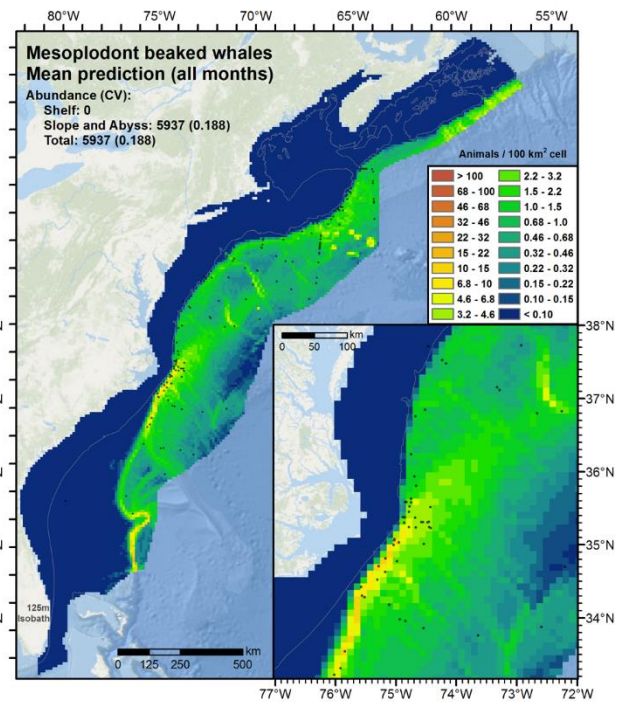
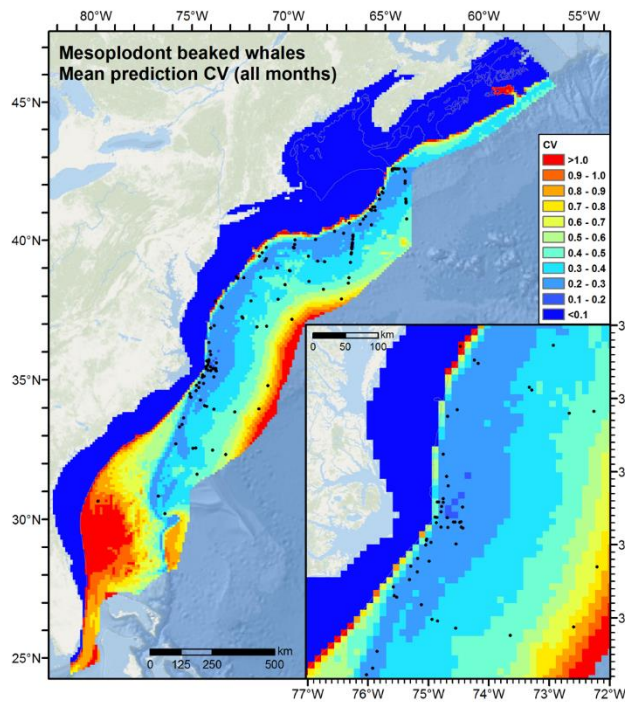
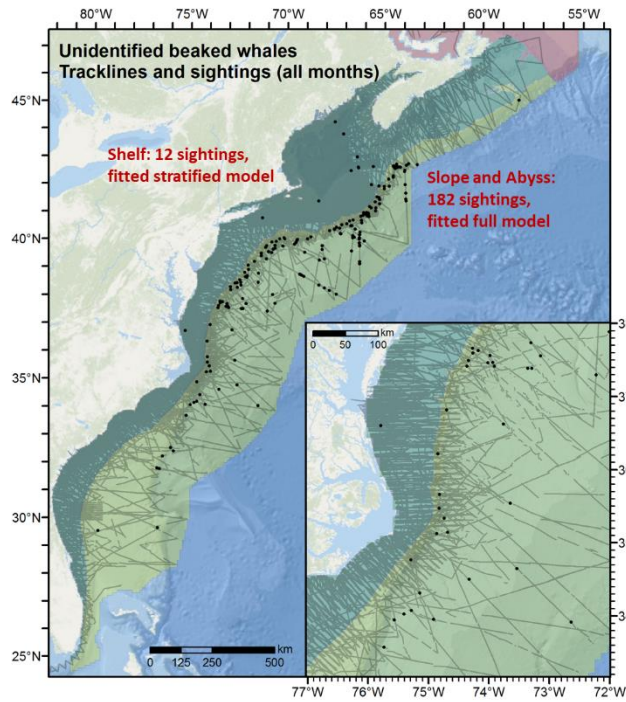


Figure 23. Left: Predicted mean coefficient of variation (CV) for *Mesoplodont* beaked whales, with sightings overlaid. Right: Predicted mean density and total abundance for *Mesoplodont* beaked whales.



Slope and Abyss

Family: Tweedie(n=1.395)
 Link function: log
 Formula:
 $Abundance \sim offset(\log(Area)) + s(\log_{10}(Depth), bs = "ts") + s(\log_{10}(Slope), bs = "ts") + s(\text{ClimDistToSSTFront}^2(1/3)), bs = "ts") + s(\log_{10}(\text{pmax}(\text{ClimTKE}, 1e-04)), bs = "ts")$
 Parametric coefficients:
 Estimate Std. Error t value Pr(>|t|)
 (Intercept) -8.5606 0.22761 -31 <2e-16 ***
 Approximate significance of smooth terms:

	edf	Ref.df	F	p-value
s(log10(Depth))	3.5359	9	7.290	2.24e-16 ***
s(log10(Slope))	0.9442	9	1.115	0.000766 ***
s(ClimDistToSSTFront^2(1/3))	0.8643	9	0.638	0.001101 **
s(1(ClimDistToSSTFront^2(1/3)))	2.6014	9	1.350	0.001627 **
s(log10(pmax(ClimTKE, 1e-04)))	1.3163	9	12.252	< 2e-16 ***

 Signif. codes: 0 '***' 0.001 '**' 0.01 '*' 0.05 '.' 0.1 ' ' 1
 R-sq. (adj) = 0.00465 Deviance explained = 49.4%
 REML = 1317.5 Scale est. = 42.732 n = 25822

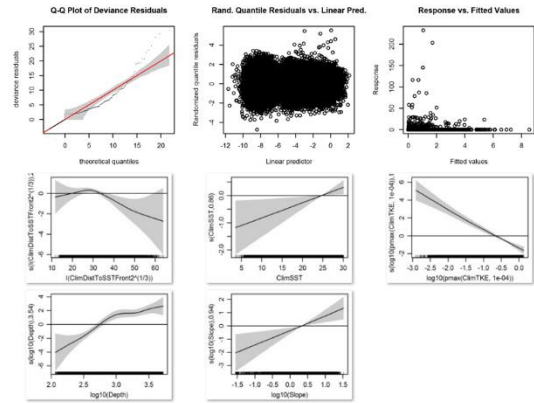


Figure 24. Left: Unidentified beaked whale model schematic. Right: spatial model selected as best.

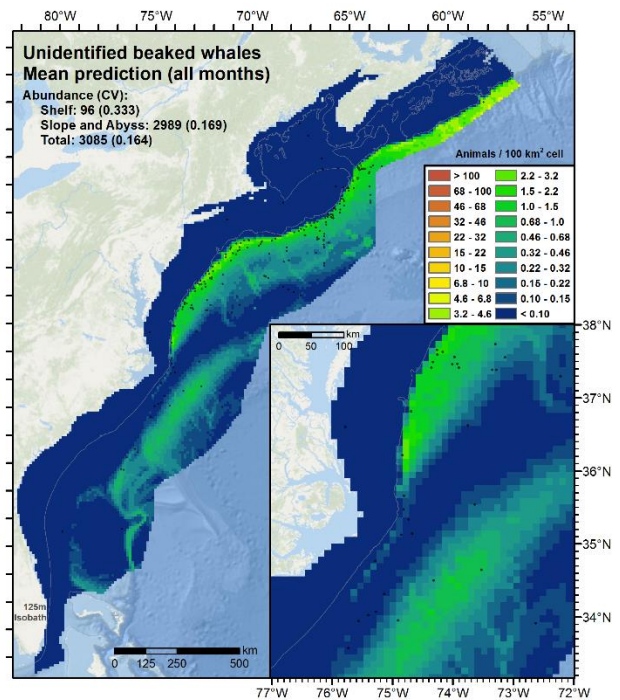
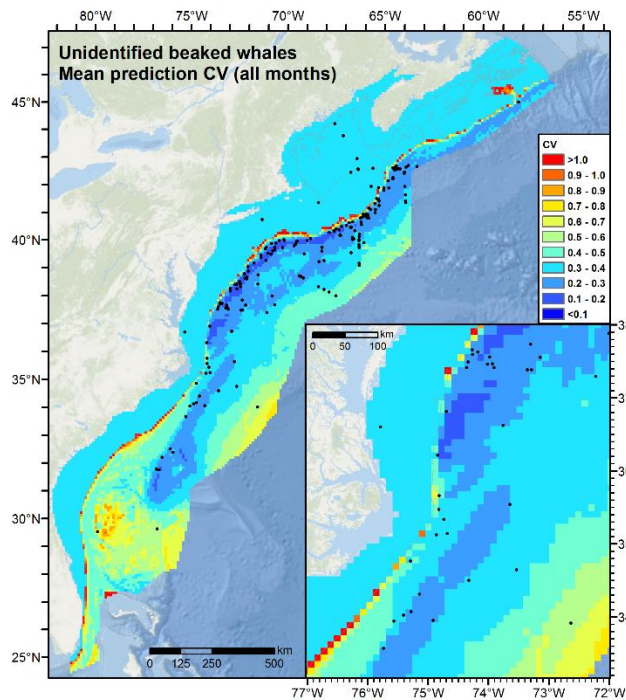


Figure 25. Left: Predicted mean coefficient of variation (CV) for unidentified beaked whales, with sightings overlaid. Right: Predicted mean density and total abundance for unidentified beaked whales.

4.2.2.5. Total abundance comparison

In aggregate, the three new beaked whales models predicted high density in similar locations (e.g. off-shelf waters along the continental slope and near submarine canyons and seamounts) as the Phase III “beaked whales” guild model. The total mean abundance predicted by the new models was about 12% higher than the Phase III model and about 23% higher than the latest NMFS Stock Assessment Reports (SARs). However, the SARs’ study area was smaller (central Florida to lower Bay of Fundy) and the methodology used for the SARs did not account for availability bias due to diving. Finally, the SARs did not provide an explicit abundance estimate for unidentified beaked whales, and it is unclear whether they were accounted for in the other two estimates (e.g. by proration) or ignored.

Table 5. Comparison of beaked whale mean total abundance (with CV) estimated by the initial Phase III model (Roberts et al. 2016a), the new models presented here, and the latest NMFS Stock Assessment Reports (SARs). Note that the CV estimates in Roberts et al. (2016a) and the new models are biased low because current statistical methods only allow them to account for uncertainty in the GAM parameter estimates. They do not include known uncertainty in $g(0)$ estimates and detection functions.

Taxon	Roberts et al. (2016a)	New models	Latest SARs
<i>Ziphius Cavirostris</i>	N/A	7,731 (0.16)	6,532 (0.32)
Mesoplodonts	N/A	5,937 (0.19)	7,092 (0.54)
Unidentified	N/A	3,085 (0.16)	NA
Total	14,491 (0.17)	16,753 (0.10)	13,624 (0.32)

4.2.3. Pilot whales model

In the initial Phase III analysis (Roberts et al. 2016a) the majority of pilot whale sightings reported in the EC region were of “unidentified pilot whale”. This trend continued with the surveys added during the Base Year and Option Year 1 (Table 6). As discussed in section 4.1 above, we investigated the possibility of classifying these into one species or the other but ultimately modeled them as a two-species guild, as was done with the original Phase III EC model.

For the updated pilot whales model we used the same $g(0)$ estimates as the Phase III model (Table 7); please see the supplementary report for the pilot whales model in Roberts et al. (2016a) for a detailed discussion.

In the Phase III model we split the study area at the shelf break under an assumption similar to that we made with beaked whales, that pilot whale foraging behavior would be different on and off the shelf, leading to different and possibly confounding species-environment relationships in the two habitats. When we tried that approach with the new data, it led to extreme winter extrapolations along the continental slope in the northern part of the study area. After trying several different model formulations, we solved this problem by eliminating the habitat split at the shelf break and fitting one model to all data (Fig. 26). The resulting model was complex, retaining 10 covariates, but the relationships expressed in the term plots made sense, and given the differing but partially overlapping habitats of the two species, a complex model is not unreasonable. The predicted density surface (Fig. 27) showed highest densities along the slope from Cape Hatteras north and near submarine canyons, known to be pilot whale habitats. Total predicted abundance was higher than in the Phase III model but much closer to the aggregate short-finned + long-finned abundance published in current NOAA Stock Assessment Reports.

Seasonal behavior of pilot whales remains relatively unknown. Telemetry of short-finned pilot whales tagged near Cape Hatteras revealed that some pilot whales maintained a relatively constrained range near the tagging location while others ranged far into the Gulf Stream, sometimes in relation to geostrophic eddies (A. Read, pers. comm.). To date, no long-finned pilot whales have been similarly tagged (A. Read, pers. comm.). In light of this lack of knowledge, we elected to provide a year-round mean density surface for pilot whales for use in the NMSDD, as we did with the original Phase III model (Roberts et al. 2016a).

Table 6. Summary of pilot whale sightings available for the updated model. “Extant” sightings were used in the Phase III regional models (Roberts et al. 2016a). “Added” sightings were incorporated during the Base Year and Option Year 1 for the updated models.

Platform	Provider	Program	G. macrorhynchus			G. melas			Unidentified		
			Extant	Added	Total	Extant	Added	Total	Extant	Added	Total
Aerial	NEFSC	Marine mammal abundance surveys							171	17	188
		NARWSS harbor porpoise survey							2		2
		NARWSS right whale surveys							433	116	549
	SEFSC	Marine mammal abundance surveys							38	38	
	UNCW	Cape Hatteras Navy Surveys	65	76	141						
		Jacksonville Navy Surveys	12	3	15						
		Norfolk Canyon Navy Surveys		35	35						
		Onslow Bay Navy Surveys	8		8						
	Right whale surveys, 2005-2008	3		3							
	All	88	114	202				606	171	777	
Shipboard	NEFSC	Marine mammal abundance surveys		3	3		2	2	98	150	248
	SEFSC	Marine mammal abundance surveys							91	94	185
	All			3	3		2	2	189	244	433

Table 7. $g(0)$ estimates used in the updated pilot whales model. These are the same as in Roberts et al. (2016a).

Platform	Surveys	Group Size	$g(0)$	Biases Addressed	Source
Shipboard	All	Any	0.585	Perception	Palka (2006)
Shipboard	NEFSC Abel-J Binocular Surveys	Any	0.50	Perception	Palka (2006)
Shipboard	NEFSC Endeavor	Any	0.67	Perception	Palka (2006)
Aerial	All	Any	0.607	Availability	Various

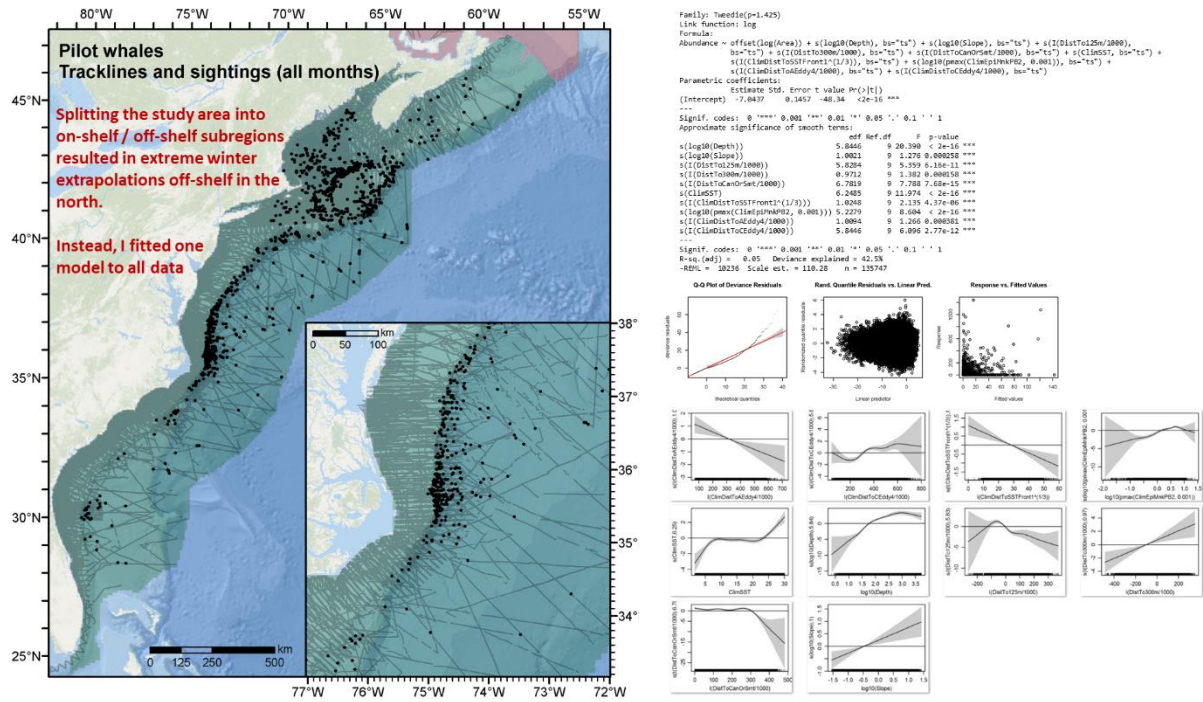


Figure 26. Left: Pilot whales model schematic. Right: spatial model selected as best.

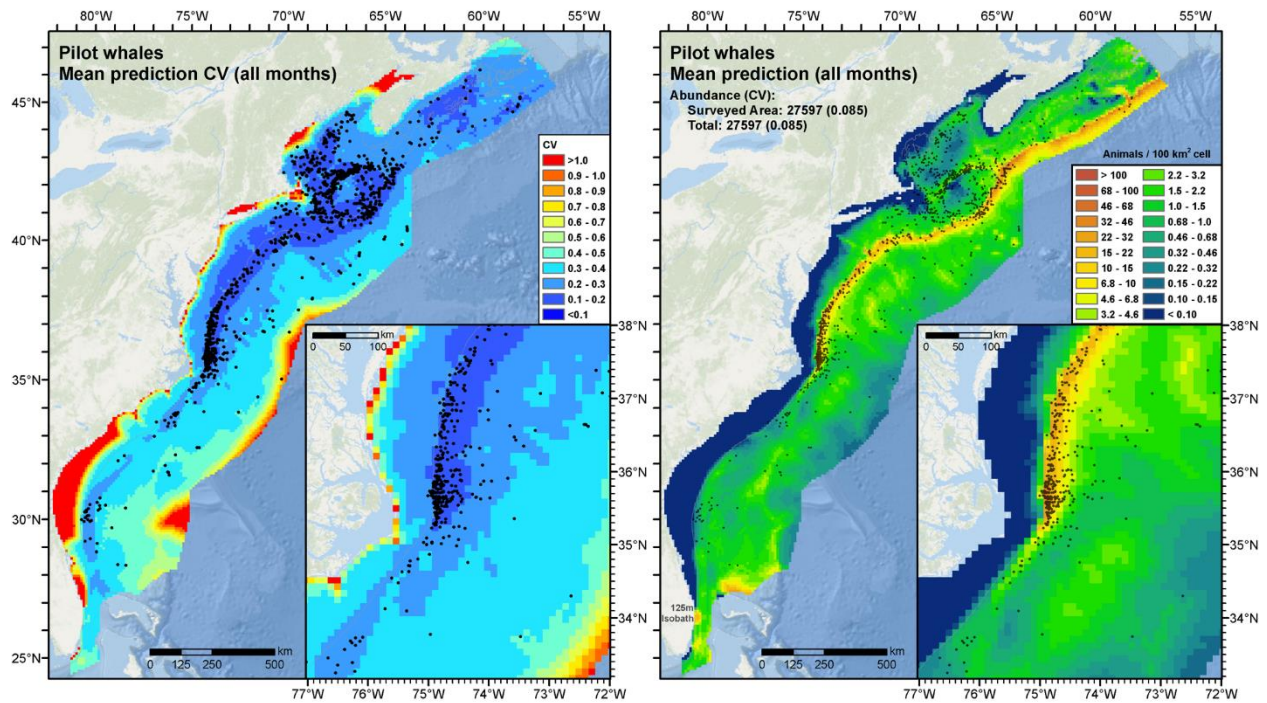


Figure 27. Left: Predicted mean coefficient of variation (CV) for pilot whales, with sightings overlaid. Right: Predicted mean density and total abundance for pilot whales.

4.2.4. Sperm whale model

For the updated sperm whale model we used the same $g(0)$ estimates as the Phase III model (Table 9); please see the supplementary report for the sperm whale model in Roberts et al. (2016a) for a detailed discussion.

Surveys of the shelf break and offshore habitat by AMAPPS and other programs contributed a large number of additional sightings of sperm whales (Table 8). We split the study area at the shelf break (Fig. 28) under an assumption similar to that we made with beaked whales, that sperm whale foraging behavior would be different on and off the shelf, leading to different and possibly confounding species-environment relationships in the two habitats. Unlike with beaked whales, for sperm whales there were sufficient sightings to fit habitat-based models to both subregions.

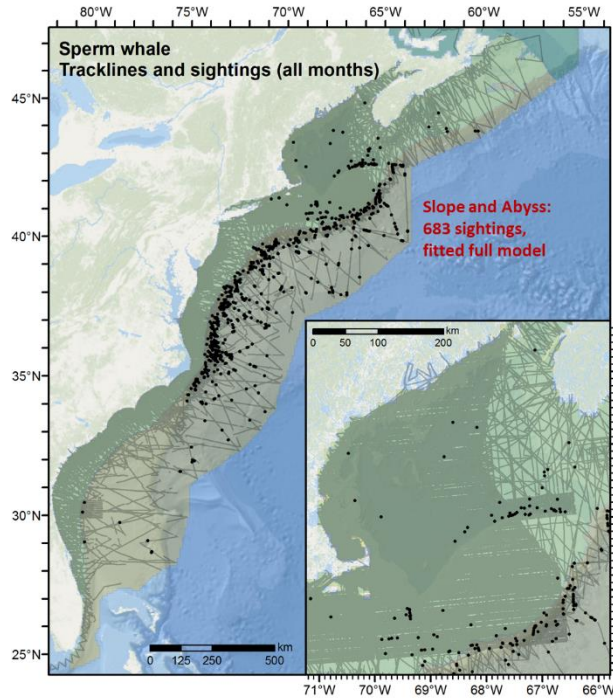
In the slope and abyss subregion, where most sperm whales were sighted, the selected model retained static and physical oceanographic covariates consistent with known sperm whale habitat associations, e.g. close to canyons, seamounts and sea surface temperature fronts (Fig. 28). Interestingly, the model discarded all biological covariates and retained sea surface temperature as the most temporally dynamic covariate. In the shelf subregion, the selected model was simpler, with fewer covariates and more linear fits, indicating high density in deep, high-slope areas close to canyons along the continental slope and the seamounts just beyond, with lower eddy kinetic energy but higher primary productivity (Fig. 29). These relationships are logical. In this subregion, primary productivity was the primary seasonal driver of the model.

Table 8. Summary of sperm whale sightings available for the updated model. “Extant” sightings were used in the Phase III regional models (Roberts et al. 2016a). “Added” sightings were incorporated during the Base Year and Option Year 1 for the updated models.

Platform	Provider	Program	Sperm whale		
			Extant	Added	Total
Aerial	NEFSC	Marine mammal abundance surveys	24	9	33
		NARWSS right whale surveys	77	12	89
	SEFSC	Marine mammal abundance surveys		8	8
	UNCW	Cape Hatteras Navy Surveys	19	8	27
		Jacksonville Navy Surveys	1	1	2
		Marine mammal surveys, 2002	1		1
		Norfolk Canyon Navy Surveys		8	8
		Right whale surveys, 2005-2008	8		8
	All	130	46	176	
Shipboard	NEFSC	Marine mammal abundance surveys	245	140	385
	SEFSC	Marine mammal abundance surveys	137	100	237
	All		382	240	622

Table 9. $g(0)$ estimates used in the updated sperm whale model. These are the same as in Roberts et al. (2016a).

Platform	Surveys	Group Size	$g(0)$	Biases	Source
				Addressed	
Shipboard	All	Any	0.53	Both	Barlow and Sexton (1996)
Shipboard	NEFSC Abel-J Binocular Surveys	Any	0.28	Perception	Palka (2006)
Shipboard	NEFSC Endeavor	Any	0.46	Perception	Palka (2006)
Aerial	All	Any	0.172	Availability	Watwood et al. (2006)



Slope and Abyss

```

Family: Tweedie(p=1.288)
Link function: log
Formula:
Abundance ~ offset(log(Area)) + s(log10(Depth), bs = "ts") +
s((DistTo125m/1000), bs = "ts") + s((DistToCanOrSmr/1000), bs = "ts") +
s((ClimSST), bs = "ts") + s((ClimDistToSSTFront3*(1/3)), bs = "ts") +
s((ClimDistToEddy9/1000), bs = "ts") + s((ClimDistToEddy9/1000), bs = "ts")
Parametric coefficients:
              Estimate Std. Error t value Pr(>|t|)
(Intercept) -7.8014      0.1589  -46.41  <2e-16 ***
Approximate significance of smooth terms:
              edf Ref.df    F    p-value
s(log10(Depth))      4.542      9  4.967 2.22e-08 ***
s((DistTo125m/1000)) 3.841      9  2.381 1.69e-05 ***
s((DistToCanOrSmr/1000)) 1.298      9 10.382 < 2e-16 ***
s((ClimSST))          3.393      9  3.321 1.73e-07 ***
s((ClimDistToSSTFront3*(1/3))) 3.127      9  3.546 1.59e-08 ***
s((ClimDistToEddy9/1000)) 3.104      9  1.564 0.000944 ***
s((ClimDistToEddy9/1000)) 6.570      9 18.179 < 2e-16 ***
---
Signif. codes:  0 '***' 0.001 '**' 0.01 '*' 0.05 '.' 0.1 ' ' 1
R-sq.(adj)  = 0.0649  Deviance explained = 42.5%
-RHL = 3574.8  Scale est. = 22.28  n = 25922

```

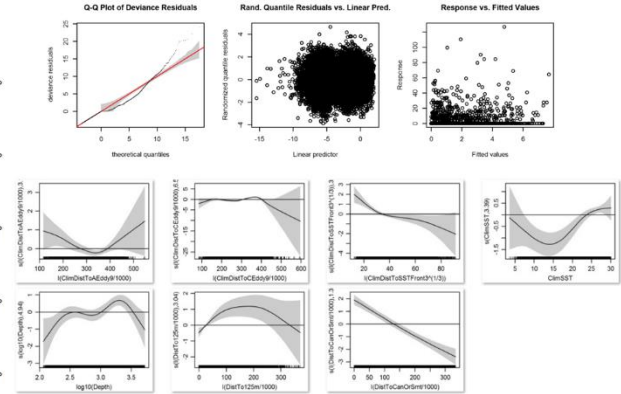
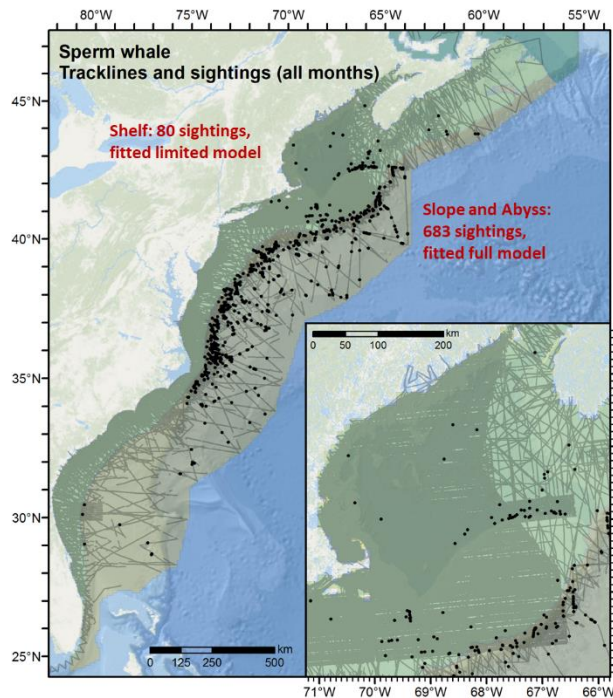


Figure 28. Left: Sperm whale model schematic. Right: spatial model that was selected as best for the Slope and Abyss region.



Shelf

```

Family: Tweedie(p=1.162)
Link function: log
Formula:
Abundance ~ offset(log(Area)) + s(log10(Depth), bs = "ts") +
s(log10(Slope), bs = "ts") + s((DistToCanOrSmr/1000), bs = "ts") +
s(log10(pmax(ClimEKE, 1e-04)), bs = "ts") + s((ClimCumVGP45*(1/3)), bs = "ts")
Parametric coefficients:
              Estimate Std. Error t value Pr(>|t|)
(Intercept) -11.8506      0.3905  -30.35  <2e-16 ***
Approximate significance of smooth terms:
              edf Ref.df    F    p-value
s(log10(Depth))      1.2666      9  5.965 1.08e-14 ***
s(log10(Slope))       0.9241      9  0.872 0.00266 **
s((DistToCanOrSmr/1000)) 1.3015      9  9.837 < 2e-16 ***
s(log10(pmax(ClimEKE, 1e-04))) 1.8496      9  1.390 1.03e-05 ***
s((ClimCumVGP45*(1/3))) 4.7390      9  7.396 1.95e-15 ***
---
Signif. codes:  0 '***' 0.001 '**' 0.01 '*' 0.05 '.' 0.1 ' ' 1
R-sq.(adj)  = 0.0025  Deviance explained = 32.8%
-RHL = 745.33  Scale est. = 28.098  n = 113184

```

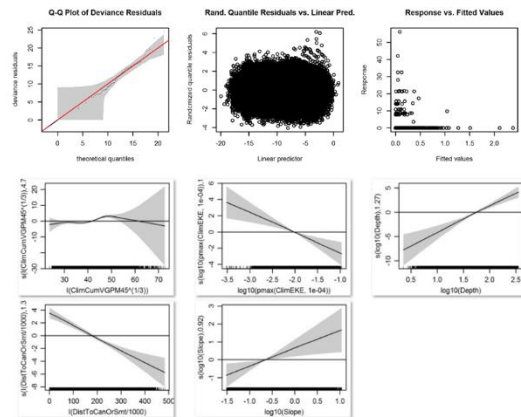


Figure 29. Left: Sperm whale model schematic. Right: spatial model that was selected as best for the Shelf region.

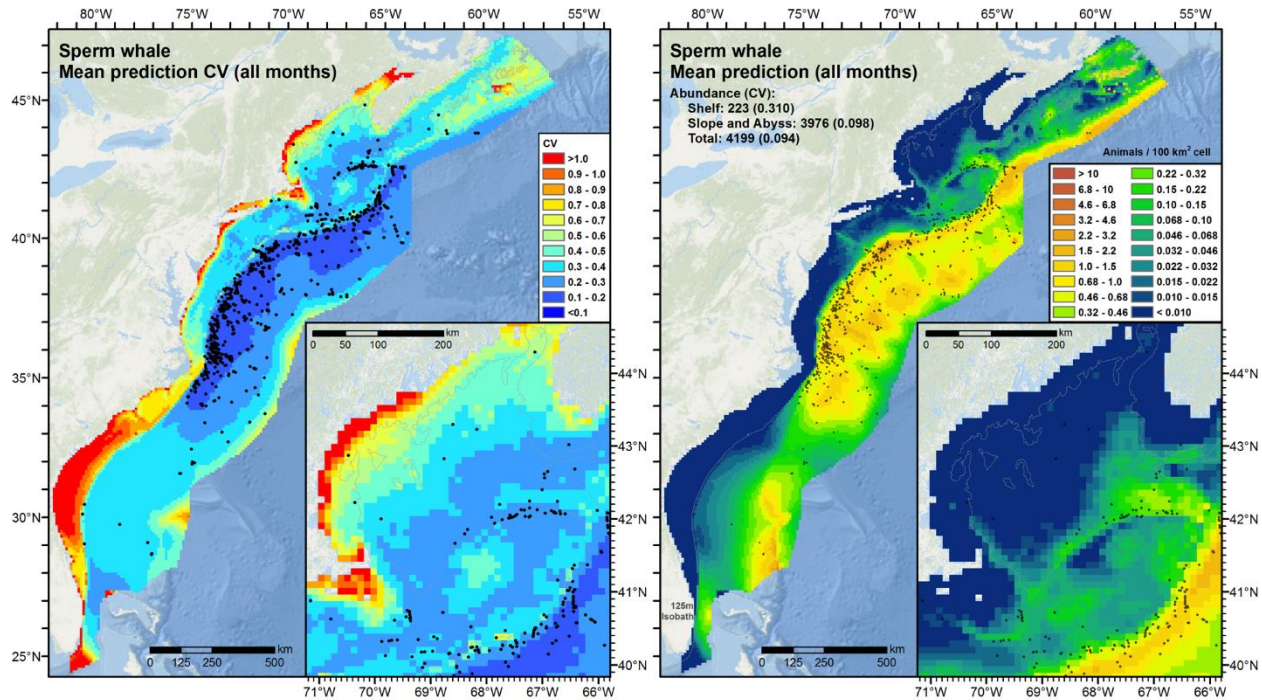


Figure 30. Left: Predicted mean coefficient of variation (CV) for sperm whale, with sightings overlaid. Right: Predicted mean density and total abundance predictions for sperm whale.

Mean predicted sperm whale density and abundance (Fig. 30) displayed a similar spatial pattern to the Phase III model but were roughly 20% lower than in the Phase III model. Coefficients of variation (CVs) were also lower in the slope and abyss subregion, where most sperm whales were sighted. At present, we have no reason to doubt either model, despite the 20% difference. The updated model incorporated several new shipboard surveys that together boosted total shipboard effort by nearly 50% (Table 2) and the total number of shipboard sperm whale sightings by over 60% (Table 8), a large change. Additionally, we refitted all detection functions from scratch. Although the old and new mean abundance estimates are not within each other's 90% confidence intervals, the estimated CVs only account for uncertainty in the spatial model parameters. If the CVs included uncertainty in detection functions and $g(0)$ estimates, the confidence limits of each estimate would expand to enclose the other estimate, suggesting that there is not a statistically significant difference between them at a 90% confidence level.

The updated model displayed a similar high-in-summer, low-in-winter trend in abundance driven mainly by sea surface temperature, like the original Phase III model. As with the Phase III model, we believe this is consistent with published findings that suggest a seasonal pattern in sperm whale abundance. Accordingly, we elected to provide monthly density surfaces for sperm whales for use in the NMSDD, for the same reasons discussed in the supplementary species report provided with the original Phase III model (Roberts et al. 2016a).

4.2.5. Harbor porpoise model

Coming into Option Year 1, we had noted several ways in which we wanted to improve upon the Phase III harbor porpoise model. First, as discussed in Section **Error! Reference source not found.** (Validation of the EC Harbor Porpoise Model with Passive Acoustic Monitoring), predictions in May and October in the mid-Atlantic showed unrealistic low-high-low spikes in density in May-June-July and September-October-November. Acoustic monitoring (Wingfield et al. 2017) provided further evidence that these spikes were spurious temporal "edge effects" that occurred during the first and last months (June and October) of the summer seasonal model when it bordered the last and first months of the winter seasonal model (May and November). We addressed this problem by moving the summer-winter transition from October-November up to September-October. While that strategy did not work with the Phase III data alone, it eliminated the edge effect from the updated model when the new data were

added. We note that Palka et al.'s (1996) summary of harbor porpoise seasonality stated that it "begins migrating out [of the northern Gulf of Maine and lower Bay of Fundy region] during September".

Second, the acoustic monitoring also suggested nearshore density predictions in the mid-Atlantic might be too low, relative to mid-shelf density predictions. We re-examined all data and covariates that we suspected could lead to this prediction and discovered a potential flaw in how we handled the NJ-DEP shipboard surveys in the Phase III models. The shipboard data provided to us by NJ-DEP was missing Beaufort sea state observations for the survey tracklines. Our harbor porpoise model was designed to utilize survey segments collected in Beaufort 2 or less, a common practice when modeling harbor porpoises (e.g., Hammond et al. (2013)) owing to the substantial difficulty in detecting them in rough seas. While the Phase III modeling procedure correctly discarded effort made in higher sea states by other surveys, it retained all of the NJ-DEP shipboard effort, because sea state was unknown.

In fall, winter, and spring in the mid-Atlantic, the ocean is windier and rougher than in summer and sea states of Beaufort 2 or less are rare. Thus most of the NJ-DEP shipboard effort from these seasons was likely Beaufort 3 or higher, and the relative lack of harbor porpoise sightings from the NJ-DEP shipboard surveys during these months was at least partially attributable to these high sea states. By failing to exclude segments of these nearshore surveys made in rough seas, we believed the Phase III models may have biased density low close to shore. To address this problem we first noted that the NJ-DEP shipboard *sightings* did include sea state estimates. We then examined each day of NJ-DEP shipboard effort and used sea state estimates from sightings made each day as a proxy for sea state on the effort segments. Finally, we excluded effort segments where sightings suggested sea state was greater than 2 or where sea state was unknown (e.g. there were no sightings made that day).

Third, in Phase III, the spatial extent of winter predictions was based on a polygon that enclosed all survey segments conducted during the seasonal model's months (October-May), regardless of Beaufort sea state. What we did not consider in Phase III when delineating that polygon was that nearly all of the off-shelf segments occurred in sea states higher than 2, and therefore were dropped from the model. Thus the model was largely extrapolating in these offshore regions. In the updated models we sought to avoid this extrapolation and redefined the model subregion as waters shallower than 1500m (Fig. 31), based on how the effort reported in Beaufort 2 or less extended roughly to this depth along the shelf break during these months. This polygon does include a large area of the Blake Plateau unsurveyed at Beaufort 2 or less, but these depths were surveyed north of Cape Hatteras, and colleagues who are experts in this stock of harbor porpoises (A. Read and D. Palka) did not raise an objection to this polygon.

Finally, summer abundance in the Phase III model averaged 45,089 across the season (June-October) and peaked in July at 48,049 (CV=0.12). This was substantially lower than the NMFS Stock Assessment Report estimate of 79,883 (CV=0.32), although the July peak was within the 90% confidence interval of the NMFS estimate. The difference could have resulted from multiple factors. One may have related to our inclusion of surveys from UNCW and Virginia Aquarium & Marine Science Center (VAMSC) that were conducted at 1000 ft altitude from aircraft (Cessna Skymasters) that had flat windows and no belly port. After discussing this with colleagues, including W. McLellan, we concluded that it was less likely that harbor porpoises could be seen as easily from these surveys as on the NMFS surveys, which were conducted at 600-750 ft. from aircraft (de Havilland Twin Otters) that have bubble windows and belly port observers. (NARWSS surveys did not have belly port observers.) Although the UNCW and VAMSC surveys occurred mostly in the southeast and mid-Atlantic where harbor porpoise density is low in summer, we excluded them from the updated model to eliminate their negative bias on density.

The additional surveys incorporated after Phase III modeling added more than 600 harbor porpoise sightings (Table 10). Most of these were reported by NARWSS and NEFSC AMAPPS aerial surveys of the Gulf of Maine; sightings occurred here in all seasons. Of particular note were three sightings reported by SEFSC AMAPPS off Virginia and Maryland (Fig. 31). These are now the southernmost sightings of harbor porpoise in our collection of surveys; in the original Phase III analysis, the southernmost sightings were off New Jersey, reported by NJ-DEP.

For the updated harbor porpoise model we used the same $g(0)$ estimates as the Phase III model (Table 11). Please see the harbor porpoise supplementary report in Roberts et al. (2016a) for a detailed discussion.

Table 10. Summary of harbor porpoise sightings available for the updated model. “Extant” sightings were used in the Phase III regional models (Roberts et al. 2016a). “Added” sightings were incorporated during the Base Year and Option Year 1 for the updated models.

Platform	Provider	Program	Harbor porpoise		
			Extant	Added	Total
Aerial	NEFSC	Marine mammal abundance surveys	411	243	654
		NARWSS harbor porpoise survey	109		109
		NARWSS right whale surveys	991	379	1370
	NJDEP	New Jersey Ecological Baseline Study	4		4
	SEFSC	Marine mammal abundance surveys		3	3
All			1515	625	2140
Shipboard	NEFSC	Marine mammal abundance surveys	349	14	363
	NJDEP	New Jersey Ecological Baseline Study	33		33
	All			382	14

Table 11. $g(0)$ estimates used in the updated harbor porpoise model. These are the same as in Roberts et al. (2016a).

Platform	Surveys	Group Size	$g(0)$	Biases Addressed	Source
Shipboard	All	Any	0.35	Perception	Palka (2006)
Aerial	All	Any	0.36	Both	Palka (2006)

4.2.5.1. Winter model

Palka et al. (1996) described the seasonal migratory pattern for the Gulf of Maine / Bay of Fundy stock of harbor porpoises. As with the Phase III models, we assumed that in summer, when harbor porpoises aggregate in the northern Gulf of Maine and southern Bay of Fundy in large numbers, species-environment relationships could be different than in other times of year, when they disperse throughout the mid-Atlantic shelf and possibly to other locations currently unknown. We therefore fitted separate seasonal models to allow for different relationships.

In the winter seasonal model, defined as October-May, we included all survey segments and sightings conducted in Beaufort sea state 2 or less in waters shallower than the 1500m isobath (Fig. 31). Mean predicted abundance for the season (13,782) (Fig. 32) was lower than the Phase III model’s prediction (17,651), and monthly predictions were lower for except for November and December. Otherwise the updated winter model was generally similar to the Phase III model.

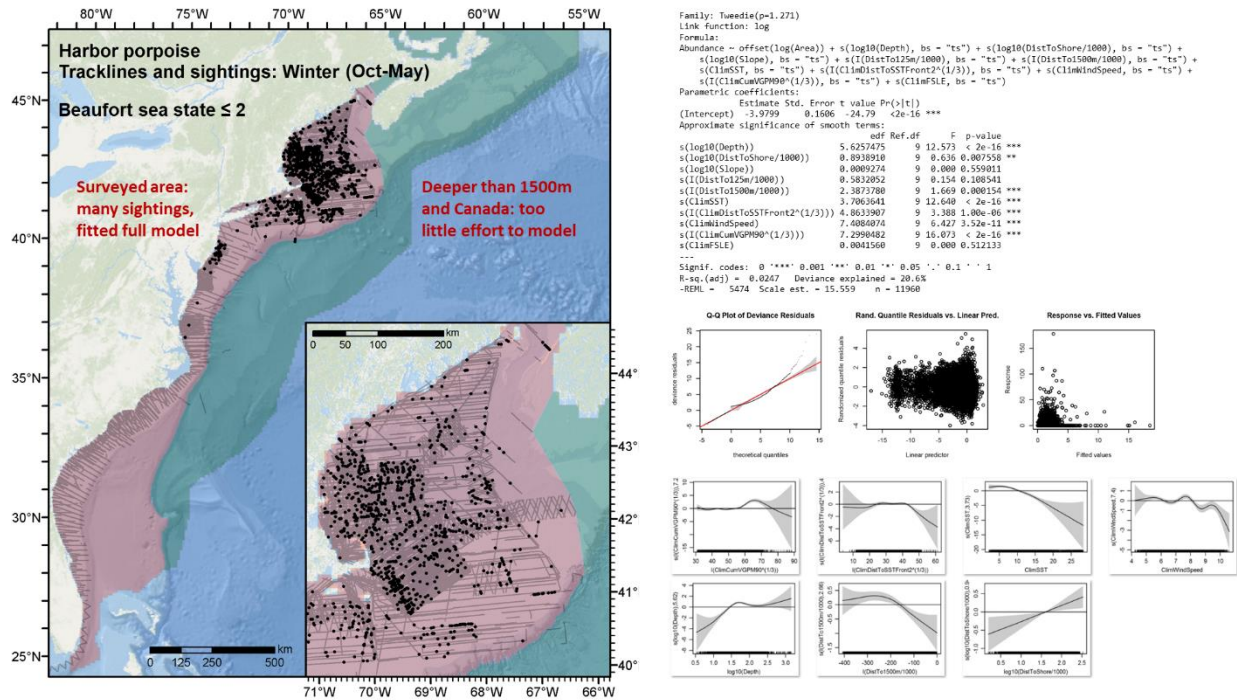


Figure 31. Left: Harbor porpoise winter model schematic. Right: spatial model that was selected as best.

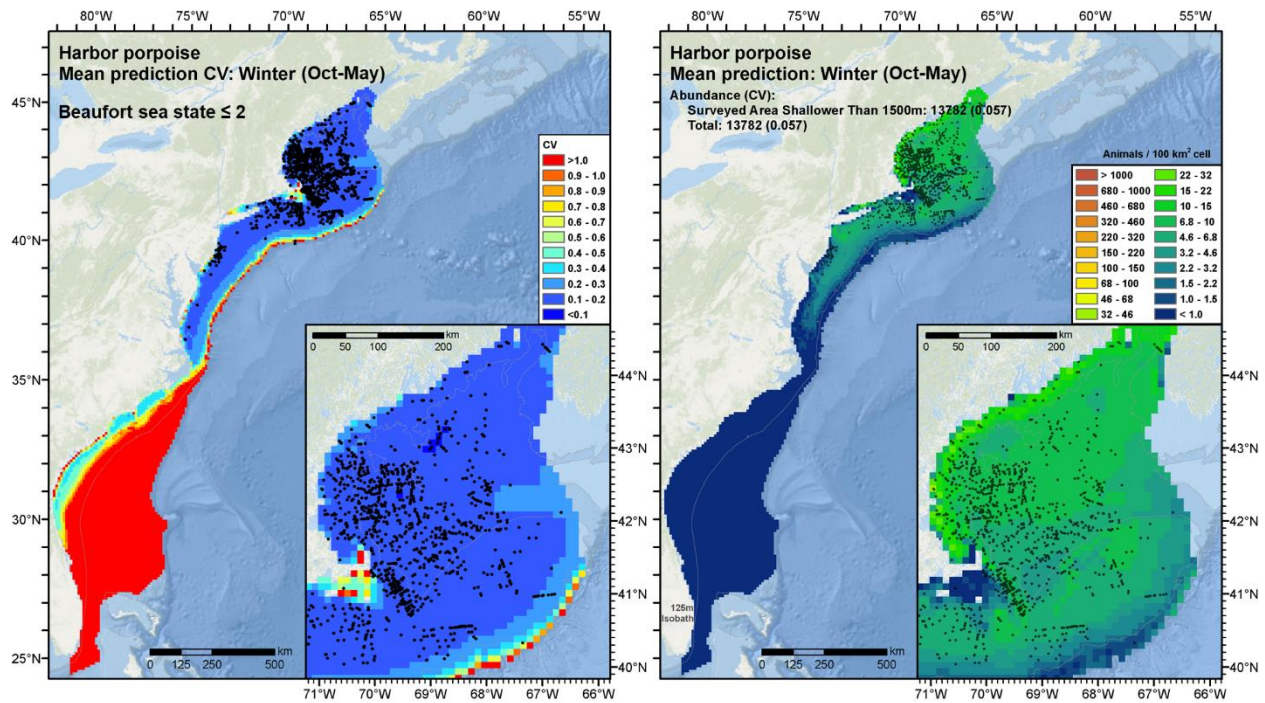


Figure 32. Left: Predicted mean coefficient of variation (CV), with sightings overlaid, for harbor porpoise for the winter season. Right: Predicted mean density and total abundance predictions for harbor porpoise for the winter season.

4.2.5.2. *Summer model*

The summer seasonal model, defined as June-September, included all survey segments and sightings conducted in Beaufort sea state 2 or less in waters north of the Gulf Stream (Fig. 33). As with the Phase III model, we assumed that abundance south of the Gulf Stream was zero in these months. Also, we placed the northern edge of the model about halfway up the Scotian Shelf, under the assumption that animals beyond this were mainly part of the Gulf of St. Lawrence stock, which we lacked sufficient data to model.

To improve model goodness of fit and reduce the tendency of the model to fit relationships to static predictors that were hard to explain ecologically, we included a bivariate smooth of spatial coordinates, a common practice in density surface modeling when the entire study area receives sufficient survey coverage, which occurred during this season. Reflecting this, the updated model retained fewer static covariates than the Phase III model (2 vs. 4) but explained 20% more deviance (57.9% vs. 37.8%). Mean predicted abundance for the season (60,281) (Fig. 34) was substantially higher than the Phase III model's prediction (45,089), with a peak of 92,309 in August.

The abundance predictions of the updated model are substantially closer to the NMFS Stock Assessment Report estimates. The summer-winter transition months of June and September do not show the unrealistic mid-Atlantic spikes that occurred with the Phase III models. It appears that the new model successfully addressed our concerns with the Phase III model. In Option Year 2, we plan to contact our collaborators and redo the density/acoustic comparison with the updated density models and updated acoustic detections.

As with the Phase III model, we believe the updated model predictions are consistent with published knowledge of harbor porpoise seasonal movements. Accordingly, we elected to provide monthly density surfaces for harbor porpoise for use in the NMSDD, for the same reasons discussed in the supplementary species report provided with the original Phase III model (Roberts et al. 2016a).

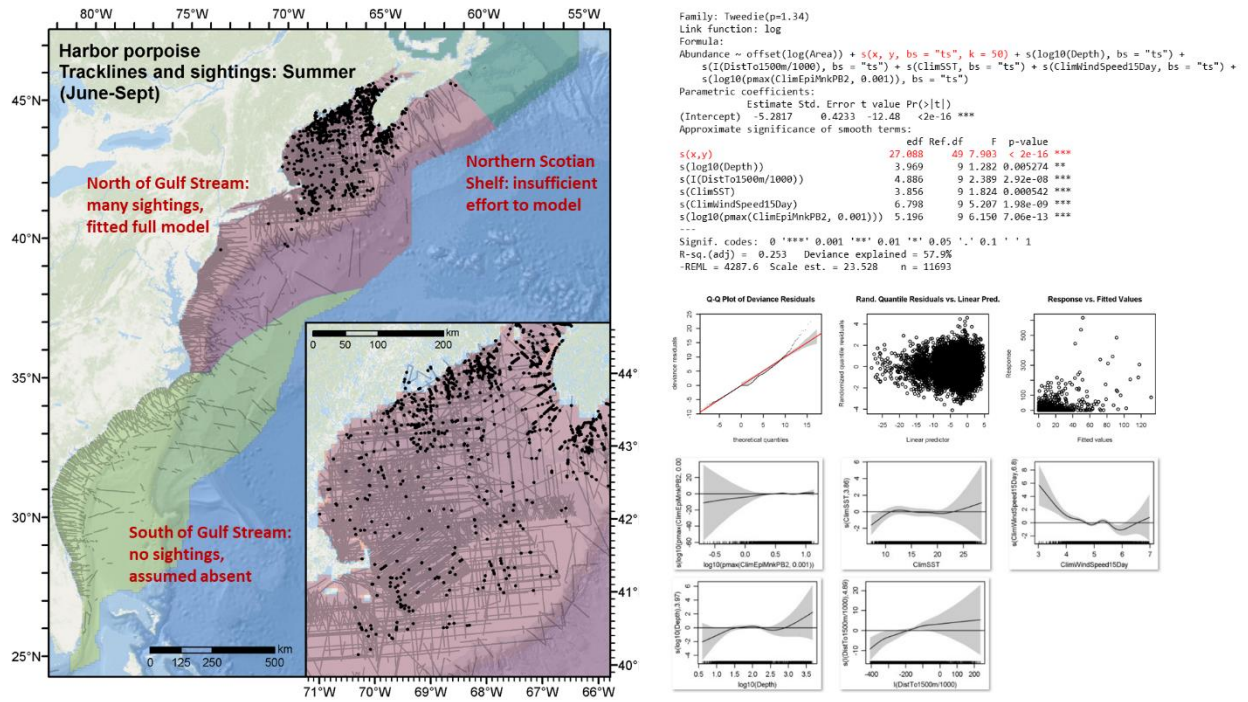


Figure 33. Left: Harbor porpoise summer model schematic. Right: spatial model that was selected as best.

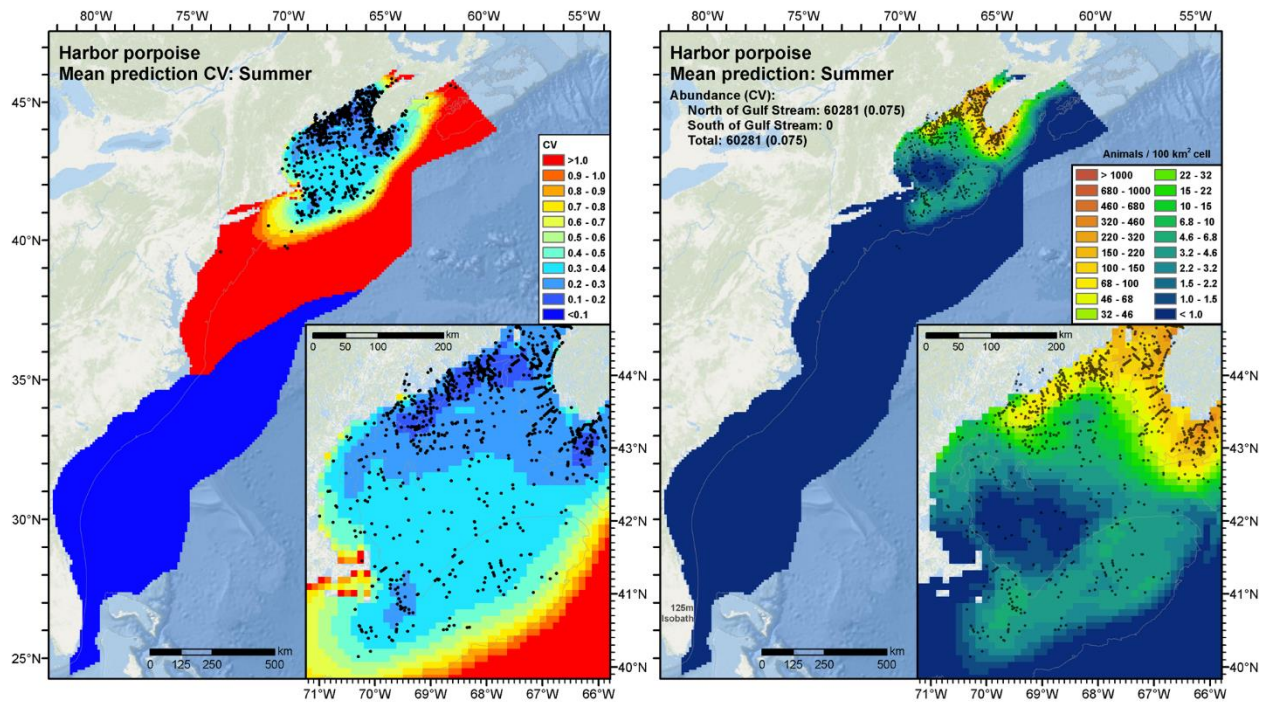


Figure 34. Left: Predicted mean coefficient of variation (CV), with sightings overlaid, for harbor porpoise for the summer season. Right: Predicted mean density and total abundance for harbor porpoise for the summer season.

4.2.6. *Humpback whale model*

The additional surveys incorporated after Phase III modeling added more than 1000 humpback sightings (Table 12). Most of these came from the three years of additional surveys from the NARWSS program. NARWSS intensively surveys the Gulf of Maine in search of right whales; this area is excellent feeding habitat for several baleen whale species, and many humpbacks were recorded. Also noteworthy were more than 50 additional sightings distributed throughout the southeast in winter (Fig. 35), sighted by the Southeast U.S. North Atlantic Right Whale (SEUS NARW) programs.

For the updated humpback whale model we used the same $g(0)$ estimates as the Phase III model (Table 13). Please see the humpback whale supplementary report in Roberts et al. (2016a) for a detailed discussion.

Readers may notice that the table of sightings (Table 12) shows approximately 700 more sightings than what appears in the model schematics (Figs. 35, 37). The missing sightings were truncated from the analysis when detection functions were fitted, with more than 500 right-truncated from the NARWSS right whale program. Observers on this program are skilled at spotting humpbacks at great distances (4 - 8km) from the aircraft, but fitting a detection function that included sightings at these distances proved problematic. Therefore we truncated them from the analysis, a practice recommended for this situation (Buckland et al. 2001; Thomas et al. 2010).

Humpbacks exhibit strong seasonal migratory behavior, with the majority of the population arriving on feeding grounds in spring and departing for calving grounds and other overwintering areas at the beginning of winter. As with the Phase III models, we split the data into summer (April-November) and winter (December-March) models, based on prior descriptions of humpback seasonality, which agreed with patterns we observed in the sightings available to us. Please see the humpback whale supplementary report in Roberts et al. (2016a) for a detailed discussion.

4.2.6.1. *Winter model*

In winter, humpbacks were scattered throughout the continental shelf of the east coast (Fig. 35). Dense clusters of sightings occurred in the western Gulf of Maine (e.g. Stellwagen Bank), near Cape Hatteras, and near core right whale calving habitat at Jacksonville, Florida. However, these areas were also the focus of intense surveying, raising the question of whether the clusters truly represented areas of high density or merely atypically intense surveying.

The resulting model (Fig. 35) and predictions (Fig. 36) suggested that humpback density was higher in the northern half of the study area, from Cape Hatteras to Nova Scotia, and much lower in the southern half except at the continental shelf break (on the Blake Plateau, the upper break, where the seafloor was still only 100-200m deep; negligible density was predicted for the lower break). The band of density predicted along the shelf break was driven by sightings of humpbacks occurring along the shelf break at many locations between 30-40°N, both north and south of Cape Hatteras. We caution that relatively little survey effort was available at deeper depths (>1500m), and while our model's prediction of near zero density at deep depths is consistent with what is known about humpbacks, it represents an area of lower confidence.

Table 12. Summary of humpback whale sightings available for the updated model. “Extant” sightings were used in the Phase III regional models (Roberts et al. 2016a). “Added” sightings were incorporated during the Base Year and Option Year 1 for the updated models.

Platform	Provider	Program	Humpback_whale			
			Extant	Added	Total	
Aerial	NEFSC	Marine mammal abundance surveys	174	63	237	
		NARWSS harbor porpoise survey	9		9	
		NARWSS right whale surveys	2549	937	3486	
	NJDEP	New Jersey Ecological Baseline Study	5		5	
	SEFSC	Marine mammal abundance surveys	4	9	13	
	SEUS NARW	FWRI surveys		32	32	
		NEAq surveys		8	8	
		SSA surveys (Skymaster)		5	5	
		SSA surveys (Twin Otter)		14	14	
		UNCW	Cape Hatteras Navy Surveys	8	1	9
		Jacksonville Navy Surveys	2	1	3	
		Marine mammal surveys, 2002	3		3	
		Norfolk Canyon Navy Surveys		4	4	
		Onslow Bay Navy Surveys	1		1	
		Right whale surveys, 2005-2008	9		9	
	VAMSC	MD Wind Energy Area surveys		2	2	
		VA Wind Energy Area surveys	11	1	12	
	All			2775	1077	3852
	Shipboard	NEFSC	Marine mammal abundance surveys	39	77	116
		NJDEP	New Jersey Ecological Baseline Study	7		7
SEFSC		Marine mammal abundance surveys		1	1	
All			46	78	124	

Table 13. $g(0)$ estimates used in the updated humpback model. These are the same as in Roberts et al. (2016a).

Platform	Surveys	Group Size	$g(0)$	Biases Addressed	Source
Shipboard	Binocular Surveys	Any	0.921	Perception	Barlow and Forney (2007)
Shipboard	NEFSC Endeavor	Any	0.88	Perception	Palka (2006)
Shipboard	Naked Eye Surveys	Any	0.38	Perception	Palka (2006)
Aerial	All	Any	0.451	Both	Heide-Jorgensen et al. (2012)

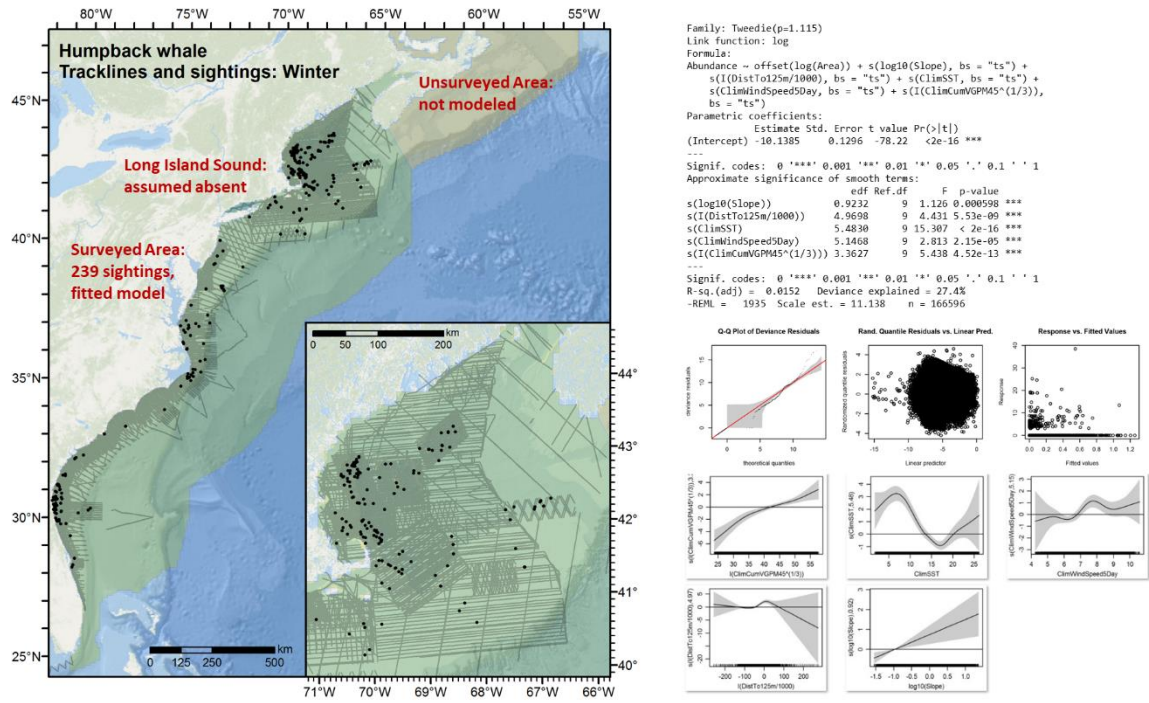


Figure 35. Left: Humpback whale winter model schematic. Right: spatial model that was selected as best.

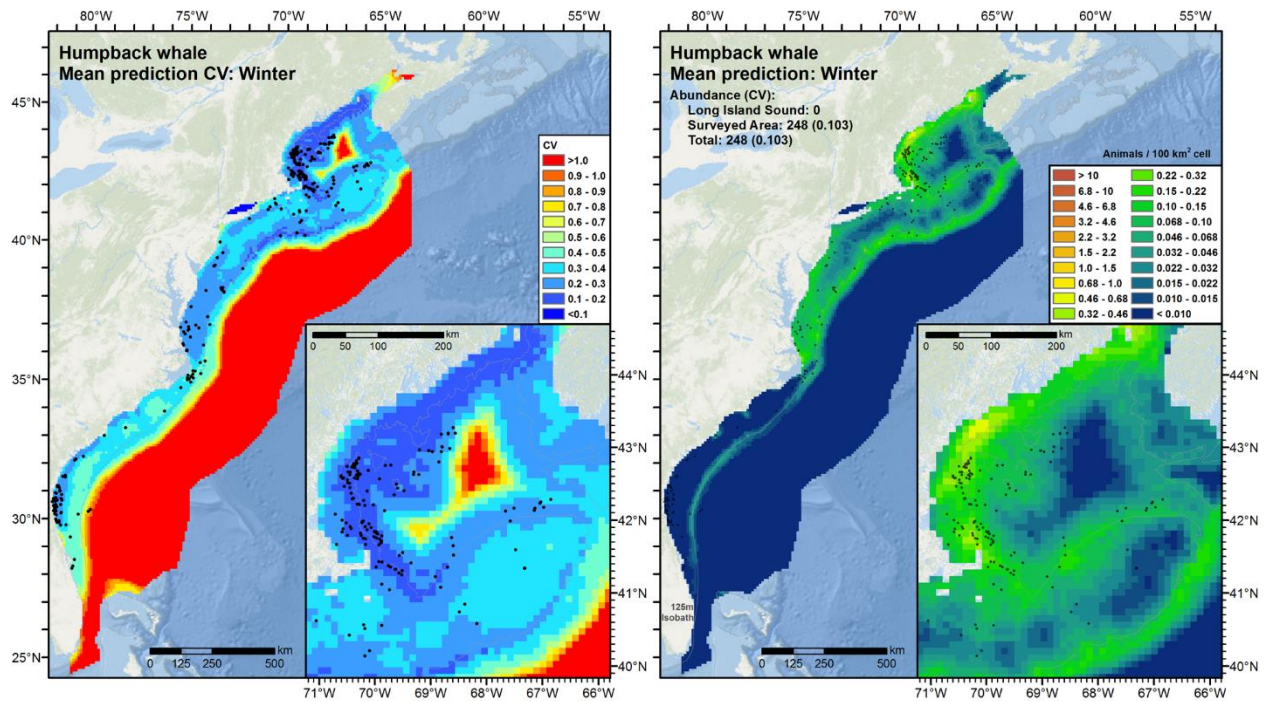


Figure 36. Left: Predicted mean coefficient of variation (CV), with sightings overlaid, for humpback whale for the winter season. Right: Predicted mean density and total abundance for humpback whale for the winter season.

4.2.6.2. *Summer model*

In summer, humpbacks aggregated in and around the Gulf of Maine, their core feeding habitat (Fig. 37). Relatively fewer were reported across the continental shelf from southern Georges Bank south to Cape Hatteras, however surveying was less intense in these areas. Many of these sightings occurred in spring, but at least one humpback was reported somewhere south of New York in all months of the year. The single sighting reported south of Cape Hatteras during this season was off South Carolina in November.

The resulting model (Fig. 37) was complex, with 9 covariates retained by the model selection procedure, reflecting the complex distribution of humpbacks throughout the season. Total mean abundance for the season, 1773 (CV=0.057), was slightly higher than that predicted by the Phase III model, 1637 (CV=0.07). Predicted spatial distributions were similar, although the new model predicted markedly lower (but still high) density off the southern edge of Nova Scotia and markedly higher density along the shelf break between Cape Hatteras and southern Georges Bank, where many additional sightings were reported.

The updated model predicts humpbacks inside Long Island Sound at low to moderate density (Fig. 38). Although humpbacks were not known to frequent Long Island Sound throughout most of the study period, they have been sighted there occasionally during the summers of 2015, 2016, and 2017. For this reason, we believe the model's prediction of low to moderate density is appropriate for use in present-day marine spatial planning applications. However, we do caution that model uncertainty was estimated relatively high here (Fig. 38).

As with the Phase III model, we believe the updated model predictions are consistent with published knowledge of humpback seasonal movements. Accordingly, we elected to provide monthly density surfaces for humpbacks for use in the NMSDD, for the same reasons discussed in the supplementary species report provided with the original Phase III model (Roberts et al. 2016a).

4.2.7. Classification of ambiguous “fin or sei whale” sightings

Fin and sei whales look and behave similarly, and unless observers are afforded an opportunity to examine them carefully, they cannot distinguish between them. Between 1992 and 2016, the surveys available in Phase III and those integrated after together reported about 2400 fin whale sightings, 800 sei whale sightings, and 800 “fin or sei whale” sightings (Table 14). These ambiguous sightings were all reported by NEFSC—both by broad scale surveys (e.g. AMAPPS) and by the NARWSS program.

As with the Phase III models, we did not want to exclude these sightings from the analysis, as they would represent a significant number of animals that were sighted but not accounted for by the models, potentially biasing abundance low. Exploratory analysis of the definitive sightings suggested that fin and sei whales exhibit some differences in seasonal timing and habitat. The ratio of sei whales to fin whales was highest in spring (Table 15), and sei whales appeared to occupy a more distinct habitat, while fin whales occurred across a broader region (Fig. 39). Density histograms of the definitive sightings of the two species across a selection of environmental covariates and day of the year revealed overlapping but differing distributions (Fig. 40). Assuming that the probability of fully identifying a fin or sei whale does not depend causally on these covariates (it is not easier to visually distinguish the species in colder water, for example), then the definitive sightings and these covariates could reasonably be used to train a model for classifying the ambiguous sightings.

4.2.7.1. Methods

To fit the classification model, we used the cforest classifier (Hothorn et al. 2006), an elaboration of the classic random forest classifier (Brieman 2001). First, we trained a binary classifier using the sightings that reported definitive species identifications (e.g. “fin whale” and “sei whale”). The training data included all on-effort sightings in the east coast region (including those in the Gulf of St. Lawrence that we did not use in fitting fin and sei whale spatial models). We used the species identification as the response variable and day of year and a selection of habitat-based environmental data as covariates.

We used receiver operating characteristic (ROC) curve analysis to select a threshold (or “cutoff”) for classifying the probabilistic predictions of species identifications made by the model into a binary result of one species or another. In the Phase III classification model, we relied on the Youden index (Perkins & Schisterman 2006) to select this threshold. While this approach could be said to optimally minimize misclassification rates, when we applied it to the definitive sightings to assess the Phase III model’s performance, although misclassification rates were fairly similar it resulted in many more fin whales being misclassified as sei whales (255) than sei whales being misclassified as fin whales (92) (Roberts et al. 2016a). Assuming this performance with the training data reflected what actually happened with the ambiguous sightings we applied the model to, the likely result was that sei whale density and abundance were biased high while fin whale density and abundance were biased low, by virtue of the classifier predicting more sei whales and fewer fin whales than is appropriate.

Although it is impossible to know if that result actually occurred—especially because habitat-based modeling was subsequently performed on the pooled classified and definitive sightings to produce density and abundance estimates—we chose a different strategy for the updated models. Here, we selected a threshold that caused the classifier to produce an equal number of misclassifications. That is, the resulting number of fin whales predicted to be sei whales was the same as the number of sei whales predicted to be fin whales. Under this philosophy, if traditional line transect density estimates were then made (without a habitat-based model), the classification would not bias abundance toward either species. The downside of this approach is that it markedly increased the rate at which sei whales were misclassified as fin whales (while marginally decreasing the rate that fin whales were misclassified as sei whales).

After fitting the classification model and selecting the threshold, we classified the ambiguous sightings as either one species or the other by processing the covariate values observed for that sighting through the fitted model. We then included the classified sightings in habitat-based spatial models of density. (But for detection functions, we used the original species identification (“fin whale”, “sei whale”, or “fin or sei whale”) as a detection function covariate. Because close sightings were more frequently fully identified, and distant sightings ambiguous, overall modeled detection probability was lower for definitive sightings and higher for ambiguous sightings.)

Table 14. Summary of fin and sei whale sightings available for the updated models. “Extant” sightings were used in the Phase III regional models (Roberts et al. 2016a). “Added” sightings were incorporated during the Base Year and Option Year 1 for the updated models.

Platform	Provider	Program	Fin whale			Sei whale			Fin or sei whale		
			Extant	Added	Total	Extant	Added	Total	Extant	Added	Total
Aerial	NEFSC	Marine mammal abundance surveys	208	55	263	8	15	23	38	13	51
		NARWSS harbor porpoise survey	13		13						
		NARWSS right whale surveys	1471	367	1838	630	166	796	536	87	623
	NJDEP	New Jersey Ecological Baseline Study	1		1						
	SEFSC	Marine mammal abundance surveys	6	21	27						
	SEUS NARW	FWRI surveys			3						
		SSA surveys (Twin Otter)			2						
	UNCW	Cape Hatteras Navy Surveys	5	4	9						
		Marine mammal surveys, 2002	1		1						
		Norfolk Canyon Navy Surveys			8						
		Onslow Bay Navy Surveys	1		1						
		Right whale surveys, 2005-2008	12		12						
	VAMSC	MD Wind Energy Area surveys			8						
		VA Wind Energy Area surveys	11		11						
		All		1729	468	2197	638	181	819	574	100
Shipboard	NEFSC	Marine mammal abundance surveys	35	103	138	6	12	18	82	31	113
	NJDEP	New Jersey Ecological Baseline Study	26		26						
	SEFSC	Marine mammal abundance surveys	11	7	18						
	All		72	110	182	6	12	18	82	31	113

Table 15. Seasonal distribution of fin and sei whale sightings. Season definitions used in this table: Winter: Jan-Mar; Spring: Apr-Jun; Summer: Jul-Sep; Fall: Oct-Dec.

Identification	Winter	Spring	Summer	Fall
Fin whale	204	1133	670	378
Sei whale	18	675	96	48
Fin or sei whale	41	446	208	93
% Ambiguous	15 %	20 %	21 %	18 %

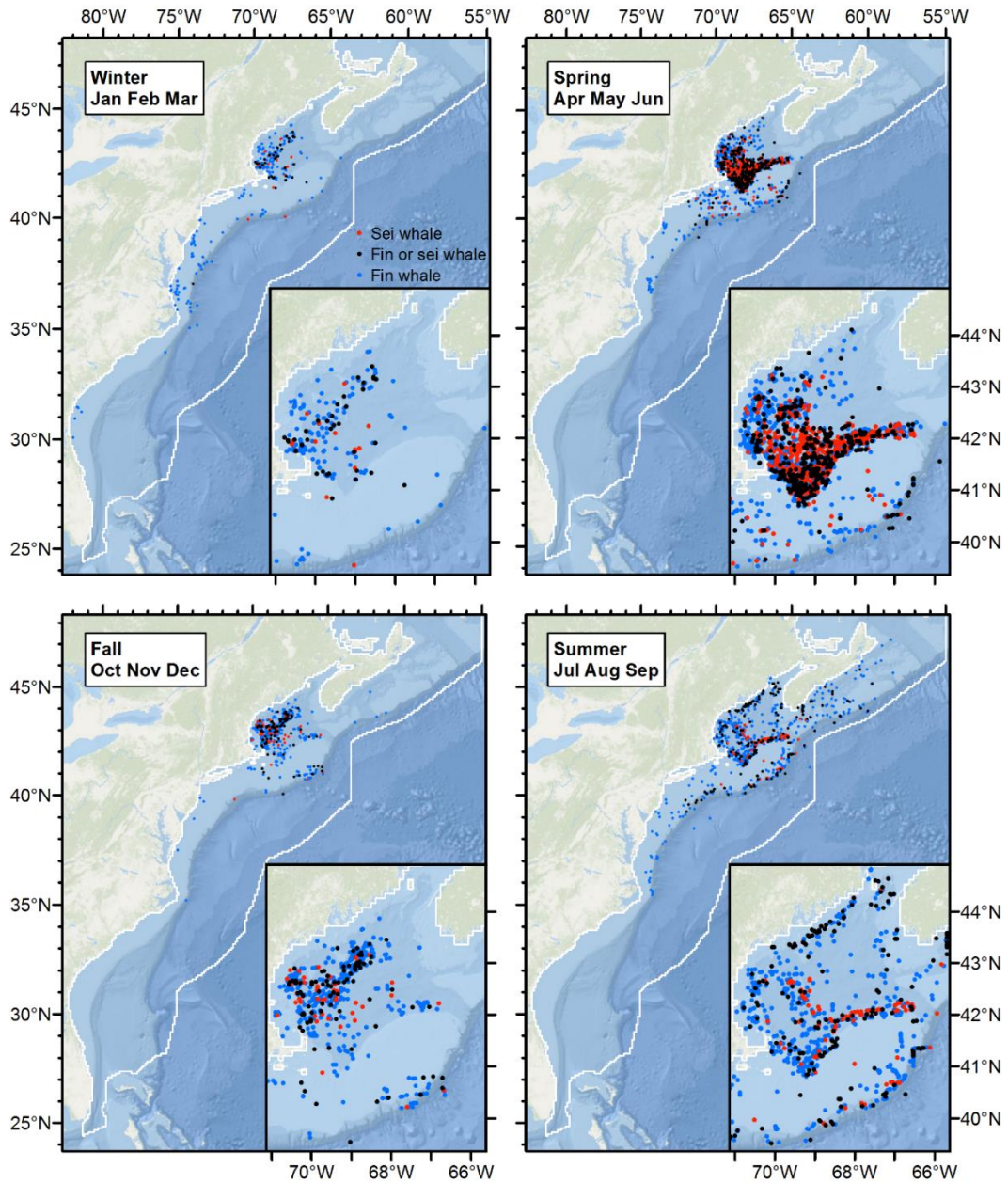


Figure 39. Seasonal maps of the fin and sei whale sightings summarized in Tables 14 and 15.

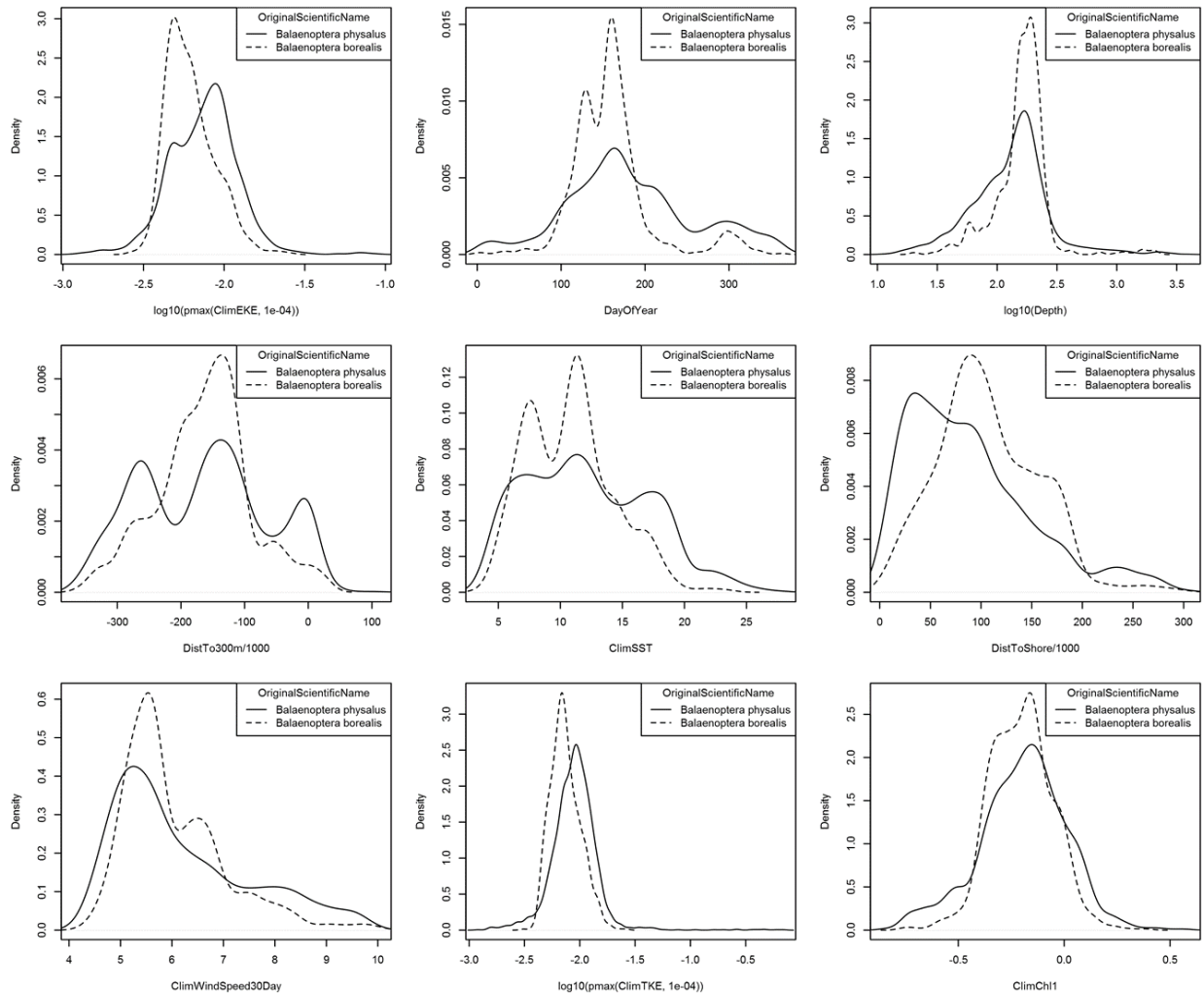


Figure 40. Density histograms of definitive fin and sei whale sightings for a selection of environmental covariates and day of the year.

4.2.7.2. Results

Eddy kinetic energy (EKE), day of year, and depth were identified as the most important covariates in training the random forest model. For the training data, the area under the ROC curve (Fig. 42) (AUC) statistic was 0.942, similar to what was obtained with the Phase III classification model. At the selected threshold (a.k.a. cutoff) value of 0.632, the misclassification rate for fin whales was 8.7% and for sei whales was 24.8%.

When we applied the classification model to the ambiguous “fin or sei whale” sightings, it predicted 588 fin whales and 227 sei whales, a ratio of 2.85 (Table 16). In the definitive sightings used to train the model, the fin/sei ratio was 2.47, suggesting that the model might be biased slightly toward fin whales. By comparison, the Phase III model predicted a ratio of 1.83 vs. a ratio of 3.00 in that model’s training data, indicating a more severe bias toward sei whales.

When applied to the ambiguous sightings, the new model predicted 216 sei whales in spring and only 11 in all other seasons combined (Table 16, Fig. 41). The fin/sei ratio in spring predictions was 1.07, vs 1.68 in the training data. However, we do not find this cause for concern, as the ambiguous sightings tended to be concentrated in the Gulf of Maine where definitive fin and sei whales were both reported, and away from clusters composed exclusively of definitive fin whale sightings (e.g. near New Jersey or off Chesapeake Bay) (Fig. 41).

Table 16. Seasonal distribution of “fin or sei whale” classification model predictions. Season definitions used in this table: Winter: Jan-Mar; Spring: Apr-Jun; Summer: Jul-Sep; Fall: Oct-Dec.

Identification	Winter	Spring	Summer	Fall	Total
Fin or sei whale	41	446	208	93	788
Classified fin	39	230	198	93	560
Classified sei	2	216	9	0	227

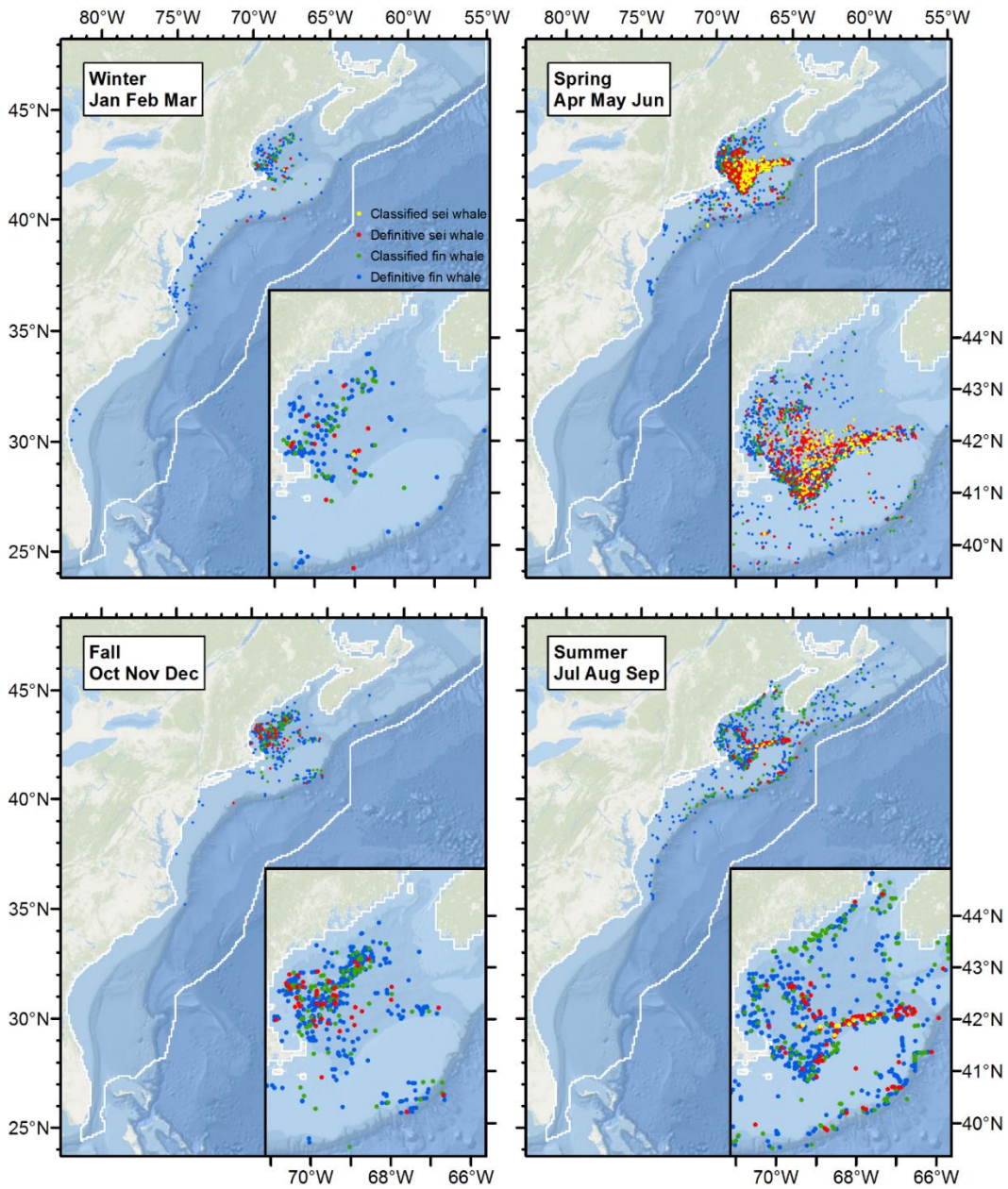


Figure 41. Seasonal maps of definitive “fin whale” (blue) and “sei whale” (red) sightings, along with ambiguous sightings classified as fin whales (green) and sei whales (yellow).

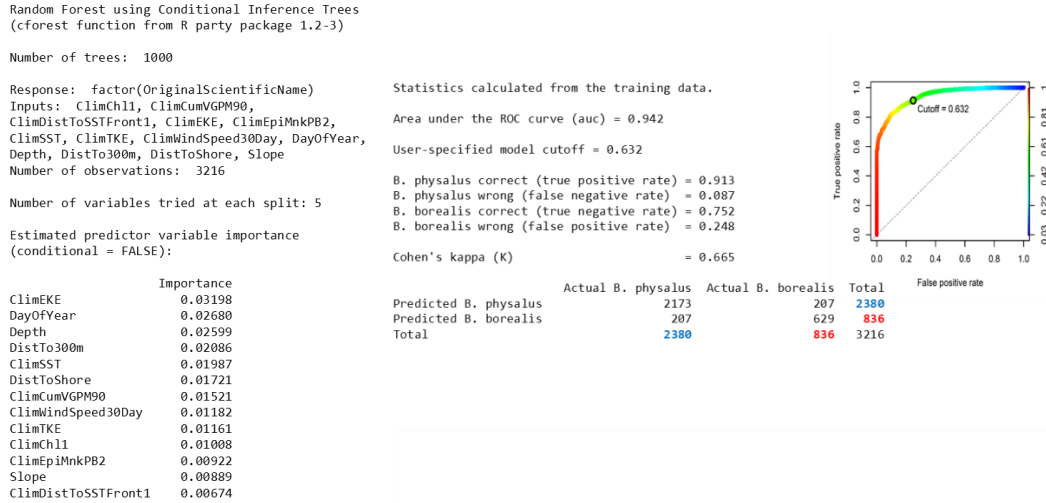


Figure 42. Statistical output from the “fin or sei whale” classification model.

4.2.8. Fin whale model

The additional surveys incorporated after Phase III modeling added more than 600 fin whale sightings, counting both the definitive sightings and ambiguous “fin or sei whale” sightings reclassified as fin whales (Tables 14, 16). Most of these came from the three years of additional surveys from the NARWSS program in the Gulf of Maine, which is known as fin whale feeding habitat, while a lesser number, reported by other programs, were distributed throughout the east coast, including five sightings at the right whale calving grounds (Fig. 43).

For the updated fin whale model we used the same $g(0)$ estimates as the Phase III model (Table 17); please see the fin whale supplementary report in Roberts et al. (2016a) for a detailed discussion.

Table 17. $g(0)$ estimates used in the updated fin whale model. These are the same as in Roberts et al. (2016a).

Platform	Surveys	Group Size	$g(0)$	Biases Addressed	Source
Shipboard	Binocular Surveys	Any	0.63	Perception	Palka (2006)
Shipboard	NEFSC Abel-J Binocular Surveys	Any	0.32	Perception	Palka (2006)
Shipboard	NEFSC Endeavor	Any	0.94	Perception	Palka (2006)
Shipboard	Naked Eye Surveys	Any	0.48	Perception	Palka (2006)
Aerial	All	Any	0.251	Availability	Lafortuna et al. (2003)

While the migratory behaviors and seasonal habitats of humpback and right whales are fairly well understood in the western North Atlantic, the seasonal movements and habitats of fin whales are relatively unknown. A 2015 review of the global distributions of fin whales noted that fin whale breeding areas are still unknown, and that while modern scientific studies and historic whaling records indicate that fin whales are more common at high latitudes in summer than in winter, some remain in higher (colder) latitudes in winter and lower (warmer) latitudes in summer (Edwards et al. 2015). These authors concluded that fin whales likely do not conduct long-distance seasonal migrations to tropical latitudes like humpback whales. Instead, some may remain at high latitudes year-round, while others may make short migrations, or something more complicated.

Sightings in the surveys available for our analysis concur with this view that fin whales inhabit U.S. waters of the western North Atlantic year-round, in both cold and warm waters, exhibiting some seasonal rise and fall in abundance but less than other baleen whales. Similar to other baleen whales, a spring rise and winter fall was

evident in monthly maps of sightings, but differences from other species were easily noted. For example, in the Gulf of Maine, known to be feeding grounds for both fin and humpback whales, fin whales were sighted in notably higher rates than humpbacks in January-March. At the warmer waters of Cape Hatteras, which is not considered prime summer feeding habitat for baleen whales, fin whales were reported in all months of July-October, while no humpbacks were reported.

Given this view, our approach to modeling fin whales was to fit a single model to all data (Fig. 43), as we did in the Phase III analysis, and rely on dynamic habitat covariates such as sea surface temperature to drive seasonal changes in fin whale density. The resulting model was complex, retaining 9 covariates; this is reasonable given the large amount of survey data used to fit the model (over 250,000 10km segments) and the distribution of fin whales over several distinct habitats (e.g. Gulf of Maine, Scotian Shelf, Mid-Atlantic Bight). Fitted relationships indicated higher density over all but the warmest and coldest temperatures, in areas of high epipelagic micronekton biomass (indicative of prey species), and in high slope habitat, especially near the shelf break (represented in the model by the 125m isobath).

Predicted mean abundance (Fig. 43) was 35% lower than for the Phase III fin whale model (3005 vs. 4633). Mean monthly abundance was lower than Phase III predictions in all months. As with Phase III, the predicted low was in February (Fig. 44) (1629 vs. 2689; new estimate 39% lower) and the high was in June (Fig. 45) (4859 vs. 6538; new estimate 26% lower). The reasons for this large difference are not immediately clear. One possibility concerns the detection functions fitted for the NARWSS Twin Otter aerial surveys, which reported over 75% of the fin whale sightings in both the Phase III model and the updated model.

The Phase III detection functions were constrained by the inability to utilize categorical covariates. The detection function selected as best was a half-normal with a third-order cosine adjustment (see Fig. 46 of the fin whale supplementary report of Roberts et al. (2016a)), which yielded a mean effective strip half width (ESHW) of 1275m, and mean probability of detection of $p=0.3188$. The new detection function, able to utilize categorical covariates, was fitted to twice as many sightings and included those identified as fin whale, sei whale, and ambiguous “fin or sei whale”, using species ID as a categorical covariate to allow the detection function to differentiate between them as supported by the data. The function selected as best was a hazard-rate with three covariates: Beaufort sea state, group size, and species ID. The mean ESHW was 1710m with $p=0.3865$.

The ESHW of the new detection function was 34% larger, and p was 21% higher, than that of the old detection function. These indicate that the new detection function considered fin whales (and sei whales) to detect than the Phase III detection function did. In a simple abundance estimate made with conventional distance sampling methodology (Buckland et al. 2001), abundance is inversely proportional to ESHW. Thus the 34% increase in ESHW that occurred in the new detection function is consistent with the 35% decrease in abundance. However, we urge caution with this interpretation, as many other aspects of the new analysis differ from the Phase III model. We will continue to investigate this further in Option Year 2. In any case, we have examined the new models carefully and have not identified anything that would give reason to doubt their abundance estimates over the Phase III model. Until we identify a reason for doubt (which we may never do), we recommend the new model over the Phase III model. We note (and discuss in detail elsewhere) that the estimated CVs of both the new model and the Phase III model only account for uncertainty in the GAM parameter estimates, and do not account for known uncertainty in the detection functions or $g(0)$ estimates.

As with Phase III, we believe that monthly predictions from the updated model resemble the current scientific consensus about fin whale seasonality in the western North Atlantic, i.e. that fin whales are present on the east coast of North America year-round, mainly north of Cape Hatteras, but that abundance is higher in summer than in winter. Although there is relatively scant knowledge of fin whale migratory behavior and no calving grounds have been identified, we believe the correspondence of model predictions with what is known is sufficient for us to recommend that monthly predictions be used for management purposes, thus we have provided monthly density surfaces for fin whales for use in the NMSDD, as we did with the original Phase III model (Roberts et al. 2016a).

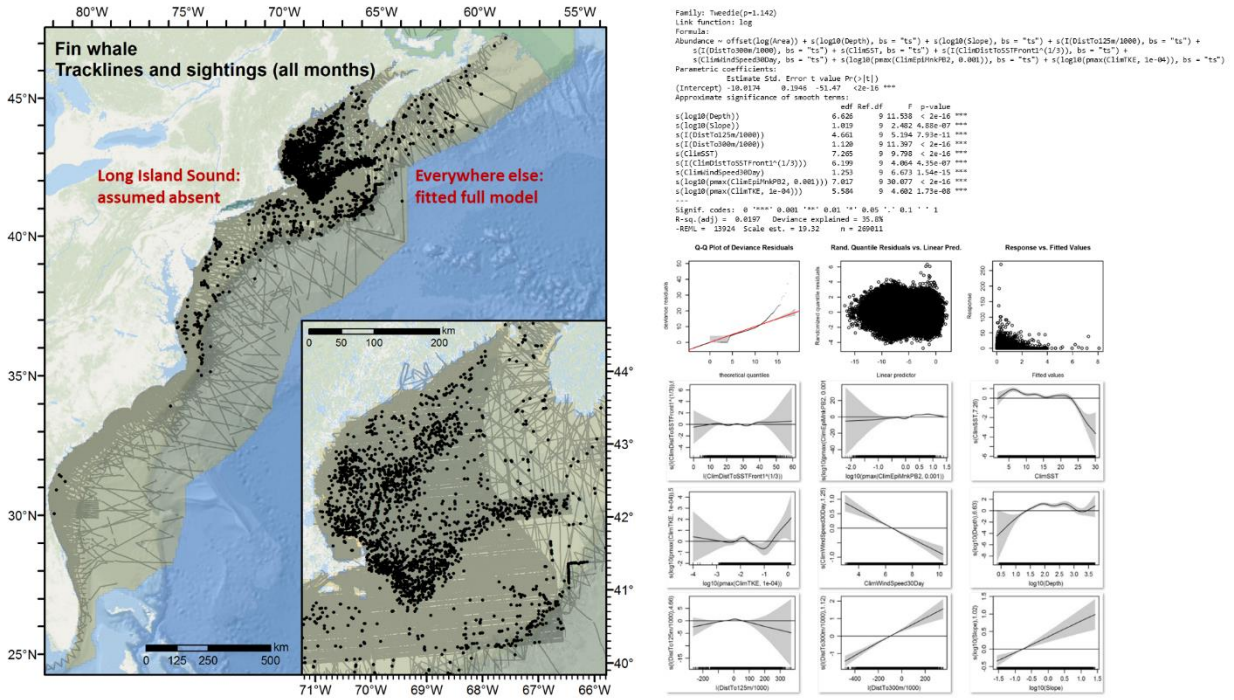


Figure 43. Left: Fin whale model schematic. Right: spatial model that was selected as best.

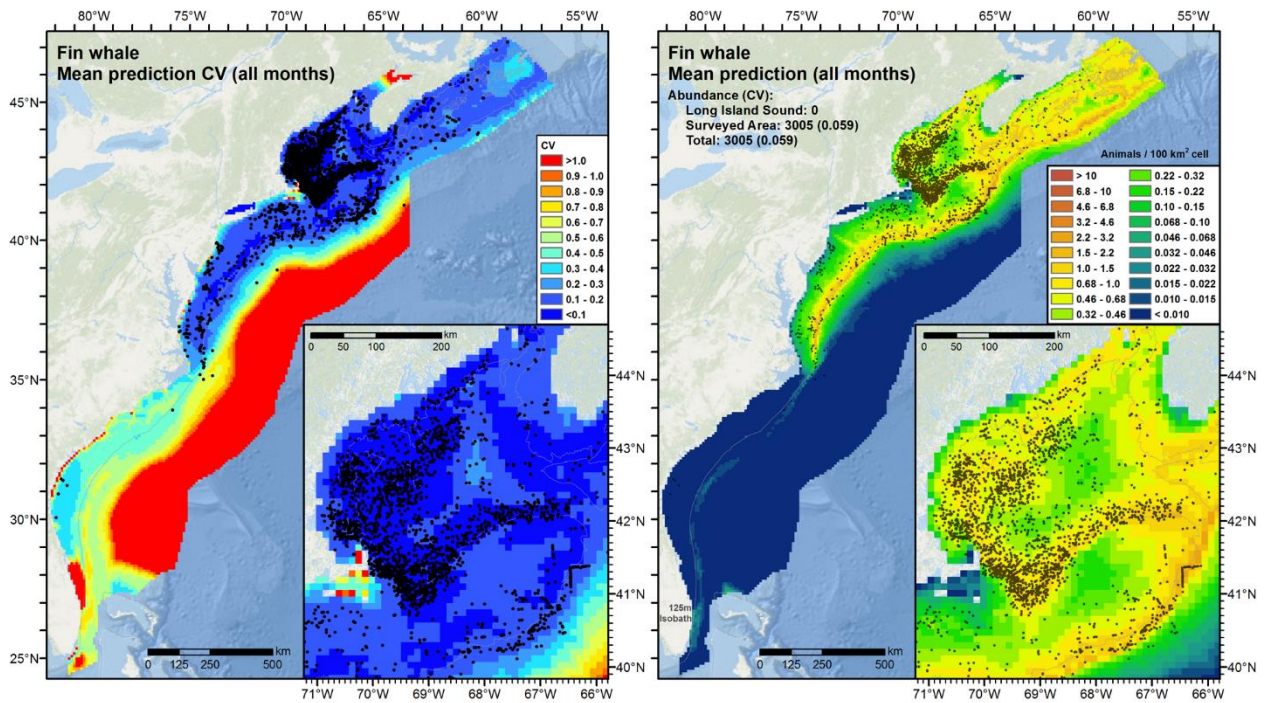


Figure 44. Left: Predicted mean coefficient of variation (CV), with sightings overlaid, for fin whale. Right: Predicted mean density and total abundance for fin whale.

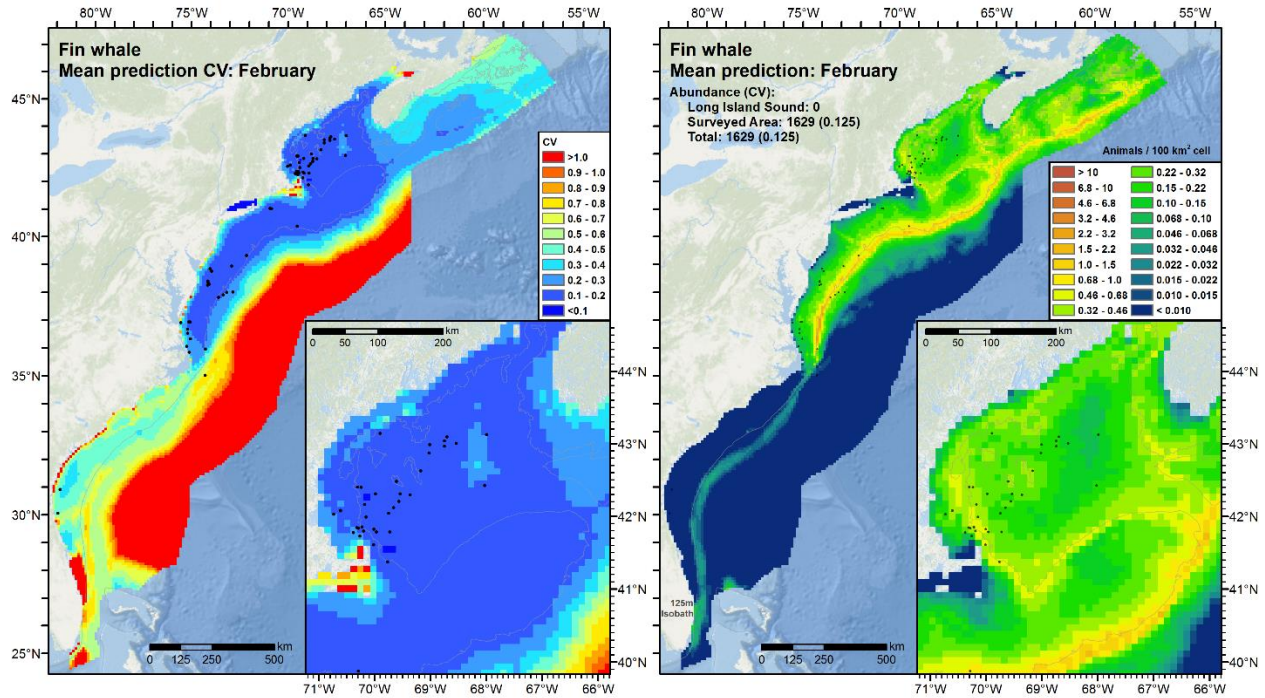


Figure 45. Left: Predicted mean coefficient of variation (CV), with sightings overlaid, for fin whale in February, the month predicted to have lowest abundance. Right: Predicted mean density and total abundance.

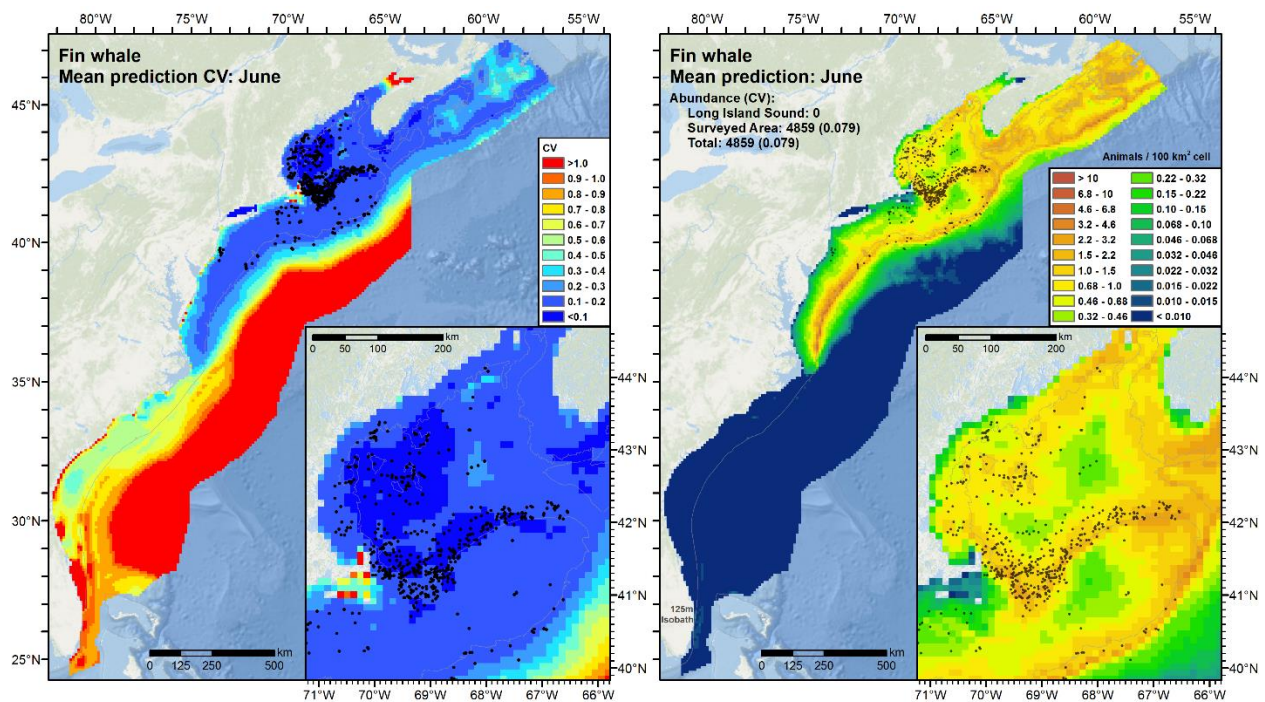


Figure 46. Left: Predicted mean coefficient of variation (CV), with sightings overlaid, for fin whale in June, the month predicted to have highest abundance. Right: Predicted mean density and total abundance.

4.2.9. Sei whale model

The additional surveys incorporated after Phase III modeling added approximately 200 sei whale sightings, counting both the definitive sightings and ambiguous “fin or sei whale” sightings reclassified as sei whales (Tables 14, 16). Most of these came from the three years of additional surveys from the NEFSC NARWSS program in the Gulf of Maine, which is known as sei whale feeding habitat, while a lesser number were reported by the NEFSC AMAPPS surveys. To date no collaborator other than NEFSC has reported a sei whale sighting except SEFSC, which reported three “Bryde’s or sei whale” sightings during the Oregon II 1992 winter cruise in the southeast. As with the Phase III models, we continued to utilize these in the sei whale model as a precautionary decision; see the sei whale supplementary report in Roberts et al. (2016a) for a detailed discussion.

For the updated sei whale model we used the same $g(0)$ estimates as the Phase III model (Table 18); please see the sei whale supplementary report in Roberts et al. (2016a) for a detailed discussion.

Table 18. $g(0)$ estimates used in the updated sei whale model. These are the same as in Roberts et al. (2016a).

Platform	Surveys	Group Size	$g(0)$	Biases Addressed	Source
Shipboard	All	Any	0.63	Perception	Palka (2006)
Shipboard	NEFSC Abel-J Binocular Surveys	Any	0.32	Perception	Palka (2006)
Shipboard	NEFSC Endeavor	Any	0.94	Perception	Palka (2006)
Shipboard	Naked Eye Surveys	Any	0.48	Perception	Palka (2006)
Aerial	All	1-5	0.53	Both	Palka (2006)
		>5	1.00	Both	Palka (2006)

Deemed the “forgotten whale” by a recent review paper, sei whales have received relatively little scientific study compared to the other baleen whales present in the western North Atlantic, and much of the knowledge of sei whale distribution and movements is still based on whaling records (Prieto et al. 2012). Sei whales are thought to follow a typical baleen whale migration pattern, moving to high latitudes in summer to feed and low latitudes in winter to breed or calve. The breeding and calving grounds for sei whales that feed in the Gulf of Maine are still unknown. Prieto et al. (2014) tracked sei whales that departed from the Azores, migrated to the Labrador Sea, and performed movements consistent with feeding. After reviewing these results and other available evidence, they concluded that the Gulf of Maine and the Labrador Sea seem to comprise two discrete feeding grounds utilized simultaneously by sei whales, but that there was insufficient evidence to conclude that sei whales feeding at these locations belonged to distinct biological stocks.

An analysis of whaling records from the Blandford, Nova Scotia whaling station reported two “runs” of sei whales, in June-July and September-October, and speculated that sei whales migrate northward from Cape Cod along the Scotian Shelf in June and July, and return again in September and October (Mitchell 1975). In the Phase III analysis, we observed a similar pattern in sei whale sightings (e.g., see DayOfYear density histogram in Fig. 39). Under the presumption that sei whales exhibit different relationships with the marine environment during different stages of this apparent multi-stage migratory pattern, we opted to fit a four-season model for the Phase III analysis.

The four-season approach had three significant drawbacks. First, in the fall season, defined as October and November, very little survey data were available for the Phase III analysis. What was available was concentrated in the Gulf of Maine, and we were forced to restrict predictions to this area in this season. Second, in the winter season (December-March), so few sei whales were present that we had to fit a stratified model. Because they were both on and off the continental shelf, we included the entire study area in this model. Our preference is to provide a habitat-based, spatially-varying model, when possible. Finally, the summer season (July-September) included a spike in abundance at the beginning of July caused by unrealistic extrapolation in Canadian waters that elevated abundance for that month to unrealistic levels.

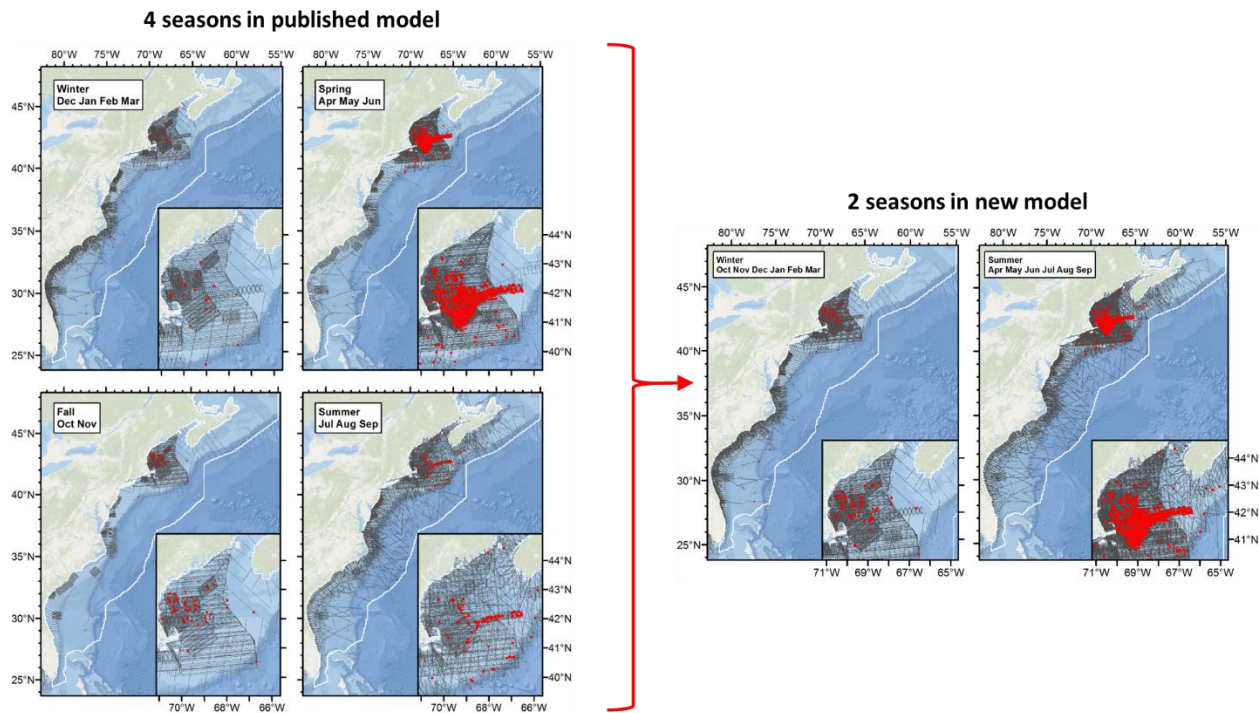


Figure 47. Seasons used in the Phase III sei whale model (left) and the new model presented here (right).

We attempted to address all of these problems by changing the seasonal configuration, including switching to a two-season model, but this yielded different problems, such as unrealistically high abundance along the shelf break south of Georges Bank in spring. Unable to discover a solution in the time available, we retained the four-season model for Phase III.

For the new model, we returned to these problems, anticipating that additional seasonal coverage provided by the newly-incorporated surveys would reduce or eliminate them. After experimenting with different seasonal configurations, we settled on a two season model that combined the spring and summer seasons of the Phase III model into the new summer season (April-September), and the fall and winter seasons of Phase III into the new winter (October-March) (Fig. 47). This configuration greatly expanded the prediction area for October and November, provided a habitat-based model for winter months, and eliminated the unrealistic spike in abundance predicted in Canadian waters in July.

4.2.9.1. Summer model

In the new summer model (April-October), similar to the humpback whale summer model, we fitted a spatial model to the survey data north of the Gulf Stream (Fig. 48), where relatively cold, nutrient-rich waters provide much better feeding habitat than the waters to the south. As with humpbacks, we did not want conditions in the south, where sei whales are clearly absent in this season, to have any possibility of confounding the spatial model in the north.

The model selected for this season was moderately complex, reflecting higher sei whale density on the deep side of the 125m isobath, in cold waters having medium levels of primary productivity measured cumulatively over the prior 90 days. These relationships are consistent with what has been reported about sei whales; the relationship with primary productivity is likely a proxy for some other condition that is of more direct importance to sei whales.

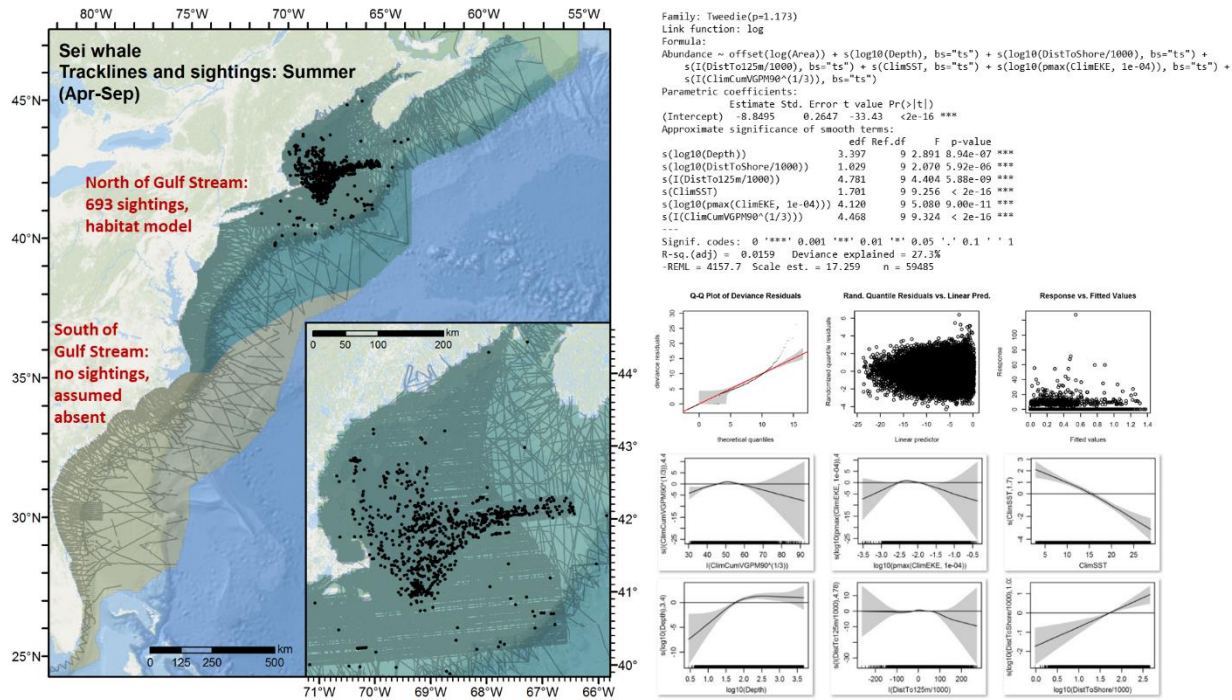


Figure 48. Left: Sei whale summer model schematic. Right: spatial model that was selected as best.

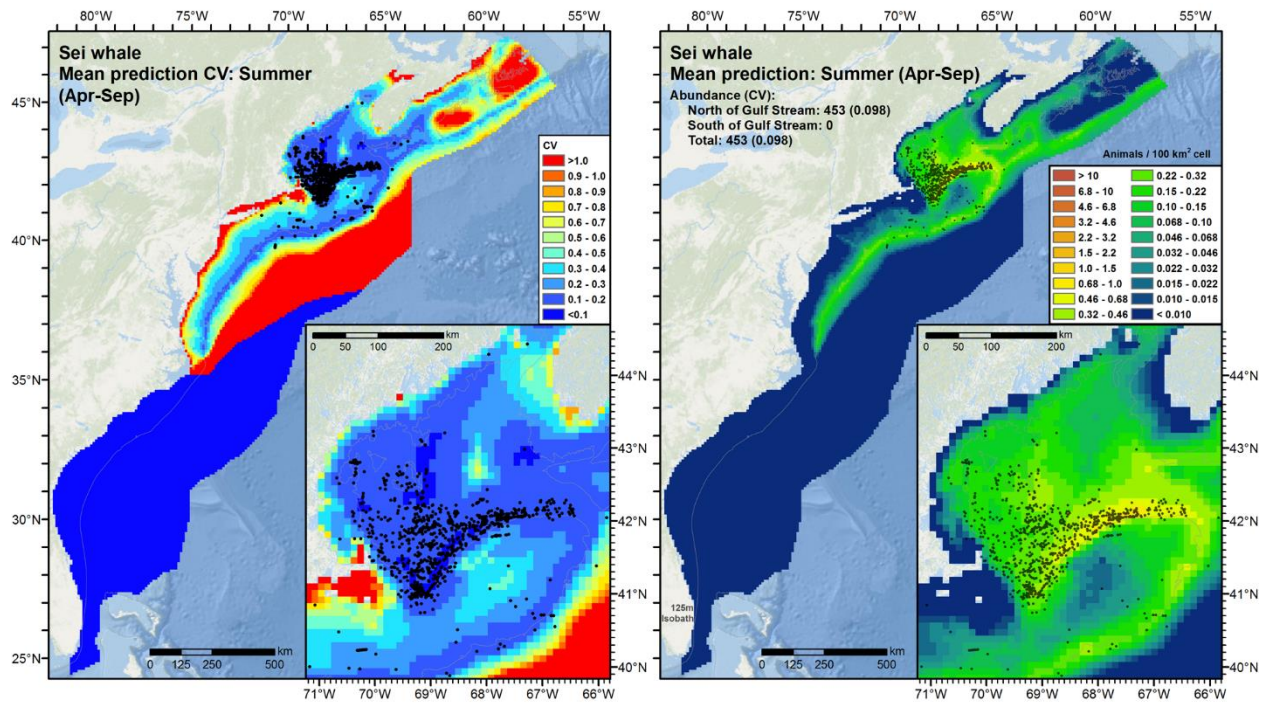


Figure 49. Left: Predicted mean coefficient of variation (CV), with sightings overlaid, for sei whale for the summer season. Right: Predicted mean density and total abundance for sei whale for the summer season.

Predicted mean abundance (Fig. 49) for the first three months of the new summer season (April-June) was close to that predicted by the Phase III model (600 in the new model vs. 627 in Phase III). It was substantially lower in the last three months (July-September) than in Phase III (298 vs. 717) but the new model did not include an unrealistic

spike in abundance; had the Phase III model not included it, it would have predicted a much closer abundance (perhaps 400-500) for those months.

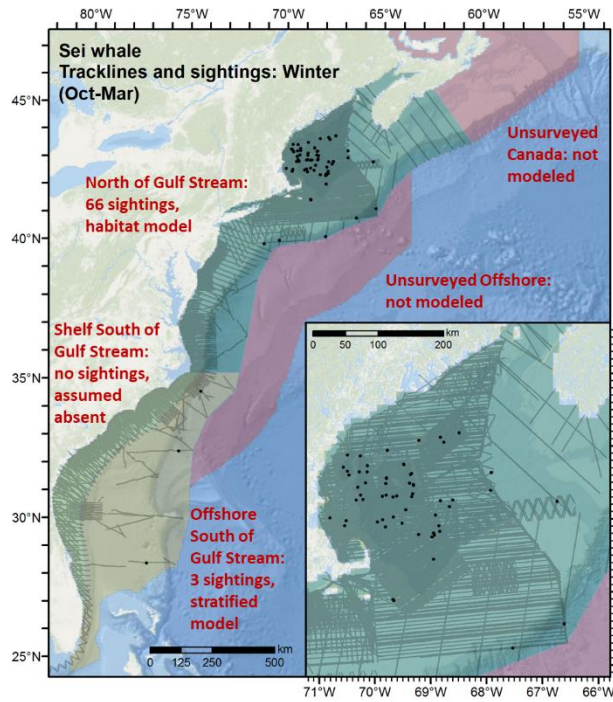
4.2.9.2. *Winter model*

In the new winter model (November-March), all but three sightings occurred north of 40°N, mostly in deeper waters of the Gulf of Maine, with a few sightings scattered along the continental slope of eastern and southern Georges Bank, right at the extreme limit of surveying conducted during this season (Fig. 50). The three sightings in the south were the “Bryde’s and sei whale” sightings reported in 1992. Two occurred over very deep waters, at or beyond the continental slope, while the other occurred over the significantly shallower Blake Plateau.

For our final model configuration (Fig. 50), we fitted a habitat-based model that tightly enclosed survey transects north of Cape Hatteras, where some sei whales were possibly overwintering in the Gulf of Maine, or possibly migrating along the continental slope. South of Cape Hatteras, we fitted a stratified model that included the three offshore sightings, bounded to the west by the shelf break (defined here as the 125m isobath) and the east by the extent of SEFSC shipboard surveys.

The selected model north of the Gulf Stream was relatively simple, with four covariates and mostly linear relationships. Higher density was modeled on the deep side of the 125m isobath in areas of high slope, high zooplankton productivity, and low total kinetic energy (Fig. 50). Low density was predicted throughout the deeper parts of the Gulf of Maine and along the continental slope adjoining the offshore Atlantic. In the offshore area south of Cape Hatteras, very low but non-zero density was estimated by the stratified model of three sightings (Fig. 51).

We experimented with but ultimately discarded various alternative models (e.g. Fig. 52) that grouped survey effort in the south with that in the north, to see what they would predict in the south. Ultimately we were unable to obtain a model that we judged was defensible. The best model exhibited a high CV in an area of high abundance (Fig. 53), and when we reviewed this model with baleen whale experts they believed it was not supportable with the data currently available. When we pointed out that the density predicted near the continental shelf could naively be viewed as similar habitat to what Prieto et al. (2014) observed in the Labrador Sea, they described the Labrador Sea as being rich in zooplankton advected from the arctic against the sub-polar continental slopes—a very different situation than what is found in the western Sargasso Sea. Accordingly we retained the stratified model (Figs. 50, 51) and discarded these alternatives. Additional surveying in the southeast in winter will help resolve uncertainty there, both for sei whales and many other species.



North of Gulf Stream

```

Family: Tweedie(p=1.062)
Link function: log
Formula:
Abundance ~ offset(log(Area)) + s(log10(Slope), bs = "ts") +
s((DistTo125m/1000), bs = "ts") + s(log10(pmax(ClimTKE,
1e-04)), bs = "ts") + s(log10(pmax(ClimPkPP2, 0.1))), bs = "ts")
Parametric coefficients:
Estimate Std. Error t value Pr(>|t|)
(Intercept) -9.8568 0.5243 -18.8 <2e-16 ***
Approximate significance of smooth terms:
s(log10(Slope)) edf Ref.df F p-value ***
s((DistTo125m/1000)) 2.4484 9 3.381 3.71e-08 ***
s(log10(pmax(ClimTKE, 1e-04))) 0.9897 9 0.743 0.005505 **
s(log10(pmax(ClimPkPP2, 0.1))) 0.9957 9 1.704 5.54e-05 ***
---
Signif. codes: 0 '***' 0.001 '**' 0.01 '*' 0.05 '.' 0.1 ' ' 1
R-sq.(adj) = 0.00257 Deviance explained = 14.0%
-REML = 527.04 Scale est. = 10.698 n = 32352

```

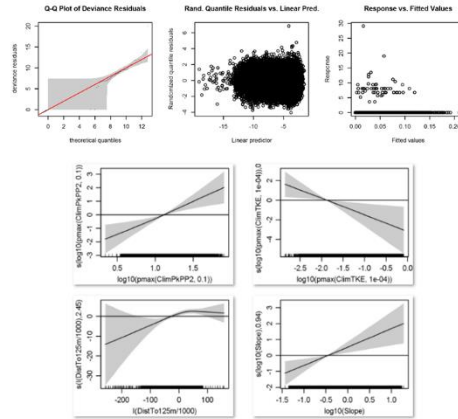


Figure 50. Left: Sei whale winter model schematic. Right: spatial model that was selected as best.

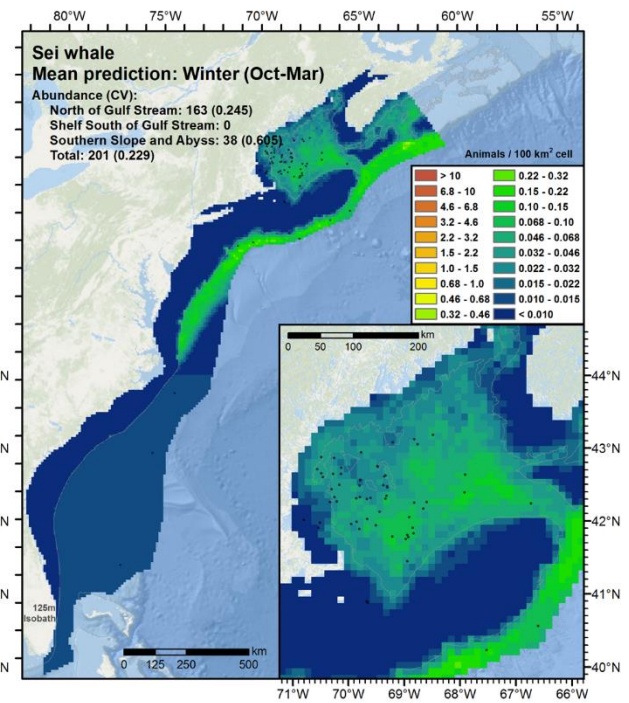
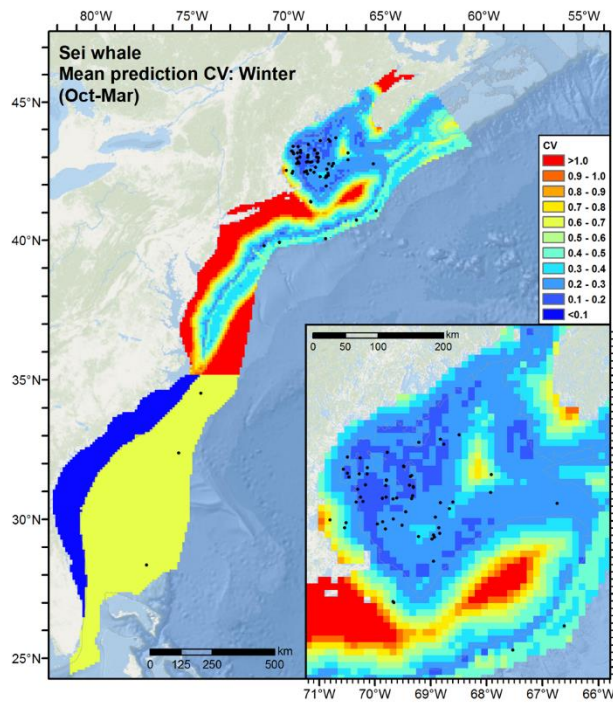


Figure 51. Left: Predicted mean coefficient of variation (CV), with sightings overlaid, for sei whale for the winter season. Right: Predicted mean density and total abundance for sei whale for the winter season.

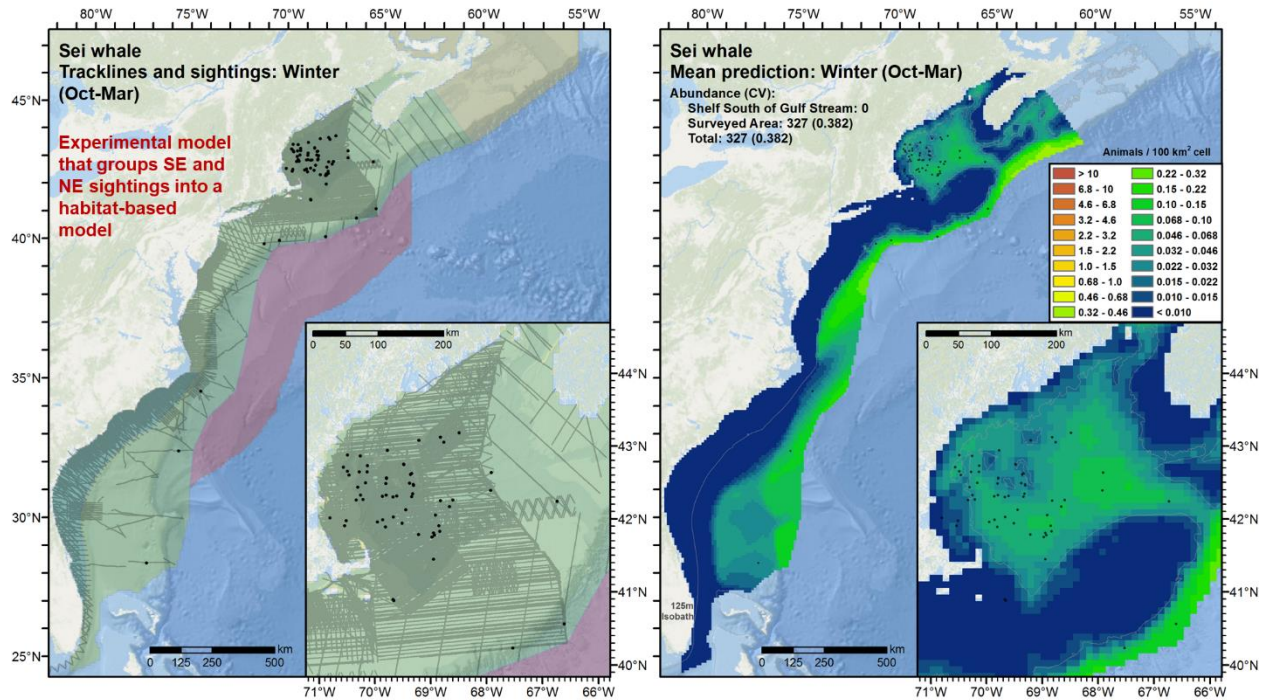


Figure 52. Left: Experimental Sei whale winter model that grouped northern and southern sightings together into a single spatial model. Right: spatial model that resulted. We ultimately discarded this model, as it yielded high CVs (Fig. 53) and lacked other evidence supporting it (see text).

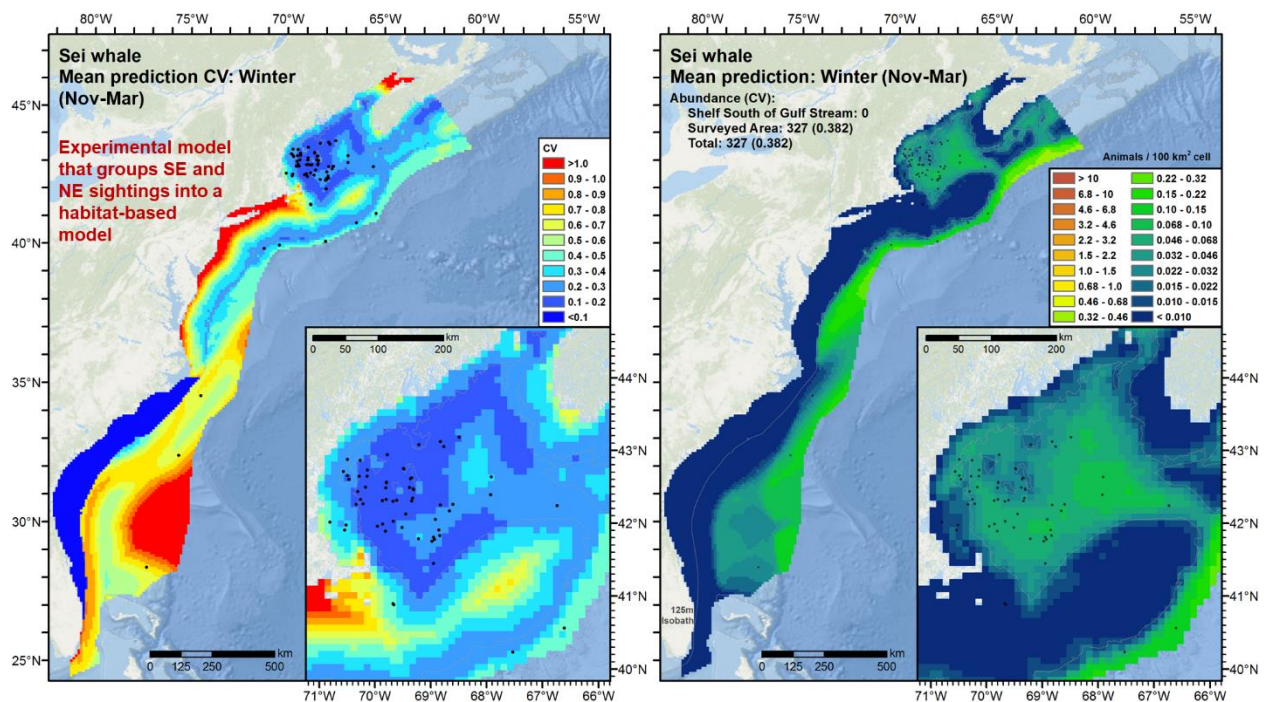


Figure 53. Left: Predicted mean coefficient of variation (CV), with sightings overlaid, for the experimental sei whale model shown in Fig. 52. Note the high CVs predicted in the southeast offshore, where moderate density is also predicted. Right: Density and abundance from Fig. 52, reproduced for comparison.

4.2.10. Minke whale model

The additional surveys incorporated after Phase III modeling added over 450 minke whale sightings (Table 19). Most of these sightings came from the three years of additional surveys from the NEFSC NARWSS program in the Gulf of Maine, which is known minke whale feeding habitat, with a lesser number reported by the NEFSC AMAPPS surveys, mostly in the northeast, and 14 sightings reported by other programs in the mid-Atlantic.

Most sightings, old and new, occurred north of Cape Hatteras on the shelf or, to a lesser degree, along the continental slope. There were two noteworthy exceptions. First, south of Cape Hatteras, 15 sightings were reported close to the shelf break, all along the deep side, spread between three sites in December and March in the years of 2009-2013. Second, a single sighting was reported by an SEFSC shipboard cruise on 10 July, 1998 at latitude 36.84°N very far offshore, approximately 200 km from the shelf break.

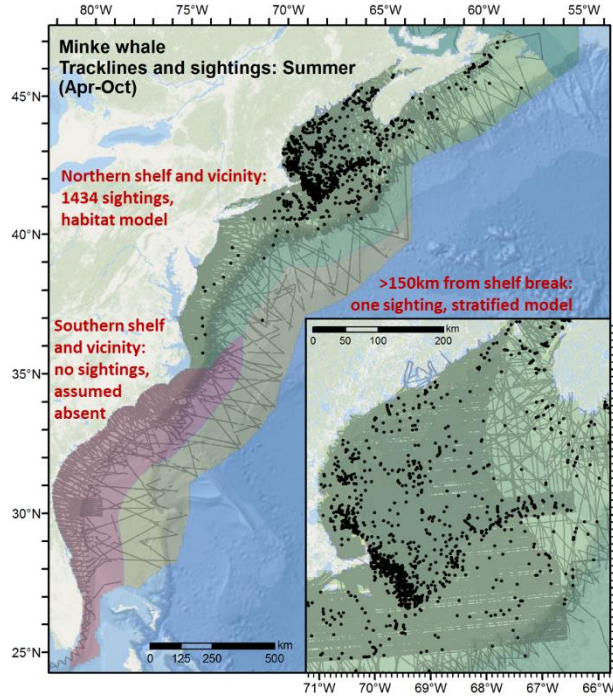
In the North Atlantic, minke whales are believed to follow a typical baleen whale migration pattern, moving to high latitudes in summer to feed and low latitudes in winter to breed or calve. Risch et al. (2014) described minke whale seasonality along the east coast of North America as observed through passive acoustic monitoring. Minkes were detected in high numbers south of Cape Hatteras from December-March, off New York in April and May, and at Stellwagen Bank, and Emerald and Roseway Basins from April through November, with a peak in September and October. Nieukirk et al. (2004) recorded minke whales at sites near the Mid-Atlantic Ridge from November to April, peaking in December-February. Minkes were also previously recorded in the West Indies and Bermuda from October-April (Nieukirk et al. 2004). As with the Phase III model, based on these results and patterns in the sightings, we split the survey data into summer (April-October) and winter (November-March) models.

Table 19. Summary of minke whale sightings available for the updated model. “Extant” sightings were used in the Phase III regional models (Roberts et al. 2016a). “Added” sightings were incorporated during the Base Year and Option Year 1 for the updated models.

Platform	Provider	Program	Minke whale		
			Extant	Added	Total
Aerial	NEFSC	Marine mammal abundance surveys	97	49	146
		NARWSS harbor porpoise survey	6		6
		NARWSS right whale surveys	834	382	1216
	SEFSC	Marine mammal abundance surveys		10	10
	UNCW	Cape Hatteras Navy Surveys	5		5
		Jacksonville Navy Surveys	9		9
		Norfolk Canyon Navy Surveys		3	3
		Onslow Bay Navy Surveys	2		2
	VAMSC	MD Wind Energy Area surveys		1	1
		VA Wind Energy Area surveys	2		2
All			955	445	1400
Shipboard	NEFSC	Marine mammal abundance surveys	101	27	128
	NJDEP	New Jersey Ecological Baseline Study	2		2
	SEFSC	Marine mammal abundance surveys	1		1
	All		104	27	131

Table 20. $g(0)$ estimates used in the updated minke whale model. These are the same as in Roberts et al. (2016a).

Platform	Surveys	Group Size	$g(0)$	Biases Addressed	Source
Shipboard	All	Any	0.69	Both	Palka (2006)
Aerial	All	Any	0.386	Availability	Carretta et al. (2000)



Family: Tweedie(p=1.207)
 Link function: log
 Formula:
 $Abundance \sim offset(\log(Area)) + s(\log_{10}(Depth), bs="ts") + s(\log_{10}(DistToShore/1000), bs="ts") + s((DistTo125m/1000), bs="ts") + s(ClimST, bs="ts") + s((ClimDistToSSTFront2*(1/3)), bs="ts") + s(ClimIndSpeed5Day, bs="ts") + s(\log_{10}(pmax(ClimP1MnkPB1, 0.001)), bs="ts")$
 Parametric coefficients:

Estimate	Std. Error	t value	Pr(> t)	
(Intercept)	-6.47744	0.08656	-74.83	<2e-16 ***

 Approximate significance of smooth terms:

	edf	Ref.df	F	p-value
s(log10(Depth))	6.2494	9	10.567	< 2e-16 ***
s(log10(DistToShore/1000))	4.3912	9	4.523	2.14e-09 ***
s((DistTo125m/1000))	6.7802	9	36.757	< 2e-16 ***
s(ClimST)	4.3788	9	15.715	< 2e-16 ***
s((ClimDistToSSTFront2*(1/3)))	0.9012	9	0.778	0.00496 **
s(ClimIndSpeed5Day)	1.2613	9	7.786	< 2e-16 ***
s(log10(pmax(ClimP1MnkPB1, 0.001)))	4.5646	9	8.739	< 2e-16 ***

 Signif. codes: 0 '***' 0.001 '**' 0.01 '*' 0.05 '.' 0.1 ' ' 1
 R-sq.(adj) = 0.0171 Deviance explained = 20.4%
 -REML = 7827.2 Scale est. = 16.301 n = 64512

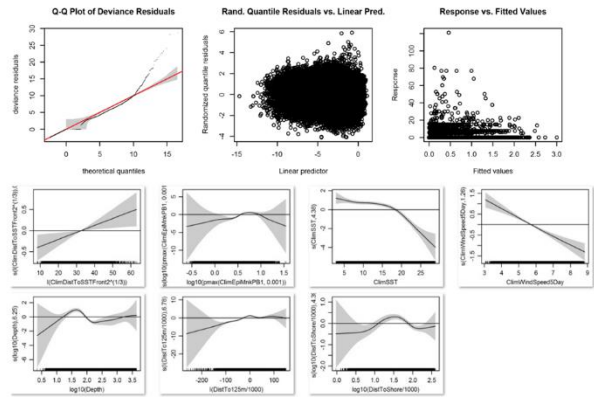


Figure 54. Left: Minke whale summer model schematic. Right: spatial model that was selected as best.

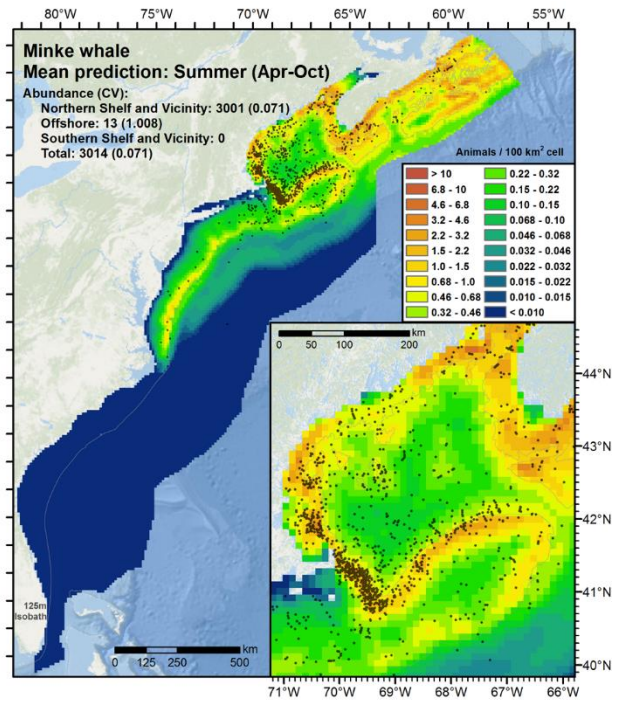
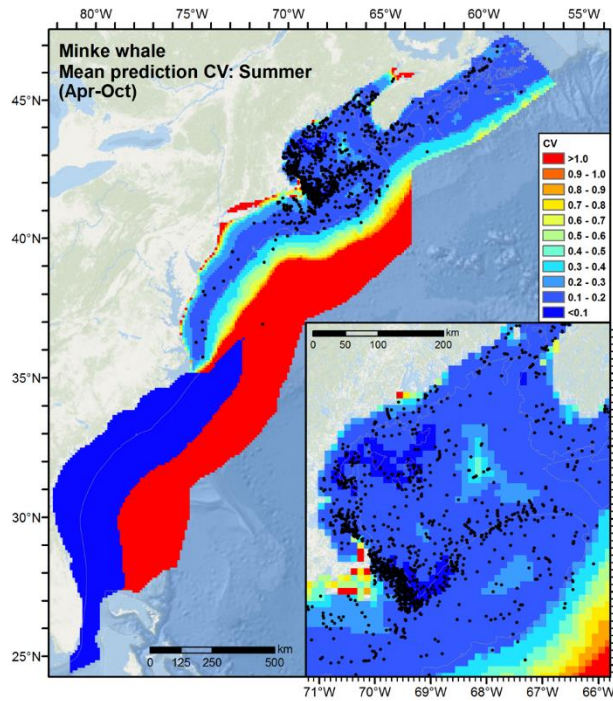


Figure 55. Left: Predicted mean coefficient of variation (CV), with sightings overlaid, for minke whale for the summer season. Right: Predicted mean density and total abundance for minke whale for the summer season.

For the updated minke whale model we used the same $g(0)$ estimates as the Phase III model (Table 20); please see the minke whale supplementary report in Roberts et al. (2016a) for a detailed discussion.

4.2.10.1. Summer model

In summer, as with other baleen whale species, we split the study area at Cape Hatteras at the north wall of the Gulf Stream and fitted a habitat-based model to data north of here (Fig. 54). To account for the offshore July 1998 outlier, we stopped the habitat model 150km from the shelf break and fitted a stratified model to surveys beyond. The offshore sighting actually occurred in the warm waters of the Gulf Stream, therefore we included waters both north and south of the Gulf Stream in the stratified model. This yielded a large area of very low density, reflecting our supposition that this sighting was rare and extralimital for minke whales in the summer.

The main model selected as best was of medium-high complexity, with seven covariates retained. Minke whale density was modeled highest at shallower depths and closer to shore than most of the other baleen whale species, in cold waters having relatively high biomass of epipelagic micronekton, indicative of prey. Mean seasonal density and total abundance (Fig. 55) were predicted to be higher than for the Phase III models (3014 vs. 2083). The new models incorporated additional sightings in the mid-Atlantic, along the continental slope adjoining the offshore Atlantic, and along the Scotian Shelf. Accordingly, the new predictions estimate higher density throughout these regions. We believe these predictions are realistic and reflect improved seasonal survey coverage.

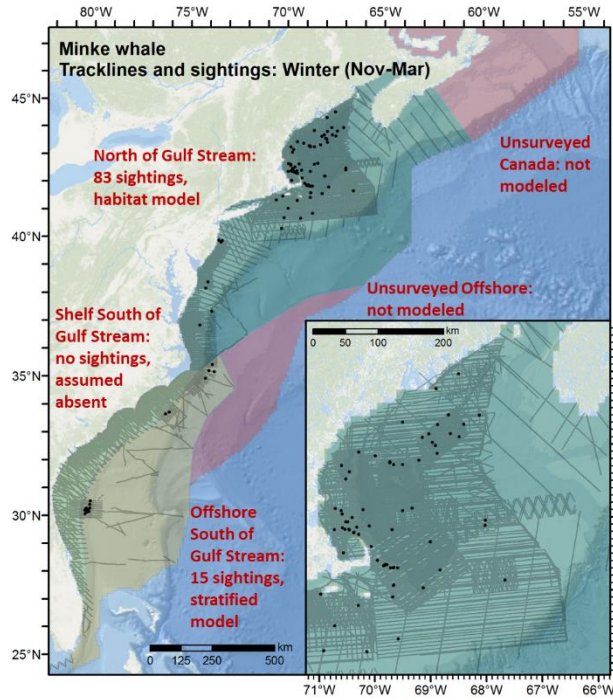
4.2.10.2. Winter model

In winter, most sightings were reported north of Cape Hatteras on the continental shelf (Fig. 56). 15 sightings were reported south of Cape Hatteras close to the shelf break (defined here as the 125m isobath), all along the deep side, at three different sites. Similar to the sei whale model, we split the study area at Cape Hatteras and fitted a habitat-based model to surveys north of the Gulf Stream. This model differed from the winter sei whale model in that we did not clip the modeled region closely to the geographic extent of the surveys, but instead allowed it to predict offshore. Because nearly all of the sightings were fully up on the shelf and some distance inside the eastern limit of surveying—rather than having a number distributed along the slope right at the edge of the survey limits, as with sei whales—we were comfortable allowing the model to extrapolate across the deeper waters of the study area north of the Gulf Stream. The resulting model (Fig. 56) was simple, modeling high density in cold waters at a specific depth range, but also at increasing distances from the 125m isobath. We believe this last relationship was used to model reduced density at nearshore locations distant from the shelf break, such as Long Island Sound and other inshore areas of the U.S. east coast.

In the south, as with sei whales, we fitted a stratified model to survey effort on the deep side of the shelf break, defined here as the 125m isobath (Fig. 56). No minke whales were reported by any survey programs on the shallow side, and Risch et al. (2014) reported that acoustic instruments deployed near Jacksonville, Florida deployed on both sides of the shelf break only detected minke whales on the deep side. To the north, we bounded the model at the north wall of the Gulf Stream. To the east, we bounded it by the eastern extent of SEFSC shipboard surveys.

As with the Phase III winter minke whale model, the resulting density and total predictions (Fig. 57) were higher in the southern stratified model than in the northern habitat based area. In the northern area, total abundance increased relative to the Phase III model (249 vs. 149), reflecting both an expansion of the study area north into Canada (enabled by AMAPPS wintertime aerial surveying) and increased density predicted for the mid-shelf in the mid-Atlantic and also the deeper waters of the Gulf of Maine. In the southern area, total abundance decreased relative to Phase III (404 vs. 591), despite an expansion of the study area, reflecting the fact that additional survey effort was added with no new sightings.

As in Phase III, we studied alternative model designs for the southern area. For example, we tested habitat-based models that incorporated both northern and southern sightings, but all of these models predicted high, isolated minke whale density in the Gulf Stream (Fig. 58), which flows along the deep side of the shelf break in this area. Risch et al. (2014) advanced a hypothesis that minke whales might use the Gulf Stream during migrations north in the spring. These alternative models would be consistent with that hypothesis, however when we discussed this with D. Risch as part of the Phase III analysis, she shared our view that evidence is too limited at this time to draw such a distinct conclusion. We revisited this discussion again for the current models with other baleen whale experts and they agreed that the more cautious stratified model (Figs. 56, 57) is appropriate until more evidence can be gathered to support such a strong winter affinity to the Gulf Stream or shelf break in the southeast.



North of Gulf Stream

```

Family: Tweedie(p=1.171)
Link function: log
Formula:
Abundance ~ offset(log(Area)) + s(log10(Depth), bs = "ts") +
s(I(DistTo125m/1000), bs = "ts") + s(ClimSST, bs = "ts")
Parametric coefficients:
              Estimate Std. Error t value Pr(>|t|)
(Intercept) -7.8420      0.2011     -39  <2e-16 ***
Approximate significance of smooth terms:
              edf Ref.df F p-value
s(log10(Depth))  3.3652      9  1.972 0.000141 ***
s(I(DistTo125m/1000)) 0.9082      9  0.786 0.004342 **
s(ClimSST)        0.8865      9  0.726 0.006118 **
---
Signif. codes:  0 '***' 0.001 '**' 0.01 '*' 0.05 '.' 0.1 ' ' 1
R-sq.(adj) = 0.00112  Deviance explained = 7.93%
-REML = 607.17  Scale est. = 19.947  n = 26662
  
```

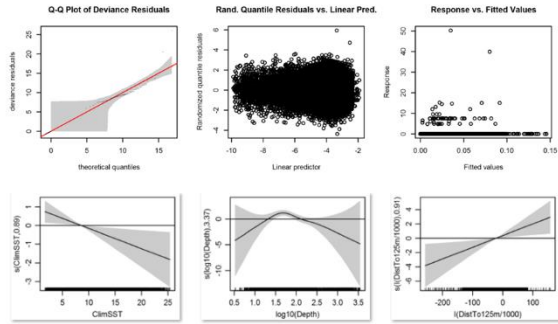


Figure 56. Left: Minke whale winter model schematic. Right: spatial model that was selected as best.

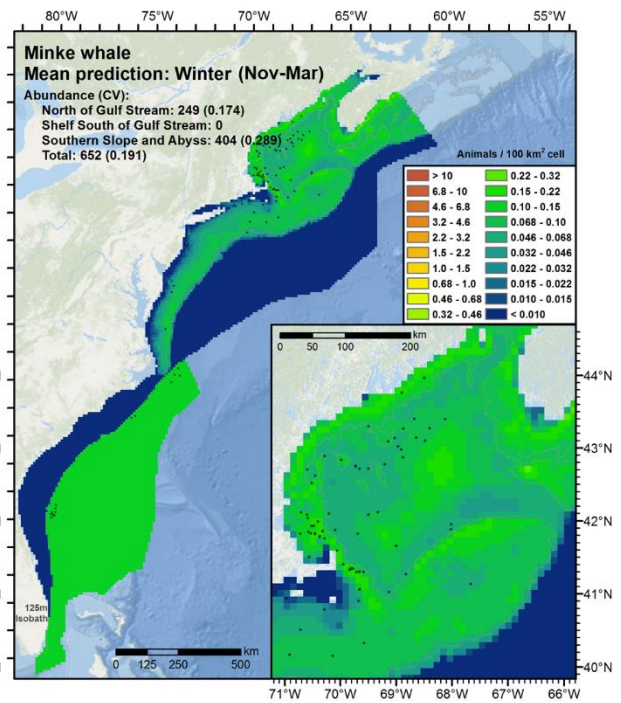
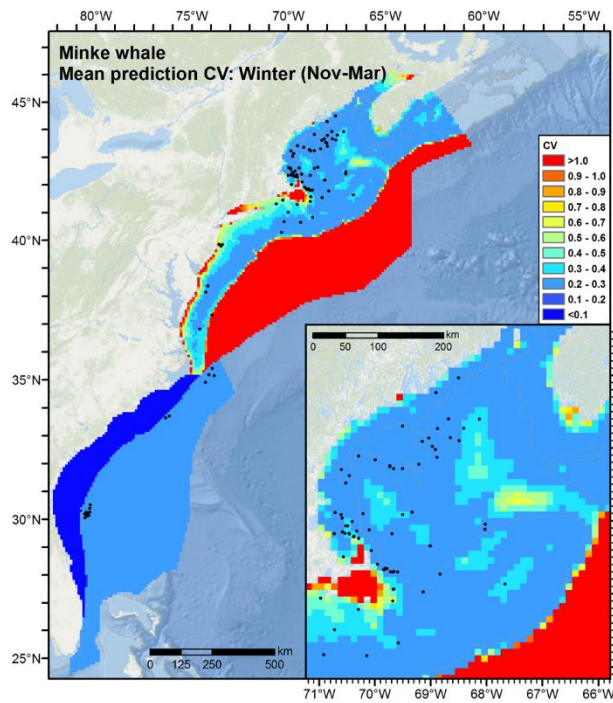


Figure 57. Left: Predicted mean coefficient of variation (CV), with sightings overlaid, for minke whale for the winter season. Right: Predicted mean density and total abundance for minke whale for the winter season.

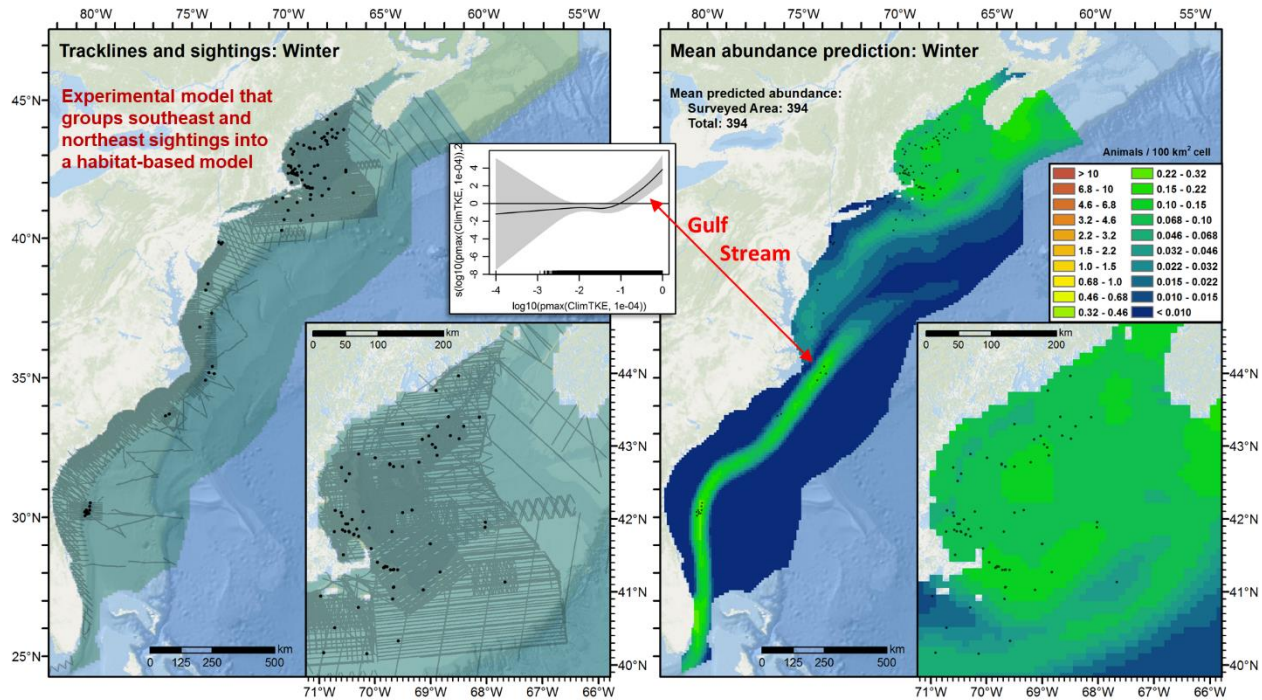


Figure 58. Left: Experimental minke whale winter model that grouped northern and southern sightings together into a single spatial model. Right: spatial model that resulted. Inset: covariate plot showing the relationship fitted to total kinetic energy (TKE), predicting high density in the Gulf Stream, the region of highest TKE in the study area. We ultimately discarded this model (see text).

4.2.11. North Atlantic right whale model

The additional surveys incorporated after Phase III modeling added over 2800 right whale sightings (Table 21), more than doubling the number available for modeling. Over 2500 were reported by the SEUS NARW survey programs, which contributed over 1.3 million km of aerial survey effort (Table 2). These were concentrated on the calving grounds during December through March (Fig. 59), with reduced numbers in the transition months of November and April, when fewer whales are believed to be on the calving grounds (but also when fewer surveys were conducted). We explicitly integrated the SEUS NARW sightings to improve our winter model of right whale density, which in Phase III was based only about 20 sightings and encompassed the area from Nantucket to southern Florida in a single model. (We discuss problems and improvements further in the winter model section below.)

In the northeast, the NARWSS and NEFSC AMAPPS programs contributed nearly 300 additional sightings, spread across all seasons, boosting the total number available in the region by about 17%. In the mid-Atlantic, an area difficult to model because of the few sightings available, the VAMSC / Riverhead Foundation survey of the Maryland Wind Energy Area and SEFSC AMAPPS sightings contributed a total of 10 sightings split across winter and spring, allowing us to improve the model of the mid-Atlantic in both seasons.

Right whales are the most critically endangered cetacean on the U.S. east coast and our objective was to re-examine all aspects of the right whale model and make as many improvements as possible. Accordingly, before revising the spatial models we revisited our $g(0)$ estimates to try and improve the models' handling of availability and perception bias.

Table 21. Summary of North Atlantic right whale sightings available for the updated model. “Extant” sightings were used in the Phase III regional model (Roberts et al. 2016a). “Added” sightings were incorporated during the Base Year and Option Year 1 for the updated model.

Platform	Provider	Program	Right whale		
			Extant	Added	Total
Aerial	NEFSC	Marine mammal abundance surveys	38	14	52
		NARWSS harbor porpoise survey	2		2
		NARWSS right whale surveys	1579	250	1829
	SEFSC	Marine mammal abundance surveys	5	6	11
		SEUS NARW FWRI surveys		797	797
			NEAq surveys		945
		SSA surveys (Skymaster)		174	174
		SSA surveys (Twin Otter)		649	649
	UNCW	Jacksonville Navy Surveys	2		2
		Marine mammal surveys, 2002	5		5
		Right whale surveys, 2005-2008	18		18
	VAMSC	MD Wind Energy Area surveys		5	5
		VA Wind Energy Area surveys	5		5
	All			1654	2840
Shipboard	NEFSC	Marine mammal abundance surveys	11	20	31
	NJDEP	New Jersey Ecological Baseline Study	2		2
	SEFSC	Marine mammal abundance surveys	1	1	2
	All		14	21	35

4.2.11.1. $g(0)$ estimates

In the Phase III right whale model, we configured $g(0)$ according to platform (aerial or shipboard), group size, and geography, using the latter as a proxy for behavior (e.g. right whales taking deeper dives at northern feeding grounds vs. spending more time at the surface at winter calving grounds). The right whale supplementary report of Roberts et al. (2016a) discusses the $g(0)$ estimates used for the Phase III model in detail.

In the updated model, we were able to improve our $g(0)$ estimates for aerial surveys in two ways. First, in the southeast, we sought to better utilize Hain et al.’s (1999) estimates of $g(0)$ based on the presence of calves. The >2500 sightings contributed by the SEUS NARW surveys all reported the number of calves per sighting. We cross-referenced this information, along with group size, to Hain et al.’s (1999) estimates and applied them to all sightings reported south of Cape Hatteras (Table 22). The waters south of Cape Hatteras are warm and relatively poor in the zooplankton that right whales prefer to consume at the summer feeding grounds to the north. Thus we judged right whale behavior here is more likely to resemble that of the calving grounds than of the Gulf of Maine, which was the other location from which we had data upon which to base $g(0)$ estimates.

Second, in the northeast, the right whale dive times reported for the southern Gulf of Maine (CETAP 1982), upon which we based our $g(0)$ estimates for Phase III, were notably shorter than those reported at more northerly feeding areas, where right whales were reported to be feeding on deep zooplankton aggregations (Baumgartner & Mate 2003). Most of the northeast sightings we had in Phase III were from the southern Gulf of Maine, and our analysis workflow at the time could not apply different $g(0)$ estimates with high geographical precision, so we utilized a $g(0)$ derived from the southern Gulf of Maine for all sightings in the northeast while acknowledging this potential bias (Roberts et al. 2016a). In the updated model, we were able to apply different $g(0)$ estimates in the northern basins, deriving $g(0)$ from the longer dive times observed there (Table 23). We also applied Hain et al.’s (1999) estimate of $g(0)$ for surface active groups (SAGs) to sightings of 5 or more animals, under the assumption that groups of this size were likely to display SAG-like behavior.

For shipboard surveys, in the updated right whale model we used the same $g(0)$ estimates as the Phase III model (Table 24); please see the right whale supplementary report in Roberts et al. (2016a) for a detailed discussion.

Table 22. Aerial $g(0)$ estimates from Hain et al. (1999), used for right whales sighted south of Cape Hatteras. Nearly all sightings listed here are from the SEUS NARW surveys of Florida, Georgia, and South Carolina. <5 sightings had a Group Size of 2 and Calf Present of “unknown”. SAG = surface active group.

Group size	Calf present	$g(0)$	Count	Notes
1	Ignored	0.434	432	$g(0)$ for single juvenile. Hain et al. did not give a $g(0)$ for single adults. Count includes 4 sightings of single calves.
2	Yes or unknown	0.729	1202	$g(0)$ for mother/calf pairs.
2	No	0.861	347	$g(0)$ for SAGs. Hain et al. included SAG of 2 in their estimate. Data providers did not systematically classify sightings as displaying SAG behavior or not.
≥ 3	Ignored	0.861	609	$g(0)$ for SAGs.

Table 23. Aerial $g(0)$ estimates used for right whales sighted north of Cape Hatteras. Most of these are from the NEFSC NARWSS program. SAG = surface active group.

Group size	Location	$g(0)$	Count	Notes
1-4	Southwest of Canadian basins	0.334	1550	From dive data reported by CETAP (1982) for whales at Stellwagen Bank, east of Cape Cod, and Great South Channel: surface 2.58 min, dive 5.65 min
1-4	Canadian basins and northeast	0.216	60	From dive data reported by Baumgartner and Mate (2003) for whales at lower Bay of Fundy and Roseway Basin: surface 3.13 min, dive 12.17 min
≥ 5	Everywhere	0.861	322	From Hain et al. (1999): $g(0)$ for SAGs

Table 24. Shipboard $g(0)$ estimates for right whales, all locations. These are the same as in Roberts et al. (2016a).

Surveys	Group Size	$g(0)$	Biases Addressed	Source
Binocular Surveys	Any	0.63	Perception	Palka (2006)
NEFSC Abel-J Binocular Surveys	Any	0.32	Perception	Palka (2006)
NEFSC Endeavor	Any	0.94	Perception	Palka (2006)
Naked Eye Surveys	Any	0.38	Perception	Palka (2006)

4.2.11.2. Season definitions

In Phase III, many aspects of our model were constrained by lack of data in the southeast in fall, winter, and spring. The seasonal definitions were determined, in part, by a need to produce a winter spatial prediction that accorded with what had already been learned about spatial distribution on the calving grounds (Keller et al. 2006; Good 2008; Keller et al. 2012; Gowan & Ortega-Ortiz 2014). The limited numbers of sightings available in different months for the Phase III model forced compromises that we would otherwise not have chosen, such as to start the winter season in November rather than December. With a very large number of sightings now available at the calving grounds, we were able to revise our seasonal definitions (Fig. 59) to better agree with what is known of right whale seasonal and spatial dynamics.

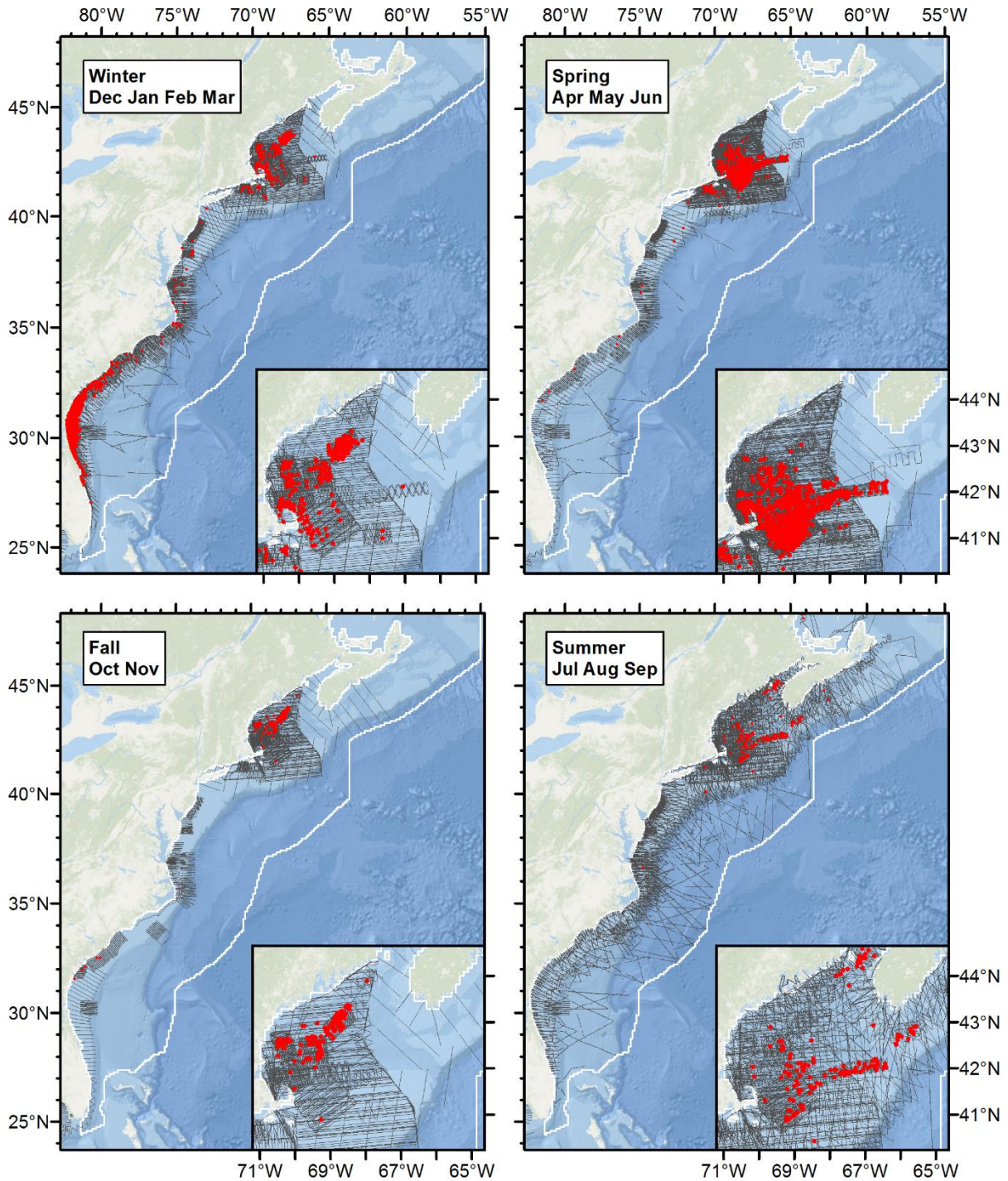


Figure 59. Season definitions used in the updated right whale model, with survey effort (grey lines) and right whale sightings (red).

First, we shifted definition of winter from November-February (Phase III model) to December-March (updated model). Patterns in aerial sightings (Gowan & Ortega-Ortiz 2014) and acoustic detections (Soldevilla et al. 2014) suggest December-March represents the core period in which right whales are most likely to be present at the calving grounds. In the northeast, this period is the time that right whales move from Canada and the northern Gulf

of Maine to the south and west and congregate in and near Cape Cod Bay (Kenney et al. 2001; Nichols et al. 2008; Brillant et al. 2015).

Next, we adjusted spring from February-March to April-June. In the updated models, spring represents the season that right whales in the northeast move east out of Cape Cod Bay into the Great South Channel and the northern slope of Georges Bank, with some starting north to Canadian waters (Kenney et al. 1996, 2001; Brillant et al. 2015). In the southeast and mid-Atlantic, the northward migration that started in late winter finishes up and most nearly all right whales are north of New York (Knowlton et al. 2002; Firestone et al. 2008) (but we caution that recent results suggest right whales may be detected in the mid-Atlantic and southeast U.S. during all parts of the year (Knowlton et al. 2002; Whitt et al. 2013; Oedekoven et al. 2015; Hodge et al. 2015)).

Finally, we adjusted summer from May-July to July-September and fall from August-October to October-November. In the updated models, summer represents the season that right whales typically depart the southern Gulf of Maine and move to feed in northern basins such as the Grand Manan Basin, Roseway Basin, and Emerald Basin (Kenney et al. 2001; Mellinger et al. 2007; Brillant et al. 2015), while fall is the season they move south and west to the central Gulf of Maine and Jeffreys Ledge area (Weinrich et al. 2000; Cole et al. 2013; Brillant et al. 2015). Overall, across the seasons, the concentrations of sightings shift around the Gulf of Maine in a counter-clockwise pattern, as has been previously noted (Brillant et al. 2015).

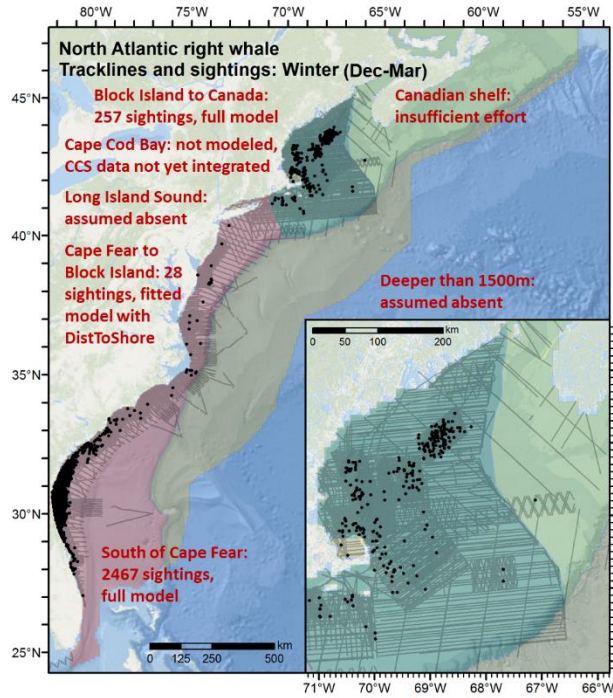
4.2.11.3. *Winter model*

In winter, we split the study area into several regions (Fig. 60) based on reports of right whale distribution and behavior in the literature and patterns we observed in the surveys available to us. First, we assumed abundance would be zero in waters deeper than 1500m. Although right whales have been observed moving into waters this deep (Baumgartner & Mate 2005), neither the surveys available to us nor the literature suggests these waters are suitable habitat for this species. Next, we excluded waters north of the U.S.-Canada boundary in the Gulf of Maine, which were relatively unsurveyed during this season. The remaining area, the U.S. continental shelf and upper slope, we split into three regions and fitted separate models to each, under the assumption that right whales exhibit different species-environment relationships in these areas, according to the differing behaviors there.

We defined the southernmost region as the waters south of Cape Fear, North Carolina, based on this being the northernmost extent of the recently-revised North Atlantic Right Whale Critical Habitat Southeastern U.S. Calving Area (50 C.F.R. 226.203 2016). This area received more survey effort than any other elsewhere in our study area—approximately 1.3 million km of aerial surveys from 2003-2016, which reported nearly 2500 sightings of during these months (December-March). Accordingly, the resulting model (Fig. 60, upper right) was complex, retaining eight covariates.

Mean total abundance predicted for this area ranged from a low of 28 in December to a high of 66 in February (Figs. 62-65), with a seasonal mean of 47 (Fig. 61). These predictions are substantially lower than in the Phase III model (Roberts et al. 2016a), but that model was based on only 21 sightings, extended from southern Florida to Nantucket, had a relatively high CV of 0.64 from the spatial model alone (detection function and $g(0)$ uncertainties were not included), and had covariates selected manually to obtain a prediction that concentrated density in the known calving area. The new model overcame all of these drawbacks and thereby offers more realistic abundance estimates. We believe these are the first such absolute abundance estimates for the southeast calving grounds.

Despite these improvements, we advise considerable caution until these results can be studied further, both by us and right whale species experts. The model's density and abundance estimates depend heavily on the $g(0)$ estimates that were used. These estimates (Hain et al. 1999) were derived from data collected in the 1990s and based on observations of a limited number of individuals. The seasonal mean of 47 predicted by our model represents only about 10% of the present-day population, which was recently estimated to have risen from 270 in 1990, peaked at 483 in 2010 and declined to 458 in 2015 (Pace et al. 2017). From the 2006/07 – 2015/16 calving seasons, the number of photo-documented calves varied widely, with a low of 7 in 2012 and a high of 39 in 2009 (Pettis & Hamilton 2016). Work by the Florida Fish and Wildlife Research Institute to estimate abundance in the southeast by synthesizing many years of photographic identifications is reaching completion; this research, when available, should provide a very interesting basis for comparison.

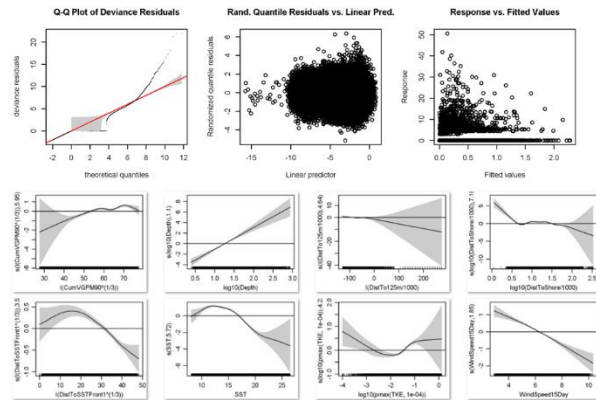


South of Cape Fear

```

Family: Tweedie(p=1.067)
Link function: log
Formula:
Abundance ~ offset(log(Area)) + s(log10(Depth), bs = "ts") +
s(log10(DistToShore/1000), bs = "ts") + s(I(DistToShore/1000),
bs = "ts") + s(SST, bs = "ts") + s(I(DistToSSTFront1*(1/3)),
bs = "ts") + s(CumVGP90*(1/3)), bs = "ts") + s(I(CumVGP90*(1/3)),
bs = "ts") + s(log10(pmax(TKE, 1e-04)), bs = "ts")
Parametric coefficients:
Estimate Std. Error t value Pr(>|t|)
(Intercept) -7.19759 0.05652 -127.3 <2e-16 ***
Approximate significance of smooth terms:
edf Ref.df F p-value
s(log10(Depth)) 1.095 9 12.502 <2e-16 ***
s(log10(DistToShore/1000)) 7.176 9 20.304 <2e-16 ***
s(I(DistToShore/1000)) 4.644 9 7.198 2.79e-15 ***
s(SST) 5.718 9 75.153 <2e-16 ***
s(I(DistToSSTFront1*(1/3))) 3.501 9 12.496 <2e-16 ***
s(WindSpeed15day) 1.848 9 22.170 <2e-16 ***
s(I(CumVGP90*(1/3))) 5.948 9 10.808 <2e-16 ***
s(log10(pmax(TKE, 1e-04))) 4.235 9 9.583 <2e-16 ***
---
Signif. codes: 0 '***' 0.001 '**' 0.01 '*' 0.05 '.' 0.1 ' ' 1
R-sq.(adj) = 0.0198 Deviance explained = 14.2%
-REML = 16507 Scale est. = 7.5363 n = 136915

```

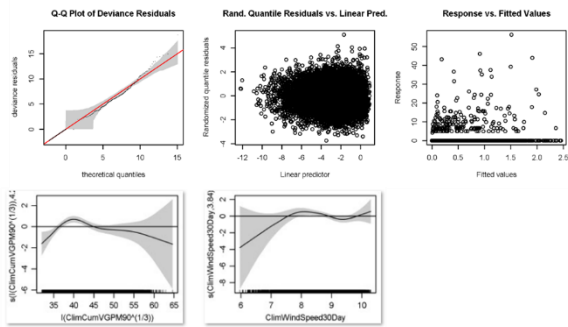


Block Island to Canada

```

Family: Tweedie(p=1.197)
Link function: log
Formula:
Abundance ~ offset(log(Area)) + s(x, y, bs="ts", k=50) +
s(ClimWindSpeed30Day, bs="ts") + s(I(ClimCumVGP90*(1/3)), bs="ts")
Parametric coefficients:
Estimate Std. Error t value Pr(>|t|)
Signif. codes: 0 '***' 0.001 '**' 0.01 '*' 0.05 '.' 0.1 ' ' 1
Approximate significance of smooth terms:
edf Ref.df F p-value
s(x,y) 28.423 49 3.757 <2e-16 ***
s(ClimWindSpeed30Day) 3.840 9 1.526 0.00233 **
s(I(ClimCumVGP90*(1/3))) 4.204 9 2.899 5.59e-06 ***
---
Signif. codes: 0 '***' 0.001 '**' 0.01 '*' 0.05 '.' 0.1 ' ' 1
R-sq.(adj) = 0.0323 Deviance explained = 20%
-REML = 1585.4 Scale est. = 16.485 n = 11684

```



Cape Fear to Block Island

```

Family: Tweedie(p=1.317)
Link function: log
Formula:
Abundance ~ offset(log(Area)) + s(DistToShore, bs = "ts")
Parametric coefficients:
Estimate Std. Error t value Pr(>|t|)
(Intercept) -8.142 0.758 -10.74 <2e-16 ***
Approximate significance of smooth terms:
edf Ref.df F p-value
s(DistToShore) 3.389 9 1.032 0.0241 *
---
Signif. codes: 0 '***' 0.001 '**' 0.01 '*' 0.05 '.' 0.1 ' ' 1
R-sq.(adj) = 0.000147 Deviance explained = 9.1%
-REML = 312.72 Scale est. = 73.671 n = 16615

```

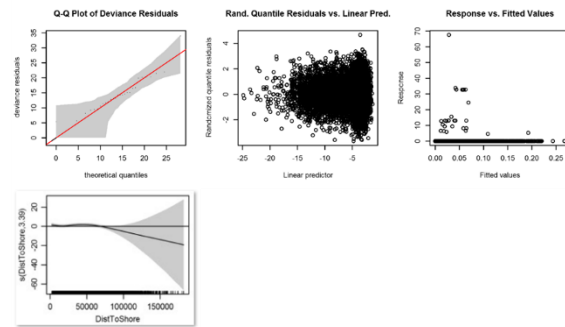


Figure 60. North Atlantic right whale winter model schematic with statistical models selected as best in each of the three regional models. The South of Cape Fear region encloses the core calving grounds. Block Island to Canada contains right whales overwintering on the core feeding grounds. Cape Fear to Block Island represents intermediate or migratory habitat between the feeding and calving grounds.

The second region we defined spanned waters from Block Island to Canada (Fig. 60), intended to represent feeding and overwintering habitat. Here, all geographic areas had been surveyed and we included a static bivariate smooth of location (longitude and latitude coordinates projected to an appropriate coordinate system with GIS) among the candidate models as a proxy for spatially-varying covariates not incorporated in the model (Miller et al. 2013). This covariate was retained, along with two others that drove dynamics in the model. Predicted mean seasonal abundance was 162 (Fig. 61), with medium to low CVs in areas of low to medium abundance.

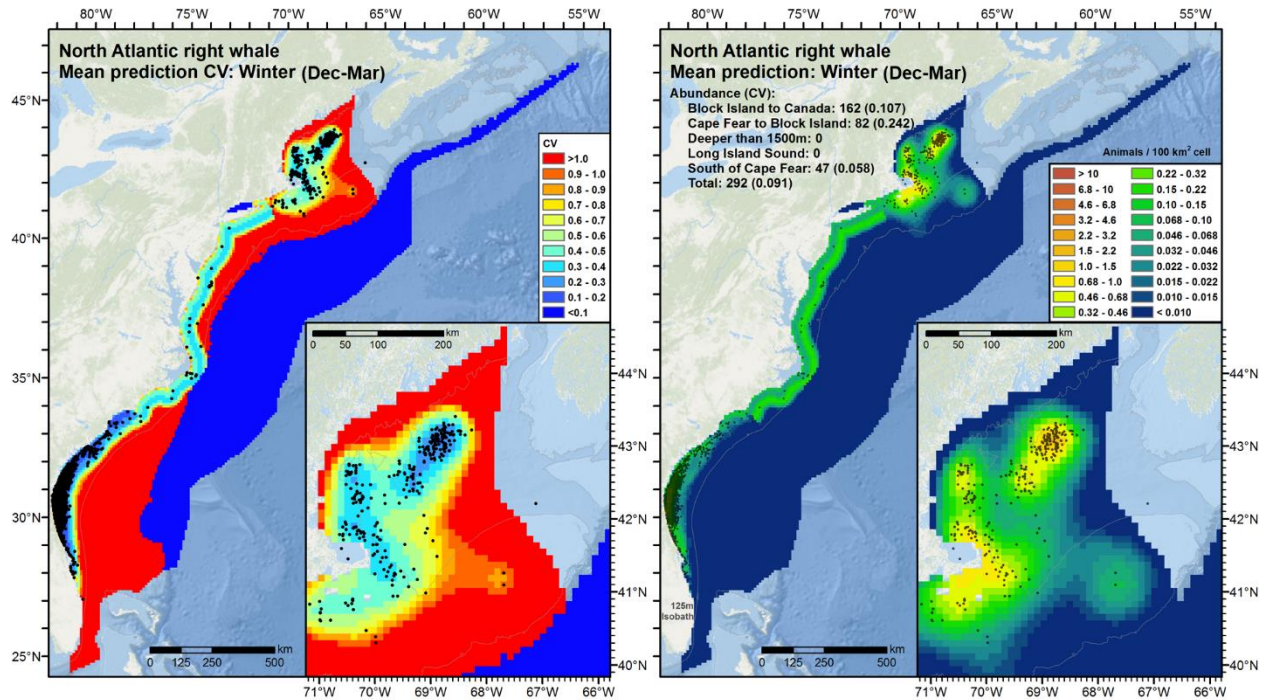


Figure 61. Left: Predicted mean coefficient of variation (CV), with sightings overlaid, for North Atlantic right whale for the winter season. Right: Predicted mean density and total abundance.

We note that we excluded Cape Cod Bay (CCB) from the model and predictions. CCB has been extensively surveyed by the Center for Coastal Studies (CCS) in Provincetown, Massachusetts, but the CCS surveys do not collect perpendicular distances to sightings and therefore require special treatment to be used under our methodology. CCB is a known winter and spring feeding area where large aggregations of right whales have been observed—for instance, CCS surveys reported 47 whales sighted in a single day, not corrected for availability or perception bias, on 4 March 1998 and 27 March 2000 (Nichols et al. 2008). Thus CCB represents an area that we cannot easily account for with the data currently utilized by our model, and total abundance should be considered an underestimate. In the future, we hope to collaborate with CCS to complete the work necessary to prepare and integrate the CCS surveys into a revised model that offers predictions for CCB.

The third region we defined spanned the area between Cape Fear and Block Island. In this region, a migration corridor between the southern calving grounds and northern feeding grounds, only 28 sightings were reported, scattered from North Carolina to New York. Survey effort was biased geographically; regional programs in Virginia, Maryland, and New Jersey surveyed certain areas monthly with densely-placed tracklines, while everywhere else was surveyed less frequently, mainly by AMAPPS. The small number of sightings necessitated a limited model. Considering this, and the fact that important habitats existed both north and south of this corridor, and that the sightings displayed a pattern of relatively few sightings far offshore, we fitted a model that used distance to shore as the only covariate (Fig. 60, lower right). This model estimated moderate density to about 80km from shore, peaking at about 50 km and rapidly dropping beyond 80 km (Fig. 60, lower right). Total abundance between Cape Fear and Block Island was estimated at 82 whales.

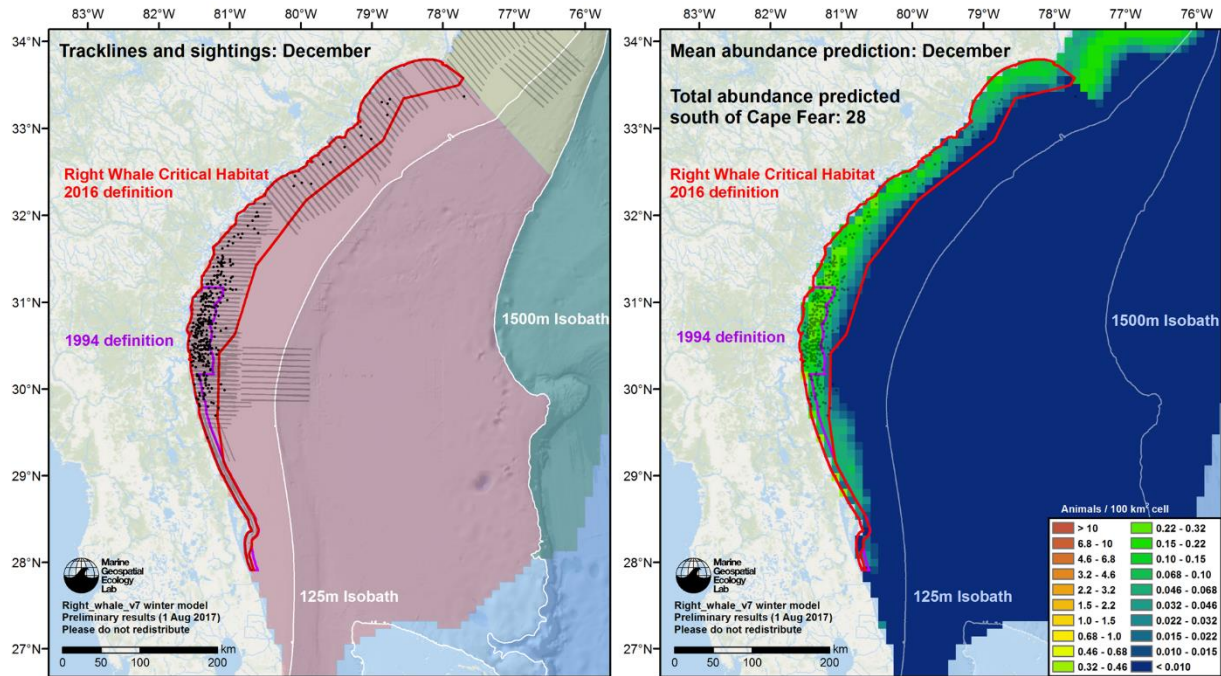


Figure 62. Left: Survey effort and sightings conducted in the South of Cape Fear modeling region (dark red background) in December of all years. Includes SEUS NARW surveys from 2003/04 – 2015/16 seasons. Right: Predicted mean density and total abundance.

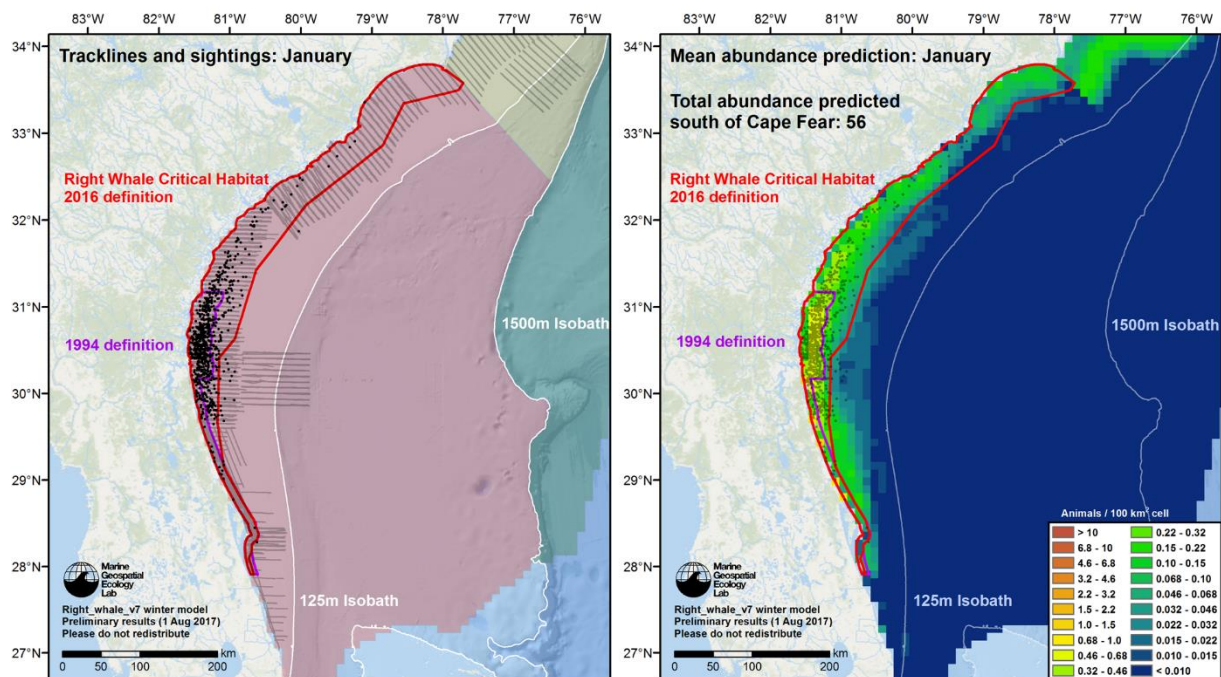


Figure 63. Left: Survey effort and sightings conducted in the South of Cape Fear modeling region (dark red background) in January of all years. Includes SEUS NARW surveys from 2003/04 – 2015/16 seasons. Right: Predicted mean density and total abundance.

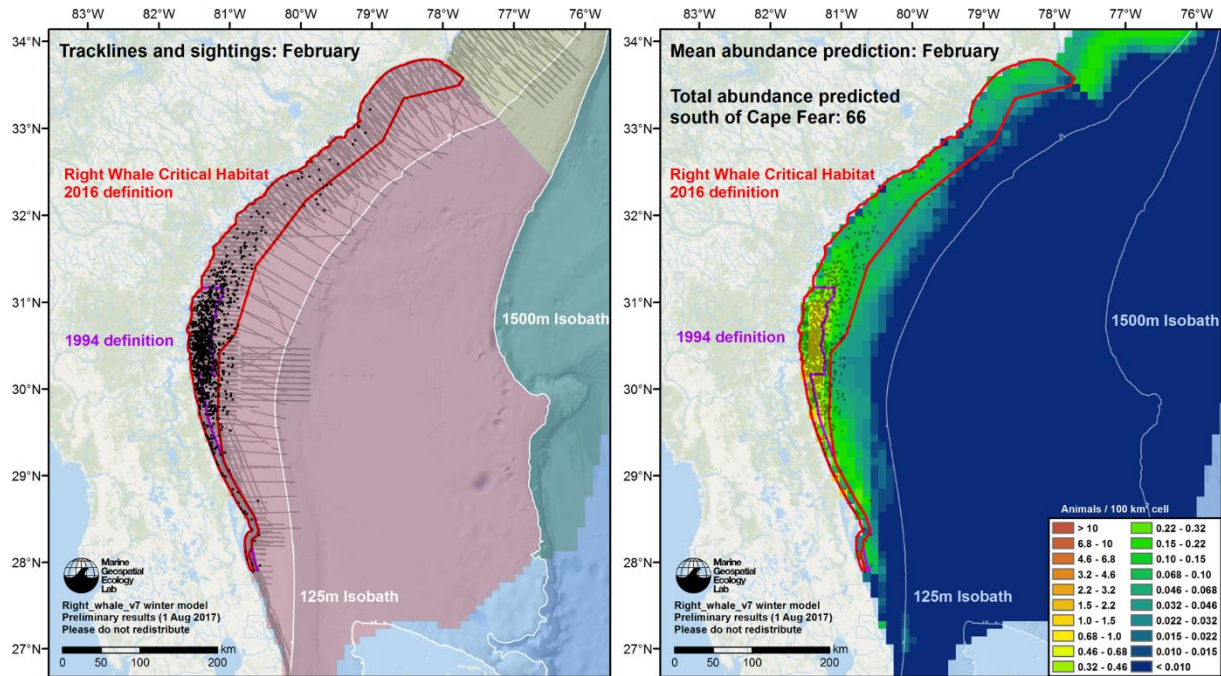


Figure 64. Left: Survey effort and sightings conducted in the South of Cape Fear modeling region (dark red background) in February of all years. Includes SEUS NARW surveys from 2003/04 – 2015/16 seasons. Right: Predicted mean density and total abundance.

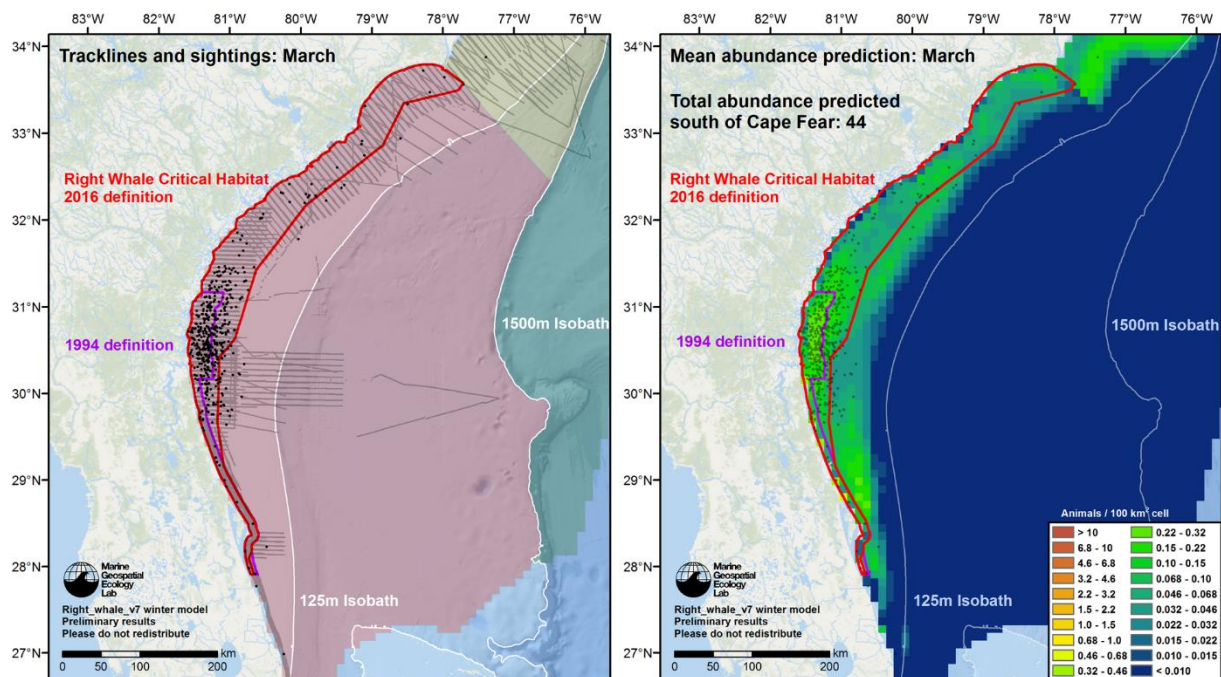


Figure 65. Left: Survey effort and sightings conducted in the South of Cape Fear modeling region (dark red background) in March of all years. Includes SEUS NARW surveys from 2003/04 – 2015/16 seasons. Right: Predicted mean density and total abundance.

4.2.11.4. Spring model

In spring (Apr-June) we retained the split at Block Island (Fig. 66), considering the area south of here to contain whales still making their northern migration and north of here to be feeding habitat. Supporting this description were sightings of nearly 100 right whales feeding in Rhode Island Sound on 20 April 2010 (NEFSC press release: https://www.nefsc.noaa.gov/press_release/2010/MediaAdv/MA1004/); 57 were sighted in the same area on 22 April 2011 (NEFSC press release: https://www.nefsc.noaa.gov/press_release/2011/SciSpot/SS1102/).

For the area south of Block Island, we only had 10 sightings for which to fit a model. Reflecting the assumption that these whales were migrating north, we tested model with SST as the only covariate (Fig. 66, bottom). The model retained the covariate as significant, showing higher density in the colder northern waters. Predictions showed total abundance decreasing as the season progressed, from 74 in April, to 39 May, to 18 in June, for a mean of 44 for the season (Fig. 67). This model and resulting predictions were logical and so we kept them.

North of Block Island we expanded the model region slightly from winter to encompass all of Georges Bank and its north slope, surveyed extensively by the NARWSS program. A model of moderate complexity was selected (Fig. 66, top right) predicting high density at Rhode Island Sound, Great South Channel, Wilkinson Basin, and the northern edge of Georges Bank. As the season progressed, monthly predictions showed density moving east (results not shown), consistent with literature reports. Predicted mean abundance in this area was 350, but as with the winter model, we excluded CCB because we did not have the CCS surveys of this region (see discussion above).

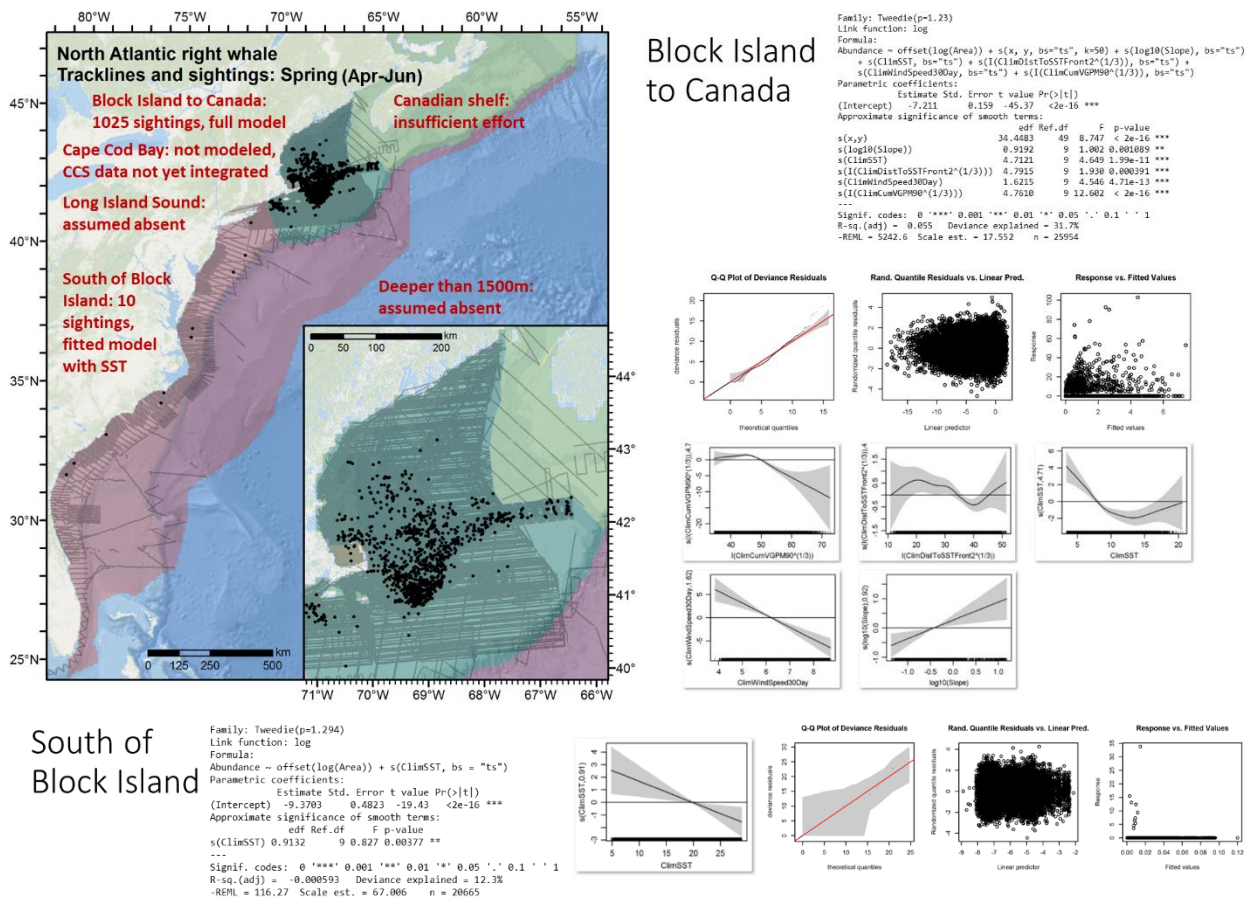


Figure 66. North Atlantic right whale spring model schematic with statistical models selected as best in each of the two regional models. The Block Island to Canada region contains right whales on the core feeding grounds. South of Block Island contains a small number of right whales still completing the springtime northward migration from the calving grounds.

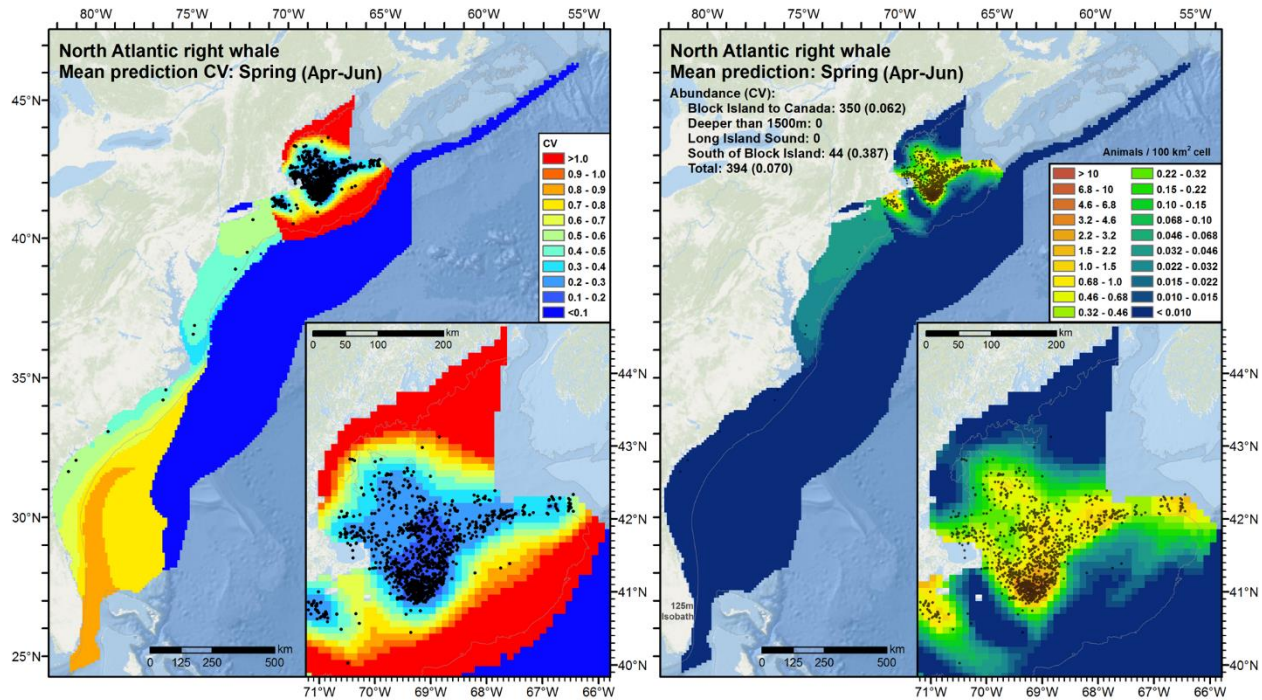


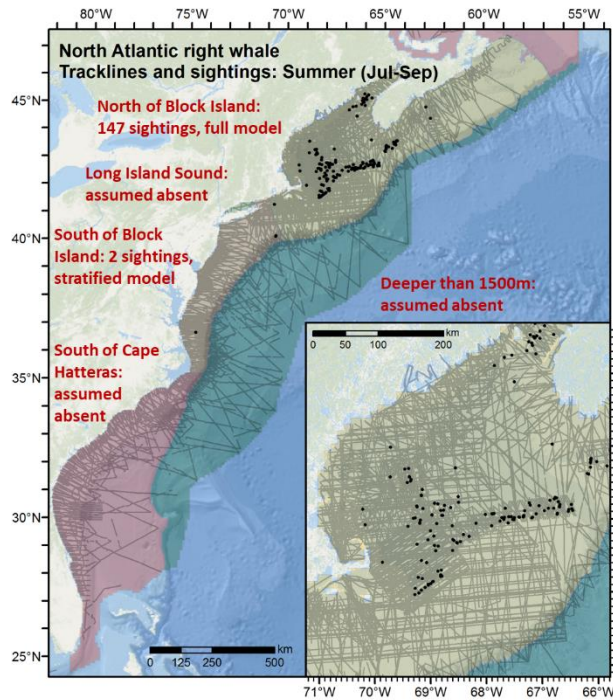
Figure 67. Left: Predicted mean coefficient of variation (CV), with sightings overlaid, for North Atlantic right whale for the spring season. Right: Predicted mean density and total abundance.

4.2.11.5. Summer model

In summer (July-September), NARWSS, AMAPPS, and historic broad-scale NEFSC aerial surveys extended coverage into Canada sufficient to extend our North of Block Island model to the Laurentian Channel at the entrance to the Gulf of St. Lawrence (Fig. 68). However, aggregate effort was less and dispersed geographically, resulting in substantially fewer sightings. Sightings were concentrated in Wilkinson Basin, the Great South Channel, the northern edge of Georges Bank, the southern Bay of Fundy, and Roseway Basin.

A model of moderate complexity was selected (Fig. 68); the resulting predictions showed high density in the expected areas, and monthly predictions showed density shifting out of the Wilkinson Basin as summer progressed into northern areas (monthly maps will appear in the supplementary report for North Atlantic right whale that will be part of our journal publication that is in preparation). Predicted mean seasonal abundance in the modeled area was 352, peaking in August at 533 but falling to 152 in September. We advise substantial caution in September, as it is one of the months of least surveying throughout the east coast. Survey effort decreased substantially in Canada, and only two right whales were reported the entire month by any surveys, both in U.S. waters. We urge additional surveying in September throughout the Gulf of Maine, in both U.S. and Canadian waters, to boost confidence of predictions during this month.

South of Block Island, two right whales were reported during this season, both north of Cape Hatteras. Accordingly we fitted a stratified model that contained no covariates to the data between Cape Hatteras and Block Island that was shallower than the 1500m isobath (Fig. 68). This model predicted a mean total abundance of 6 whales distributed evenly throughout the modeled region.



North of Block Island

```

Family: Tweedie(p=1.223)
Link function: log
Formula:
Abundance ~ offset(log(Area)) + s(x, y, bs="ts", k=50) +
s(log10(Depth), bs="ts") + s(log10(DistToShore/1000), bs="ts") +
s(ClimSST, bs="ts") + s(ClimWindSpeed5Day, bs="ts") +
s(log10(pmax(ClimPKPB2, 0.01))), bs="ts")
Parametric coefficients:
Estimate Std. Error t value Pr(>|t|)
(Intercept) -9.9870 0.5811 -17.19 <2e-16 ***
Approximate significance of smooth terms:
s(x,y) 27.0643 49 2.325 2.09e-15 ***
s(log10(Depth)) 3.4329 9 2.929 5.78e-07 ***
s(log10(DistToShore/1000)) 0.9656 9 0.579 0.06526 **
s(ClimSST) 3.7930 9 3.031 0.00667 ***
s(ClimWindSpeed5Day) 1.0201 9 1.741 2.18e-05 ***
s(log10(pmax(ClimPKPB2, 0.01))) 0.9191 9 0.934 0.00093 ***
---
Signif. codes: 0 '***' 0.001 '**' 0.01 '*' 0.05 '.' 0.1 ' ' 1
R-sq. (adj) = 0.0582 Deviance explained = 49.5%
-REML = 896.75 Scale est. = 18.432 n = 12742

```

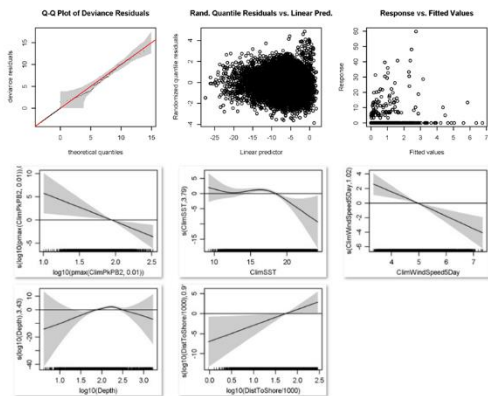


Figure 68. North Atlantic right whale summer model schematic with statistical model selected as best in the region of the study area that was modeled with a habitat-based density model.

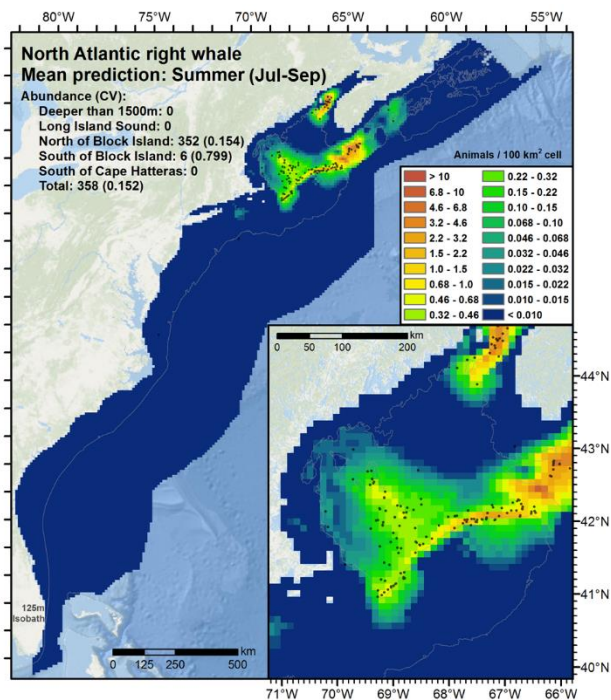
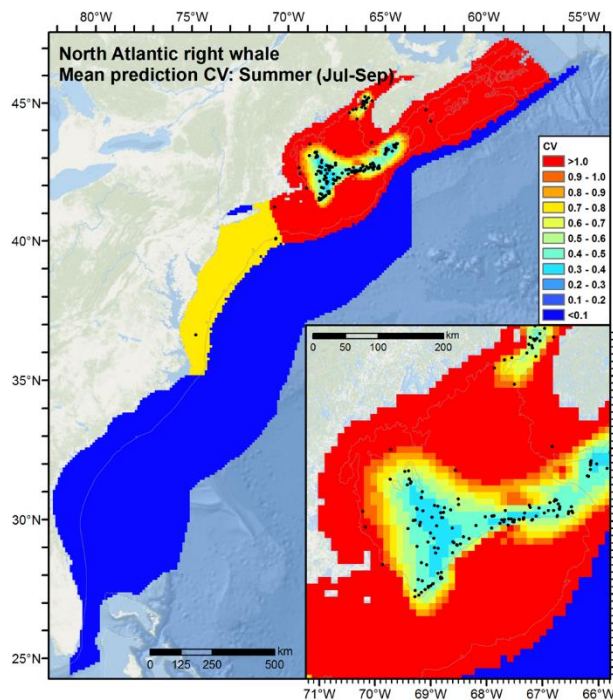


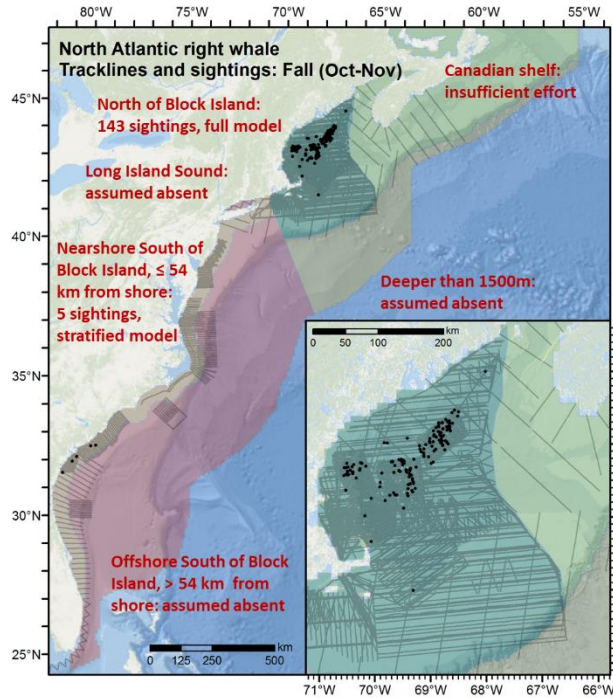
Figure 69. Left: Predicted mean coefficient of variation (CV), with sightings overlaid, for North Atlantic right whale for the summer season. Right: Predicted mean density and total abundance.

4.2.11.6. *Fall model*

In fall (October-November), surveying was sparse throughout the east coast. In the northeast NARWSS and AMAPPS provided good coverage of the U.S. Gulf of Maine but surveying was insufficient in Canada to for us to confidently offer predictions there (Fig. 70). Accordingly we stopped our North of Block Island model at the U.S.-Canada border. In this region, sightings were concentrated in the central Gulf of Maine and at Jeffreys Ledge, with a lesser number of sightings scattered south toward Cape Cod. A relatively simple model was selected (Fig. 70); the resulting predictions showed high density in the expected areas but a relatively low mean abundance of 117 (97 in October, 136 in November), with few sightings and very little additional abundance predicted elsewhere in the study area.

South of Block Island, surveying was very patchy and only five sightings were reported, all in the southeast approaching the calving grounds (Fig. 70). We judged that the only appropriate treatment for these sightings under our process was to incorporate them into a stratified model, but we faced an important question: all of these sightings were in November, very close to shore; how far out should we extent the modeled region? We considered the 1500 m isobath, which we used in other seasons. But wintertime models in both the calving grounds and the migratory area suggested right whales did not frequent areas far from the shelf in this area. Instead, we set the outer boundary at 54 km on the basis that 99% of the right whales sighted south of Block Island were within this distance of shore. The resulting total abundance estimate was 7 whales (Fig. 71).

These are the months were our confidence in the available data and the resulting models is the lowest. The acoustic validation exercise (section 3.1 above) showed acoustic detections at low rates throughout the U.S. east coast (Fig. 11, left) but there were no visual sightings at any of the monitored locations. Clearly a large portion of the population is elsewhere, perhaps in Canada or even the offshore Atlantic Ocean. To resolve this mystery, we recommend additional visual surveying and acoustic monitoring throughout the eastern seaboard in these months, particularly in Canada and the U.S. mid-Atlantic. Additional satellite tracking could also be extremely informative, providing it could be done without imposing additional health risks on this highly endangered population.



Block Island to Canada

```

Family: Tweedie(p=1.211)
Link function: log
Formula:
Abundance ~ offset(log(Area)) + s(x, y, bs="ts", k=50) +
s(log10(Depth), bs="ts") + s(log10(pmax(ClimTKE, 1e-04)), bs="ts")
Parametric coefficients:
Estimate Std. Error t value Pr(>|t|)
(Intercept) -9.852 1.867 -9.224 <2e-16 ***
Approximate significance of smooth terms:
          edf Ref.df F p-value
s(x,y)    22.5698  49 2.822 < 2e-16 ***
s(log10(Depth)) 0.9513  9 1.304 0.000171 ***
s(log10(pmax(ClimTKE, 1e-04))) 0.9887  9 1.720 4.34e-05 ***
---
Signif. codes:  0 '***' 0.001 '**' 0.01 '*' 0.05 '.' 0.1 ' ' 1
R-sq.(adj) = 0.0556  Deviance explained = 43.8%
-REML = 796.12  Scale est. = 16.723  n = 8888

```

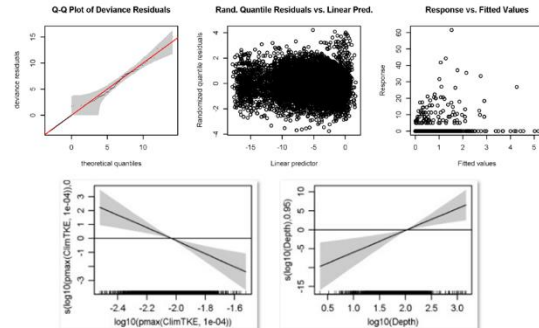


Figure 70. North Atlantic right whale fall model schematic with statistical model selected as best in the region of the study area that was modeled with a habitat-based density model.

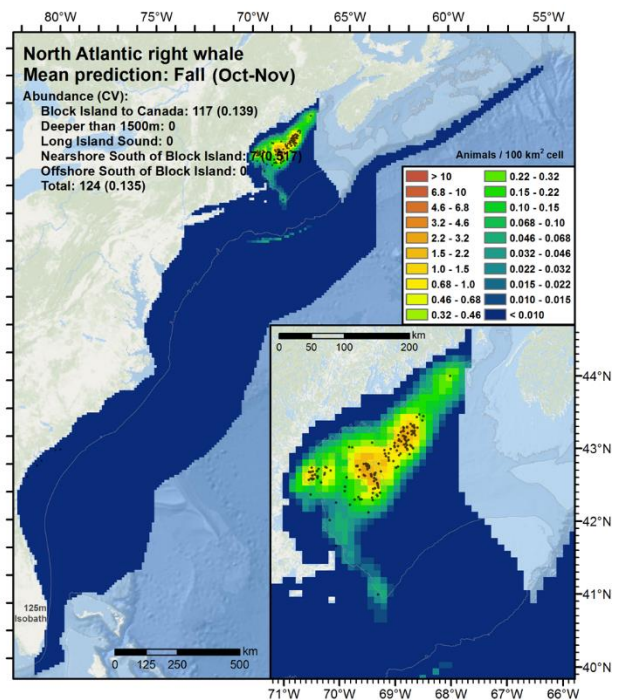
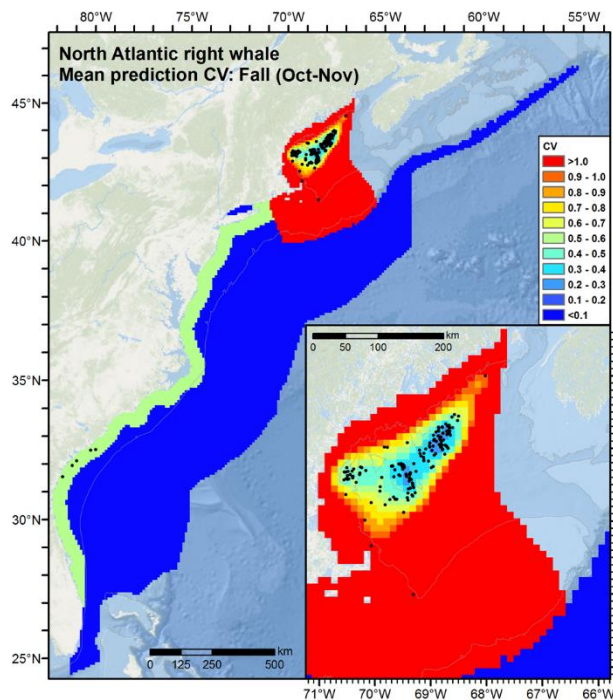


Figure 71. Left: Predicted mean coefficient of variation (CV), with sightings overlaid, for North Atlantic right whale for the fall season. Right: Predicted mean density and total abundance.

4.3. *Special challenges to building sea turtle density models*

In our investigation of the feasibility of building sea turtle density models, we identified several challenges specific to sea turtles that should be addressed. The effort required for them was too much to allow development of sea turtle density models in Option Year 1. If the Navy prioritizes sea turtle density models in a future Option Year, we should start by discussing these challenges.

4.3.1. *Not all surveys recorded sea turtle sightings*

Not all surveys recorded turtle sightings, and of those that did, not all recorded distances to turtles. Before doing any modeling, it will be necessary to conduct a small feasibility analysis. The analysis would first carefully review all of the surveys to determine the subset that could be used for turtle models. To use our current methodology, which requires distances to the sighted animals in order to model and correct for the influence of distance on detectability using the Horvitz-Thompson approach (Miller et al. 2013) advocated by University of St. Andrews, we must discard all surveys that did not record distances to turtles. We would likely be left only with broadscale abundance surveys conducted by NMFS (e.g. AMAPPS). The analysis should examine the seasonal consequences of doing this, relative to the Navy's need for turtle predictions in all seasons.

The analysis should also examine, and ideally prototype, whether an alternative modeling approach might allow utilization of surveys that did not report distances if some assumptions are made, e.g. (a) Develop detection functions from surveys that did record distances. Restrict the detection functions to only use segment-level covariates (we couldn't use group size as covariate, but turtles are mainly solitary). (b) Estimate effective strip width (ESW) from those surveys. Apply this to other surveys that recorded turtle sightings with no distances, under the assumption that they are similar. (c) Use a density formulation that allows the use of ESW, rather than the Horvitz-Thompson approach.

4.3.2. *SEFSC did not provide sea turtle sightings for AMAPPS surveys*

These would be critical to modeling sea turtles in the southeast U.S. As far as we know, SEFSC would provide them if we asked. But given the time required for NMFS to provide AMAPPS cetacean data—which required SEFSC to first send the data to NEFSC for preparation, then for NEFSC to release it to us—some time could be required. If the Navy decides to prioritize sea turtles for modeling, we should jointly make the request as soon as possible.

4.3.3. *There are many “unidentified hardshell sea turtle” sightings*

Density would be biased low unless we classified or modeled these somehow. We could try to classify them using a habitat-based approach, similar to how we have done for cetaceans (e.g. “fin or sei whale”). But hardshell turtle habitats overlap somewhat, so this approach might not be successful. Alternatively we could model unidentified hardshell turtles separately, as was done in the AFTT Phase II models, known as the Navy OPAREA Density Estimates (NODEs) models.

4.3.4. *Sea turtle availability bias varies by species, space, time, and age class*

Sea turtles dive longer in some seasons, in some places, and at some age classes. Correcting for this bias may be hard relative to cetaceans. The approach we would use, piloted by a Navy-funded study by researchers at CREEM at University of St. Andrews, is to have a separate habitat-based model of availability bias derived from dive data. We could use the CREEM model in some situations but definitely not all (e.g. not for leatherbacks, not in the Gulf of Mexico). Fitting our own model would require gaining access to a large quantity of satellite telemetry data that included dive information. This would require new collaborations with researchers in the sea turtle community; it could prove challenging to establish these collaborations.

4.4. New uncertainty estimates for the AFTT models

In the wider AFTT area, beyond the extent of the regional east coast and Gulf of Mexico models, or for certain rare species that were better modeled AFTT-wide rather than with regional models, we base our estimates on AFTT-wide models that incorporate data from the east coast, Gulf of Mexico, and select datasets beyond the AFTT to improve model extrapolation performance (Mannocci et al. 2017). As the Navy did not indicate that it was a priority to update or refine these models, we did not update them in Option Year 1, and continue to base predictions in the wider AFTT region on models developed for Phase III. However, the AFTT model predictions published in the NMSDD for Phase III did not include coefficients of variation (CVs) for these predictions (leaving the UNCERTAINTY field of the NMSDD at NULL), as the predictions represented extrapolations beyond surveyed areas and thus the model CVs might underestimate true uncertainty.

As part of the process of publishing these models (Mannocci et al. 2017), we produced CVs for the AFTT models and studied this problem further. To try to avoid underestimating CVs, we utilized a method that accounts for covariance between covariates when combining multiple predicted density surfaces into an aggregate (e.g. year-round) density surface (Miller et al. 2013). In consultation with peer modelers, we reviewed the estimated CVs and concluded that while they may still underestimate uncertainty to some degree, they would be appropriate for use in the NMSDD, applied cautiously. As with the regional density models, the AFTT CVs represent uncertainty in the parameter estimates of the spatial model only, and do not account for known uncertainty in detection functions or $g(0)$ estimates. For warm water dolphins modeled with SST as the single covariate (e.g., Clymene dolphin), we note that CVs are extremely high in the northern part of the AFTT area. These very high CVs result from very low densities predicted in coldest waters where these species are absent.

Because these CVs do not reflect true uncertainty in the extrapolated part of the AFTT area, we also investigated techniques to better characterize extrapolation in the AFTT area. In Phase III, we only characterized extrapolation in univariate space (i.e. with respect to the range of individual covariates) (Fig. 72).

In Option Year 1, we conducted experiments to characterize AFTT model extrapolation in multivariate space. In multivariate space, predictions within the range of individual covariates can encompass novel combinations of covariates and therefore require extrapolation (Fig. 73). To examine extrapolation in multivariate space, we applied two multivariate metrics derived from the convex hull and the Gower's distance.

The convex hull of a set of points is defined as the smallest convex set that contains these points. Predictions inside the convex hull are interpolations while predictions outside the convex hull are extrapolations. The convex hull of a single covariate is the interval between the minimum and maximum data points (i.e., a univariate environmental envelope). The convex hull of two covariates is a polygon with vertices at the extreme points of the data points (i.e., a bivariate environmental envelope). A convex hull can be defined for any number of covariates, although visualization becomes difficult for more than two covariates and computational power starts to limit calculations for more than ten covariates (King & Zeng 2007).

The Gower's non-parametric distance between points i and j belonging to the calibration and prediction datasets respectively, is defined as the average absolute distance between the values of these two points in each dimension divided by the range of the data (Gower 1971; King & Zeng 2007). With K environmental dimensions:

$$G_{ij}^2 = \frac{1}{K} \sum_{k=1}^K \frac{|x_{ik} - x_{jk}|}{r_k}$$

where r_k is the difference between the largest and the smallest values of the calibration dataset for the k th covariate. Because of range standardization, covariates have equal contribution to the Gower's distance. We considered a prediction point was in the neighborhood (in environmental space) of calibration data points if it was situated within a radius of one geometric mean Gower's distance of all pairs of calibration data points (King & Zeng 2007). The larger the proportion of prediction points "near" calibration data points, the more reliable the extrapolation.

While the convex hull allows a binary distinction between interpolation and extrapolation (Fig. 73), the metric derived from the Gower's distance provides a quantitative way of assessing prediction reliability (Fig. 74). We used

the WhatIf package (version 1.5-6) (Stoll et al. 2005) in R (version 3.1.1) to calculate the convex hulls and Gower's distances.

We presented and discussed these examples in a review workshop with the Navy and collaborators in May 2017. In discussions, it was pointed out that the Navy Acoustic Effects Model (NAEMO), the Navy system that uses the density estimates in the NMSDD to model exposure of marine mammals to anthropogenic sound sources, does not currently have the capability of considering uncertainty metrics aside from coefficient of variation. Thus we did not prepare them for the NMSDD in Option Year 1, as producing them is highly computationally intensive, and storing them in the NMSDD would require that additional fields be added. However, if the Navy expresses interest in Option Year 2 or a later period, we can compute and add them to a future NMSDD update.

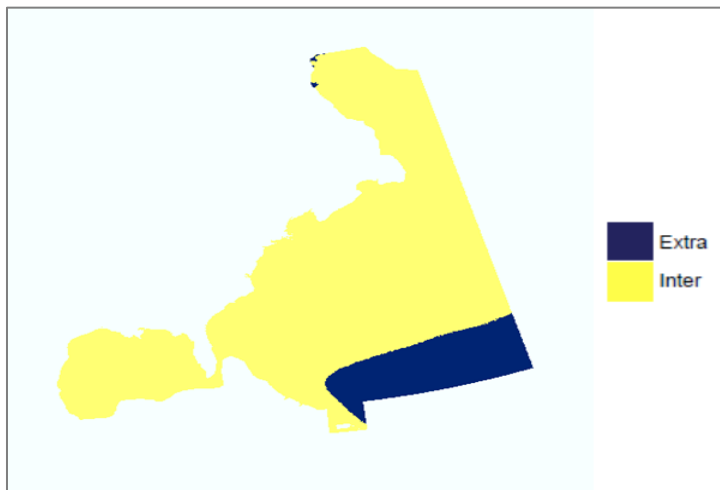


Figure 72. Example of a binary qualitative uncertainty surface in univariate space, prepared for the Phase III NMSDD from the AFTT fin whale model for the month of July. Yellow: interpolation (i.e., within the range of individual covariates (UNCER_QUAL set to “AFTT model” in the NMSDD)); blue: extrapolation (i.e., outside the range of individual covariates (UNCER_QUAL set to “AFTT model out of range”)).

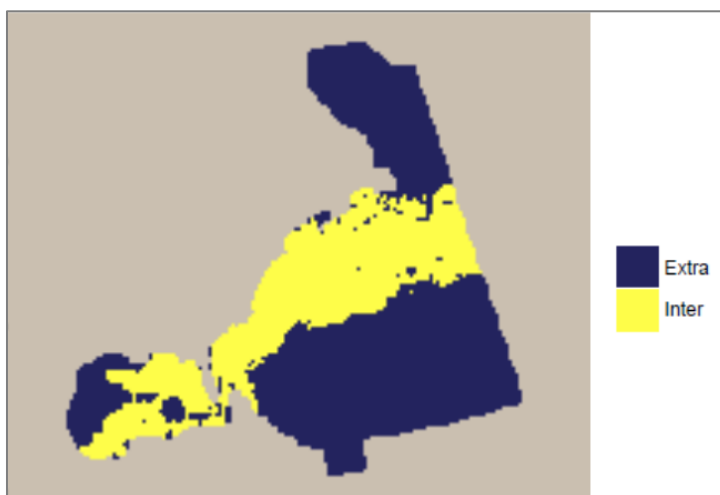


Figure 73. Example of a binary qualitative uncertainty surface in multivariate space, derived from the convex hull for the AFTT fin whale model for the month of July. Yellow: interpolation (i.e., within the multivariate convex hull); blue: extrapolation (i.e., outside the multivariate convex hull). The extent of the blue (extrapolation) area is larger than in Fig. 72 as it includes novel combinations of predictors.

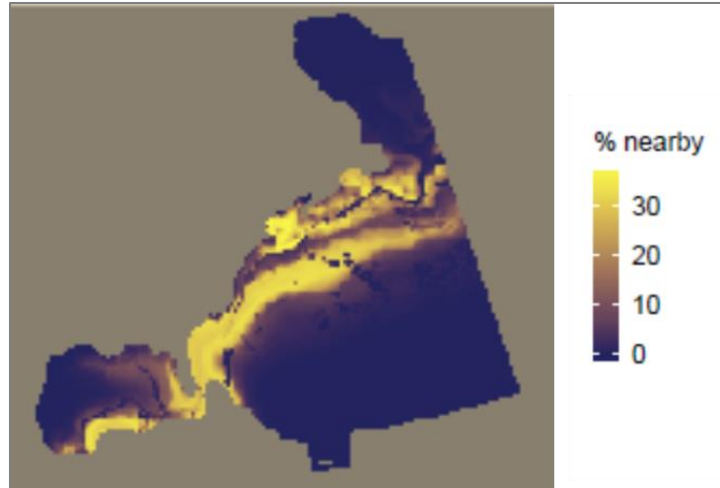


Figure 74. Example of a quantitative uncertainty surface derived from Gower’s distances for the AFTT fin whale model for the month of July. Cell values show the percentage of calibration data “near” that cell in multivariate covariate space. The higher the percentage, the more reliable the prediction.

5. [Omitted]

[This section contains information unrelated to the updated density models.]

6. Acknowledgements

Above all, we thank the observers, scientists, engineers, pilots, captains, and crews who collected and shared line transect survey data with us; thank you for the opportunity to analyze the data you produced. Beth Josephson, Debi Palka, and Lance Garrison preprocessed the AMAPPS data and prepared it for our use. Lance Garrison also contributed the pre-AMAPPS GU-06-03 survey. Tim Gowan and Katie Jackson preprocessed and prepared the Southeast Right Whale Surveys for our use. Barb Zoodsma facilitated communications that established the collaborations necessary for us to use those data. Tim Cole and Christian Khan contributed the NARWSS surveys. Bill McLellan and his team contributed the UNC Wilmington surveys. Sarah Mallette, Gwen Lockhart, and Susan Barco contributed the VAMSC surveys of the Maryland and Virginia Wind Energy Areas.

Thanks to Sofie Van Parijs, Genevieve Davis, Danielle Cholewiak, Mark Baumgartner, and Julianne Gurnee for sharing right whale acoustic detections for validation of our right whale density models. Many thanks to their numerous collaborators who deployed the instruments, shared the data, and allowed such a comprehensive acoustic record to be assembled and utilized. Thanks to Helen Bailey, Jessica Wingfield, Aaron Rice, and their collaborators for undertaking the work to compare our harbor porpoise density model predictions to their acoustic detections.

7. References

- Barlow J. 1999. Trackline detection probability for long-diving whales. Pages 209–221 *Marine Mammal Survey and Assessment Methods*. Balkema, Rotterdam, The Netherlands.
- Barlow J, Sexton S. 1996. The effect of diving and searching behavior on the probability of detecting track-line groups, go, of long-diving whales during linetranssect surveys. Page

21. Administrative Report LJ-96-14. NOAA National Marine Fisheries Service, Southwest Fisheries Center.
- Baumgartner MF, Mate BR. 2003. Summertime foraging ecology of North Atlantic right whales. *Marine Ecology Progress Series* **264**:123–135.
- Baumgartner MF, Mate BR. 2005. Summer and fall habitat of North Atlantic right whales (*Eubalaena glacialis*) inferred from satellite telemetry. *Canadian Journal of Fisheries and Aquatic Sciences* **62**:527–543.
- Brieman L. 2001. Random Forests. *Machine Learning* **45**:5–32.
- Brillant SW, Vanderlaan AS, Rangeley RW, Taggart CT. 2015. Quantitative estimates of the movement and distribution of North Atlantic right whales along the northeast coast of North America. *Endangered Species Research* **27**:141–154.
- Buckland ST, Anderson DR, Burnham KP, Laake JL, Borchers DL, Thomas L. 2001. *Introduction to Distance Sampling: Estimating Abundance of Biological Populations*. Oxford University Press, Oxford, UK.
- CETAP. 1982. A characterization of marine mammals and turtles in the mid- and North Atlantic areas of the U.S. outer continental shelf, final report, Cetacean and Turtle Assessment Program, University of Rhode Island. Page 576. #AA551-CT8-48. Bureau of Land Management, Washington, DC.
- Cole T, Hamilton P, Henry A, Duley P, Pace R, White B, Frasier T. 2013. Evidence of a North Atlantic right whale *Eubalaena glacialis* mating ground. *Endangered Species Research* **21**:55–64.
- Edwards EF, Hall C, Moore TJ, Sheredy C, Redfern JV. 2015. Global distribution of fin whales *Balaenoptera physalus* in the post-whaling era (1980–2012). *Mammal Review* **45**:197–214.
- Firestone J, Lyons SB, Wang C, Corbett JJ. 2008. Statistical modeling of North Atlantic right whale migration along the mid-Atlantic region of the eastern seaboard of the United States. *Biological Conservation* **141**:221–232.
- Forney KA. 2000. Environmental Models of Cetacean Abundance: Reducing Uncertainty in Population Trends. *Conservation Biology* **14**:1271–1286.
- Good CP. 2008. Spatial ecology of the North Atlantic right whale (*Eubalaena glacialis*).
- Gowan TA, Ortega-Ortiz JG. 2014. Wintering Habitat Model for the North Atlantic Right Whale (*Eubalaena glacialis*) in the Southeastern United States. *PLoS ONE* **9**:e95126.
- Gower JC. 1971. A General Coefficient of Similarity and Some of Its Properties. *Biometrics* **27**:857.

- Hain JHW, Ellis SL, Kenney RD, Slay CK. 1999. Sightability of right whales in coastal waters of the southeastern United States with implications for the aerial monitoring program. Pages 191–207 *Marine Mammal Survey and Assessment Methods*. Balkema, Rotterdam.
- Hammond PS et al. 2013. Cetacean abundance and distribution in European Atlantic shelf waters to inform conservation and management. *Biological Conservation* **164**:107–122.
- Hedley SL, Buckland ST. 2004. Spatial models for line transect sampling. *Journal of Agricultural, Biological, and Environmental Statistics* **9**:181–199.
- Hodge K, Muirhead C, Morano J, Clark C, Rice A. 2015. North Atlantic right whale occurrence near wind energy areas along the mid-Atlantic US coast: implications for management. *Endangered Species Research* **28**:225–234.
- Hothorn T, Hornik K, Zeileis A. 2006. Unbiased Recursive Partitioning: A Conditional Inference Framework. *Journal of Computational and Graphical Statistics* **15**:651–674.
- Keller C, Garrison L, Baumstark R, Ward-Geiger L, Hines E. 2012. Application of a habitat model to define calving habitat of the North Atlantic right whale in the southeastern United States. *Endangered Species Research* **18**:73–87.
- Keller CA, Ward-Geiger LI, Brooks WB, Slay CK, Taylor CR, Zoodsma BJ. 2006. North Atlantic Right Whale Distribution in Relation to Sea-Surface Temperature in the Southeastern United States Calving Grounds. *Marine Mammal Science* **22**:426–445.
- Kenney RD, Mayo CA, Winn HE. 2001. Migration and foraging strategies at varying spatial scales in western North Atlantic right whales: a review of hypotheses. *Journal of Cetacean Research and Management* **2**:251–260.
- Kenney RD, Payne PM, Heinemann DW, Winn HE. 1996. Shifts in Northeast shelf cetacean distributions relative to trends in Gulf of Maine/Georges Bank finfish abundance. Pages 169–196 *The Northeast Shelf Ecosystem: Assessment, Sustainability, and Management*. Blackwell Science, Cambridge, MA.
- King G, Zeng L. 2007. When can history be our guide? The pitfalls of counterfactual inference. *International Studies Quarterly* **51**:183–210.
- Knowlton AR, Ring JB, Russell B. 2002. Right whale sightings and survey effort in the Mid Atlantic Region: Migratory corridor, time frame, and proximity to port entrances. Report submitted to the NMFS Ship Strike Working Group, Silver Spring, Maryland.[PDF available from <http://www.nero.noaa.gov/shipstrike/ssr/midatanticreportrFINAL.pdf>]. Available from <http://www.nero.noaa.gov/shipstrike/midatanticreportrFINAL.pdf> (accessed May 27, 2014).
- Kraus SD et al. 2016. Northeast Large Pelagic Survey Collaborative Aerial and Acoustic Surveys for Large Whales and Sea Turtles, OCS Study BOEM 2016-054. US Department of the Interior, Bureau of Ocean Energy Management, Sterling, Virginia. Available from <https://www.boem.gov/RI-MA-Whales-Turtles/> (accessed November 4, 2016).

- Mannocci L, Roberts JJ, Miller DL, Halpin PN. 2017. Extrapolating cetacean densities to quantitatively assess human impacts on populations in the high seas. *Conservation Biology* **31**:601–614.
- Mellinger DK, Nieukirk SL, Matsumoto H, Heimlich SL, Dziak RP, Haxel J, Fowler M, Meinig C, Miller HV. 2007. Seasonal Occurrence of North Atlantic Right Whale (*Eubalaena glacialis*) Vocalizations at Two Sites on the Scotian Shelf. *Marine Mammal Science* **23**:856–867.
- Miller DL, Burt ML, Rexstad EA, Thomas L. 2013. Spatial models for distance sampling data: recent developments and future directions. *Methods in Ecology and Evolution* **4**:1001–1010.
- Mitchell E. 1975. Preliminary report on Nova Scotia fishery for sei whales (*Balaenoptera borealis*). *Rep. Int. Whal. Comm* **25**:218–225.
- Nichols OC, Kenney RD, Brown* MW. 2008. Spatial and temporal distribution of North Atlantic right whales (*Eubalaena glacialis*) in Cape Cod Bay, and implications for management. *Fishery Bulletin* **106**:270–280.
- Nieukirk SL, Stafford KM, Mellinger DK, Dziak RP, Fox CG. 2004. Low-frequency whale and seismic airgun sounds recorded in the mid-Atlantic Ocean. *The Journal of the Acoustical Society of America* **115**:1832–1843.
- Oedekoven CS, Fleishman E, Hamilton P, Clark JS, Schick RS. 2015. Expert elicitation of seasonal abundance of North Atlantic right whales *Eubalaena glacialis* in the mid-Atlantic. *Endangered Species Research*. Available from <https://research-repository.st-andrews.ac.uk/handle/10023/7921> (accessed February 10, 2016).
- Pace RM, Corkeron PJ, Kraus SD. 2017. State-space mark-recapture estimates reveal a recent decline in abundance of North Atlantic right whales. *Ecology and Evolution*. Available from <http://doi.wiley.com/10.1002/ece3.3406> (accessed September 30, 2017).
- Palka DL. 2006. Summer abundance estimates of cetaceans in US North Atlantic navy operating areas. Page 41. 06–03, Northeast Fish Sci Cent Ref Doc. U.S. Department of Commerce, Woods Hole, MA. Available from <http://www.nefsc.noaa.gov/publications/crd/crd0603/crd0603.pdf> (accessed March 5, 2014).
- Palka DL, Read AJ, Westgate AJ, Johnston DW. 1996. Summary of current knowledge of harbour porpoises in US and Canadian Atlantic waters. *Reports of the International Whaling Commission* **46**:559–565.
- Perkins NJ, Schisterman EF. 2006. The Inconsistency of “Optimal” Cutpoints Obtained using Two Criteria based on the Receiver Operating Characteristic Curve. *American Journal of Epidemiology*:670–675.
- Pettis HM, Hamilton PK. 2016. North Atlantic Right Whale Consortium annual report card. Report to the North Atlantic Right Whale Consortium, November 2016. Available from

<http://www.narwc.org/pdf/2016%20Report%20Card%20final.pdf> (accessed September 30, 2017).

- Prieto R, Janiger D, Silva MA, Waring GT, GonçAlves JM. 2012. The forgotten whale: a bibliometric analysis and literature review of the North Atlantic sei whale *Balaenoptera borealis*: North Atlantic sei whale review. *Mammal Review* **42**:235–272.
- Prieto R, Silva MA, Waring GT, Gonalves JMA. 2014. Sei whale movements and behaviour in the North Atlantic inferred from satellite telemetry. *Endangered Species Research* **26**:103–113.
- Risch D et al. 2014. Seasonal migrations of North Atlantic minke whales: Novel insights from large-scale passive acoustic monitoring networks. *Movement Ecology* **2**:24.
- Roberts JJ. 2015. Estimates of bottlenose dolphin density for estuaries in the AFTT area for the Phase III NMSDD, Document version 1.2. Duke University Marine Geospatial Ecology Lab, Durham, NC.
- Roberts JJ et al. 2016a. Habitat-based cetacean density models for the U.S. Atlantic and Gulf of Mexico. *Scientific Reports* **6**:22615.
- Roberts JJ, Mannocci L, Halpin PN. 2015. Marine mammal density models for the U.S. Navy Atlantic Fleet Training and Testing (AFTT) study area for the Phase III Navy Marine Species Density Database (NMSDD), Document Version 1.1. Duke University Marine Geospatial Ecology Lab, Durham, NC.
- Roberts JJ, Mannocci L, Halpin PN. 2016b. Final Project Report: Marine Species Density Data Gap Assessments and Update for the AFTT Study Area, 2015-2016 (Base Year), Document Version 1.0. Duke University Marine Geospatial Ecology Lab, Durham, NC.
- Soldevilla M, Rice A, Clark C, Garrison L. 2014. Passive acoustic monitoring on the North Atlantic right whale calving grounds. *Endangered Species Research* **25**:115–140.
- Stanistreet JE, Nowacek DP, Baumann-Pickering S, Bell JT, Cholewiak DM, Hildebrand JA, Hodge LEW, Moors-Murphy HB, Van Parijs SM, Read AJ. 2017. Using passive acoustic monitoring to document the distribution of beaked whale species in the western North Atlantic Ocean. *Canadian Journal of Fisheries and Aquatic Sciences*:1–12.
- Stoll H, King G, Zeng L. 2005. WhatIf: R software for evaluating counterfactuals. *Journal of Statistical Software* **15**. Available from <https://dash.harvard.edu/handle/1/3445051> (accessed September 27, 2017).
- Thomas L, Buckland ST, Rexstad EA, Laake JL, Strindberg S, Hedley SL, Bishop JRB, Marques TA, Burnham KP. 2010. Distance software: design and analysis of distance sampling surveys for estimating population size. *Journal of Applied Ecology* **47**:5–14.
- Watwood SL, Miller PJ, Johnson M, Madsen PT, Tyack PL. 2006. Deep-diving foraging behaviour of sperm whales (*Physeter macrocephalus*). *Journal of Animal Ecology* **75**:814–825.

- Weinrich MT, Kenney RD, Hamilton PK. 2000. Right whales (*Eubalaena glacialis*) on Jeffreys Ledge: A habitat of unrecognized importance? *Marine Mammal Science* **16**:326–337.
- Wenger SJ, Olden JD. 2012. Assessing transferability of ecological models: an underappreciated aspect of statistical validation. *Methods in Ecology and Evolution* **3**:260–267.
- Whitt A, Dudzinski K, Laliberté J. 2013. North Atlantic right whale distribution and seasonal occurrence in nearshore waters off New Jersey, USA, and implications for management. *Endangered Species Research* **20**:59–69.
- Wingfield JE, O'Brien M, Lyubchich V, Roberts JJ, Halpin PN, Rice AN, Bailey H. 2017. Year-round spatiotemporal distribution of harbour porpoises within and around the Maryland wind energy area. *PLOS ONE* **12**:e0176653.